Firing of Hippocampal Neurogliaform Cells Induces Suppression of Synaptic Inhibition

Gengyu Li

St Edmund Hall

Trinity Term, 2014

Thesis submitted for the degree of

Doctor of Philosophy

at the

University of Oxford

ACKNOWLEDGMENTS

I would like to thank my supervisor Marco Capogna for taking me on as a D.Phil student and for his constant guidance, support and encouragement throughout my time in the Capogna lab. I have learnt a lot from him, benefiting me not only as a scientist but also as a person. I have been lucky to have him as a mentor and I am grateful to be his student.

I would also like to thank Prof. Peter Somogyi and the Medical Research Council for giving me the opportunity to work in the MRC Anatomical Neuropharmacology Unit. It is an exciting and enriching environment for research and my heartfelt gratitude goes to everyone in the Unit.

I extend my gratitude also to the members of the Capogna lab: Mira Manko, Thomas Bienvenu, Michael Bazelot, Marco Bocchio and Katie Whitworth, for their friendship and continuous assistance. I extend my thanks also my many friends outside the department, who have made my time at Oxford memorable.

I would like to thank Prof. Keith Gull for admitting me to St Edmund Hall and for his advice and support during my D.Phil study.

I would also like to thank Glenn Wong for proofreading the thesis.

Finally, I would like to dedicate this thesis to my parents as I am grateful for the selfless love and support they have given me throughout my life.

Firing of Hippocampal Neurogliaform Cells Induces Suppression of Synaptic Inhibition

Gengyu Li

St Edmund Hall, Trinity Term 2014

Thesis submitted for the degree of Doctor of Philosophy at the University of Oxford

ABSTRACT

The hippocampus contains more than 21 types of inhibitory interneurons that express different proteins and innervate different sub-domains of pyramidal cells to regulate the spatiotemporal integration of excitatory postsynaptic potentials (EPSPs) and to define temporal windows for spiking. Neurogliaform cells (NGFCs), form synapses on the distal tufts of pyramidal cell apical dendrites alongside excitatory inputs from the entorhinal cortex. NGFCs express neuronal nitric oxide synthase (nNOS), are often synaptically coupled, and fire rhythmically during theta oscillations *in vivo*.

In this thesis, I describe a novel form of synaptic communication between these interneuron types, hereafter referred to as the firing induced suppression of inhibition (FSI). Specifically, I found that when a theta-associated activity patterns were evoked in NGFCs from rodent hippocampal slices, the cells exhibited a transient reduction in unitary IPSP amplitude. My data suggest that FSI requires the backpropagation of action potentials, calcium influx through L-type calcium channels, nNOS activity within the dendrites of interneurons, and the activation of NO-sensitive guanylyl cyclase (NOsGC) receptors that are present on presynaptic terminals. My results also demonstrate the physiological impact of this phenomenon by showing that when FSI occurs, the strength of incoming excitatory postsynaptic potentials onto NGFCs are transiently sharpened. Specifically, FSI indirectly increased the amplitude of EPSPs. Thus FSI may enhance spatial and temporal summation of excitatory inputs to NGFCs and regulate their inhibition of pyramidal cells.

DECLARATION

All the work in this thesis was done by myself, Gengyu Li, except for what is mentioned below.

I am grateful to have had the opportunity of collaborating with other scientists. Their contribution to the work presented in this thesis is outlined as the following.

Dr Marco Canepari and Dr Robert Stewart wrote the software to analyse voltage sensitive dye and calcium imaging data. Additionally, I have benefited greatly from their assistance in analysing the imaging data.

Dr Marco Canepari helped to set up the voltage imaging and calcium imaging equipment and participated in the acquisition of imaging data.

Mr Ben Micklem performed the confocal imaging of biocytin and Lucifer Yellow filled cells presented in Figure 3.2.1.

Dr Peter Magill, Dr Paul Dodson and Mr Marco Bocchio performed perfusion-fixation of the brains used for cell counting experiments presented in Figure 3.6.6.

Mr Szabolcs Biró performed the immunofluorescence labelling with NOS and CCK antibodies presented in Figure 4.7.2.

The *in vivo* firing pattern that was used in this study was recorded by Fuentealba et al. (Fuentealba et al., 2010).

The dynamic clamp sequence used in this study presented in Figure 3.8.2 was recorded by Price et al. from the Capogna lab (Price et al., 2005).

LIST OF ABBREVIATIONS

4-AP	4-aminopyridine
aIPSC/P	autaptic inhibitory postsynaptic current/potential
AP	action potential
bAP	backpropagating action potential
BAPTA	1,2-bis(o-aminophenoxy)ethane- N,N,N',N'-tetraacetic acid
CB	calbindin
CB1R	canabinoid receptor type 1
CCK	cholecystokinin
dEPSC/P	synthetic (dynamic clamp) excitatory postsynaptic current/potential
DG	dentate gyrus
DSI	depolarisation induced suppression of inhibition
eCB	endocannabinoid
EC	entorhinal cortex
EPSC/P	excitatory postsynaptic current/potential
FSI	firing induced suppression of inhibition
GABA	γ-aminobutyric acid
IPSC/P	inhibitory postsynaptic current/potential
L-NAME	NG-Nitro-L-arginine methyl ester hydrochloride
LTD	long term depression
LTP	long term potentiation
LTP-GABA	LTP of inhibitory synapse
NGFC	neurogliaform cell
NMDA	N-methyl-D-aspartate

nNOS	neuronal nitric oxide synthase
NO	nitric oxide
NOS	nitric oxide synthase
NOsGC	nitric oxide sensitive soluble guanylyl cyclase
NPY	neuropeptide Y
ODQ	1H-[1,2,4]Oxadiazolo[4,3-a]quinoxalin-1-one
O-LM	oriens-lacunosum moleculare
PV	parvalbumin
SC	Schaffer collateral
SEM	standard error of the mean
sIPSC/P	spontaneous inhibitory postsynaptic current/potential
SL	stratum lacunosum
SM	stratum moleculare
SLM	stratum lacunosum moleculare
SNP	sodium nitroprusside
SO	stratum oriens
SOM	somatostatin
SNARE	soluble NSF attachment protein receptor
SP	stratum pyramidale
SR	stratum radiatum
SR95531	6-Imino-3-(4-methoxyphenyl)-1(6H)-pyridazinebutanoic acid hydrobromide
STDP	spike timing dependent plasticity
TEA	tetraethylammonium
TTX	tetrodotoxin
uIPSC/P	unitary inhibitory postsynaptic current/potential
VIP	vasoactive intestinal peptide

VTA	ventral segmental area
VGCC	voltage gated calcium channel
τ	membrane time constant

LIST OF FIGURES

TABLE OF CONTENTS

1. INTRODUCTION

1.1. The Hippocampus

1.1.1. Hippocampus and memory

The hippocampus is a brain structure that is well-known for its involvement in memory formation. Memory, as Richard Morris describes, “transcends the immediate moment” and is monumental for the survival of an animal. In unstable environments, it is critical for an animal to process and store external information to optimise their future behaviour, such as remembering the location of safety and food source. To achieve this, the hippocampus and other brain areas have evolved to inhabit the property of activity dependent plasticity.

Two types of memory have been described, namely, declarative or non-declarative memory. The subdivision of memory storage in different structures of the brain is evident in lesion studies. For example, lesion studies from patients like HM (Scoville and Milner, 1957) revealed that this patient had severe anterograde amnesia following a medial temporal lobectomy for an epilepsy treatment. HM and other patients who sustain similar injuries cannot form new memories that involve facts and events (declarative memories), but their acquisition of motor skills remained intact (non-declarative memories). The hippocampus is an important site for the maintenance of declarative memory, particularly for episodic memory (events). For example, the CA1 pyramidal cells of the hippocampus can act as placement cells that respond to the environmental location of the animal (O’Keefe and Dostrovsky, 1971).

The structure and function of the hippocampus and associated structures in the

medial temporal lobe are conserved between species (Manns and Eichenbaum, 2006). Importantly, the rodent is a suitable and relevant model for understanding human hippocampal function as its medial temporal lobe architecture resembles its human counterpart.

1.1.2. Anatomy of the hippocampus

The hippocampal formation is a C-shaped tube structure in 3D and is located in the medial temporal lobe of the brain. It consists of the dentate gyrus (DG), the hippocampus proper (CA3, CA2 and CA1), the subicular complex (subiculum, presuiculum, and parasubiculum), and the entorhinal cortex (EC). At greater resolution, functional subdivision of the hippocampus is evident in the form of a layered structure, where each layer is described as a stratum (Figure 1.1.2.1).

CA1 pyramidal cells are primarily responsible for hippocampal output and are located to one long continuous layer called the stratum pyramidale (SP). These cells extend their primary apical dendrites to the border of the DG, passing through the stratum radiatum (SR) in the process and terminates at the stratum lacunosum moleculare (SLM). Their basal dendrites, however, extend in the opposite direction and arrive at the stratum oriens (SO). The SR, SLM and SO host several types of GABAergic interneurons, which form synapses at different sub-regions of the pyramidal cells and/or with each other (Klasuberger and Somogyi, 2008). These GABAergic interneurons are thought to be the key regulators of hippocampal output, and will be discussed in detail in later sections.

In terms of input, the perforant pathway forms the classical tri-synaptic hippocampal loop (Andersen et al., 1971), where axons from layer 2 of the EC, primarily glutamatergic, synapse to the granule cells in the DG of the hippocampus. The granule cells then transduce the signal via mossy fibres that are present on CA3 pyramidal cells; these cells in turn synapse with the proximal and basal dendrites of CA1 pyramidal cells via the Schaffer collateral (SC), thereby completing the tri-synaptic pathway. Additionally the EC also projects directly to CA3, CA1 and the subiculum. This forms a shorter loop, where inputs from layer 3 of the EC synapse directly with the distal dendrites of the CA1

pyramidal cells, which then output to the subiculum and EC to close the loop (Figure 1.1.2.2).

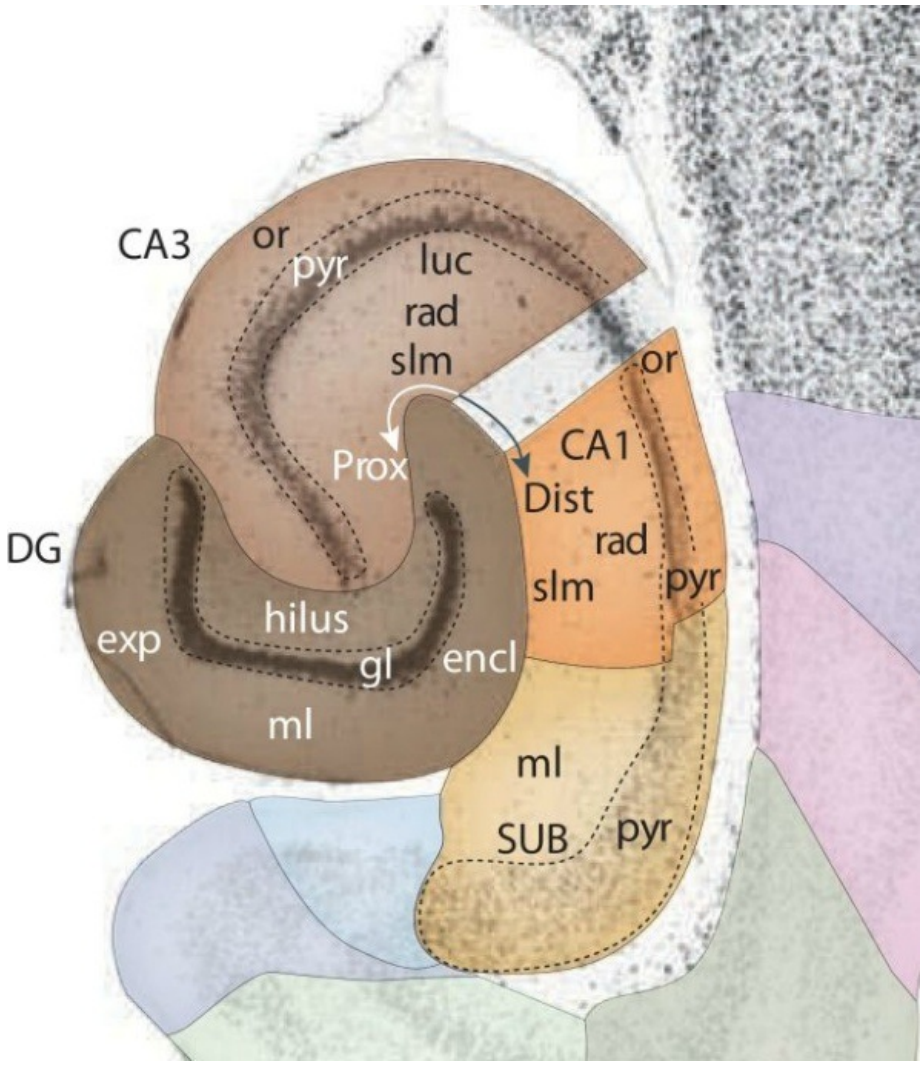

Figure 1.1.2.1 Representation of the hippocampal formation

CA, cornu ammonis; dist, distal; encl, enclosed blade of the DG; exp, exposed blade of the DG; gl, granule cell layer; luc, stratum lucidum; ml, molecular layer; or, stratum oriens; prox, proximal; pyr, pyramidal cell layer; rad, stratum radiatum; slm, stratum lacunosum-moleculare.

Figure taken from http://www.temporal-lobe.com

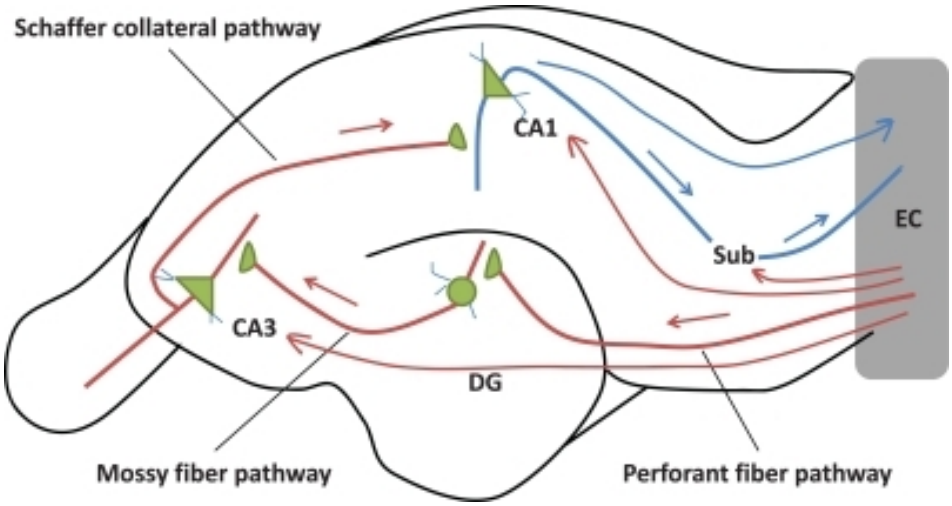

Figure 1.1.2.2 The input and output pathways of hippocampal formation

The entorhinal cortex (EC) is the main input to the hippocampus. The EC projects to the dentate gyrus (DG) via perforant pathway and provides the critical input to CA3 via the mossy fiber pathway, then to CA1 by means of the Schaffer collateral pathway. In addition, the EC can also project directly to CA3, CA1 and subiculum (Sub). Furthermore, the EC is the major output of the hippocampus. Arrows denote the direction of impulse flow.

Figure taken from Zhang and Zhu, 2011.

1.1.3. Flow of information in the hippocampus

A few intriguing hypotheses have been advanced to explain the ability of the hippocampus to encode and store environmental information. At the cellular level, the mechanisms for memory storage are thought to occur through Hebbian-style modifications in synaptic strength, i.e. the coordination of presynaptic and postsynaptic activity to enhances synaptic strength or “cells that fire together wire together” (Hebb, 1949).

Synaptic plasticity was then demonstrated by Bliss and Lømo in 1973, who described a phenomenon known as long-term potentiation (LTP) in the hippocampus of an anaesthetised rabbit (Bliss and Lømo, 1973). In this process, a brief train of high-frequency stimulation of the perforant pathway causes an abrupt yet sustained increase in synaptic strength on hippocampal granule cells. Thus, memory can be represented by modifications to synaptic strength. Pharmacological studies further dissected the key components that are involved in the initiation and maintenance of LTP, including the involvement of NMDA receptors in the formation of episodic memory (Morris et al., 1986). In addition, pyramidal cells within the CA1 hippocampus were found to respond to locations in space. These cells are referred to as “place cells” as they respond to changes in the environment by firing in a specific pattern to represent a place cell map (O’Keefe and Dostrovsky, 1971).

An interesting feature of CA3 pyramidal cells is their extensive recurrent connectivity. Their anatomical properties suggests that pattern completion could occur during memory recall, as demonstrated by a correlation matrix (Marr, 1971). For example, the hippocampus encodes new perceptual representations of the spatiotemporal context into unique sets of synaptic weight changes, and when the animal re-experiences a partial representation, such as a cue (activity of a subset of

neurons), the activity spreads across synapses that had initially been modified and reproduces a pattern of activity that closely matches the original. This phenomenon is known as the autoassociative model of memory storage and retrieval, and supports the notion that memory storage is occurs in the CA3 region. Evidence supporting this argument includes: 1) the extensive recurrent connections of the axons of CA3 pyramidal cells; 2) the observation that the participating synapses undergo LTP; 3) LTP at these synapses are Hebbian in nature. Nevertheless, whether the CA3 represents the sole region where a recurrent network exists remains unclear. In principle, recurrent connections are known to exist between hilar mossy cells and granule cells, and also within the granule cell-CA3-granule cell loop (Lisman, 1999).

1.1.4. Oscillations in the brain

It is evident that the animal brain shows a different band of oscillations and there are solid evidence which demonstrate that oscillations, which can be recorded as electroencephalogram (EEG), are key to information processing in the brain (Buzsáki, 2002). The EEG reflects the activity of a large number of neurons in the brain and could be recorded *in vivo* by placing a recording electrode in specific brain regions such as the hippocampus *in vivo*. Four bands of rhythmic oscillations have been identified: theta (4 - 12 Hz), beta (12 - 25 Hz), gamma (25 - 100 Hz) and ripple (100 - 200 Hz). Studies have shown that these oscillations represent more than just 'background hum' as they perform an important functions in the brain.

One function of these oscillations is to facilitate spike synchrony, which encodes an additional level of information beyond the contribution of individual spikes (Salinas and Sejnowski, 2001). Accordingly, these oscillations could provide an answer to the binding problem, such that different attributes of sensory or memory objects are brought together by spike synchrony rather than physical synaptic connections (Jensen and Lisman, 2005). Specifically, when distinct neuronal groups become entrained in synchronous oscillations, they tend to emit spikes in synchrony - this concerted response enhances the neuronal impact that coordinated output signals will have on target cells.

Oscillations also function to provide a common reference signal that might be used for temporal coding. An example of this is the observation that the spike timing of hippocampal pyramidal cells relative to ongoing theta oscillations provides information concerning the location of an animal (O'Keefe and Recce, 1993). Specifically, studies have shown that place cells progressively fire earlier in the theta cycle as the animal approaches and then pass through the centre of the place field, a phenomenon called phase precession (O'Keefe and Recce, 1993). Interestingly, different bands of

oscillations have distinct behaviour correlates. For example, theta and gamma oscillations are prominent during exploratory behaviours (Bragin et al., 1995a), and place cells replay previous firing during sharp-wave ripples (Carr et al., 2011). However, the causal relationships between network oscillations and information processing require further addressing.

One hypothesis for a mechanism underlying network oscillations is thought to come from the action of inhibitory interneurons. Specifically, spike timing is modulated through synaptic inhibition and/or shunting inhibition by GABAergic interneurons that synapse to various compartments of the CA1 pyramidal cells (Cobb et al., 1995). The oscillation cycle can be subdivided into depolarising and hyperpolarising phases. During the depolarising phase, EPSPs can effectively contribute to the excitation of the cells and trigger spikes. The probability of generating spikes increases gradually and is highest at the peak of the depolarising cycle. However, a strong excitatory drive can also generate spikes before reaching the peak of the depolarising cycle; in this case, the spike timing depends on the strength of the excitatory drive. A stronger excitatory drive causes earlier discharges. Thus, the amplitude of an excitatory drive can be predicted by spike timing, whereby spike timing relative to the peak of the depolarising cycle of the oscillation is a direct measurement of the input intensity. This relation allows the conversion of rate coded amplitude values to the temporal code of spike timing. The second phase of the oscillation, the hyperpolarising phase, is generated by a large number of IPSPs from various interneurons. During this phase, cells are unlikely to respond to the excitatory drive as both the shunting and hyperpolarising effect of IPSPs prevent an effective summation of the EPSPs.

In addition to signal processing, the precise adjustment of timing of action potentials (APs) relative to oscillation cycles is also important for learning and memory. For example, use-dependent synaptic modifications are very sensitive to timing relations

between pre- and post- synaptic activation (spike timing dependent plasticity, STDP). This indicates that in oscillating networks, the phase relations between the timing of spikes relative to the oscillation cycle will determine whether synaptic strength will be enforced or depressed, as has been demonstrated *in vitro* (Wespatat et al., 2004).

1.2. Modes of GABAergic neurotransmission

1.2.1. Pre- post-synaptic communication

GABA is synthesised by the decarboxylation of glutamate via the enzyme glutamic acid decarboxylase (GAD). Two isoforms of GAD exists, namely GAD67 and GAD65, they synthesise GABA at different locations in the neuron and at different development times. This difference is thought to reflect a functional specialisation. The enzyme GAD67 is expressed throughout the cytoplasm and synthesises GABA for neurotransmission-independent activities, such as synaptogenesis and protection from neuronal injury (Pinal and Tobin, 1998). On the other hand, GAD65 is expressed at presynaptic terminals and synthesises GABA during neurotransmission (Pinal and Tobin, 1998). Once synthesised, GABA is then packed into vesicles at the presynaptic terminal through the potential gradient formed by high intra-luminal hydrogen ions, possibly with the aid of a vesicular transporter VGAT (McIntire et al., 1997), or without them as reported in a subset of GABAergic terminals (Chaudhry et al., 1998).

At the presynaptic terminal, vesicles filled with GABA are tethered by synapsin molecules to an actin scaffold in the presynaptic terminal. Three distinct populations of vesicles are known: vesicles that are docked and primed for release at a specialised presynaptic membrane region (active zone) are called the readily releasable pool; vesicles that are located near the active zone but not yet primed for release are called the recycling pool; and vesicles that are located further away from the active zone and mobilised only during period of higher presynaptic activity are called the reserve pool (Rizzoli and Betz, 2005).

When action potential is evoked in the presynaptic terminal, depolarisation enables the opening of voltage gated calcium channels (VGCCs) that leads to a rise in

intracellular calcium concentration. In most synapses, presynaptic calcium influx occurs through P/Q or N-type calcium channels, whereas R and L-type calcium channels are less involved (Sudhof, 2004). In response to the presynaptic calcium concentration, primed vesicles begin fusing with the membrane mediated by the SNARE protein and driven by the energy provided from the SNARE complex. The elevation in calcium that triggered this event is sensed by the calcium-binding protein called synaptotagmin. The importance of SNAREs in mediating this calcium-dependent fusion has been demonstrated in mutants or knockouts of Drosophila or mice (Sudhof, 2004). The mechanism by which vesicles fuse with membrane is still under debate. Two main models exist, namely the full collapse fusion model and the kiss-and-run model (He and Wu, 2007).

Once in the synaptic cleft, neurotransmitters such as GABA diffuses through the synaptic space to activate receptors located postsynaptically, and usually from another neuron. Although in some cases, presynaptic receptors may also become activated (autoreceptors); and the presynaptic cell may synapse to itself as well (autapses). GABA binds to two types of GABA receptors: ionotropic $GABA_A$ receptors and metabotropic $GABA_B$ receptors, to modify postsynaptic activity. The binding of GABA to $GABA_A$ receptors allows the opening of chloride channels which results in fast inhibitory postsynaptic potentials (IPSPs) and shunting inhibition. Activation of $GABA_B$ receptor triggers G-protein coupled signalling pathway and this may leads to the opening of K^+ channels, which further leads to slower, longer IPSP, as well as suppressing of presynaptic calcium channels (through presynaptically located $GABA_B$ receptors) and reduce transmitter release.

$GABA_A$ receptors are a pentameric complex of subunits that are permeable to chloride ions. Five subunits can combine in different ways to form $GABA_A$ receptors, the

minimal requirement is the inclusion of both α and β subunits (Connolly et al., 1996). In particular, the most common type in the brain is a pentamer comprising two α's, two β's, and a γ, arranged as γ-β-α-β-α (Baumann et al., 2002). Distinct types of $GABA_A$ receptors exist, due to different subunits compositions. For example, $GABA_A$ receptors expressed on axo-axonic cells contain several subunits including the α1 and α2 subunits (Somogyi et al., 1996); $GABA_A$ receptors found on PV basket cells are predominantly composed of the α1 subunit (Klausberger et al., 2002), whereas the α2 subunit is used in CCK basket instead (Nyiri et al., 2001). In particular, $GABA_A$ receptors expressed on NGFCs contain α1, α5 and δ subunits (Szabadics et al., 2007). The subunits composition determines the biophysical properties of $GABA_A$ receptors. For example, the EC_{50} value, as a measure of sensitivity of the receptor to GABA, is ranked differently for different subunits: α6<α1<α2<α4<α5<α3 (from higher sensitivity to lower sensitivity) (Bollan et al., 2003).

1.2.2. Autapses

Autapse refer to synapses formed by the axon of a neuron onto its own soma or dendrites. In the brain, several types of GABAergic interneurons are often found to exhibit autapses; whereas autpases are less common in pyramidal cells (Tamas et al., 1997). For example, autapses are frequently found in parvalbumin (PV)-positive basket cells and neurogliaform cells (NGFCs). The presence of autapses is cell-type specific, for example, ~85% of neocortical fast-spiking PV-positive cells (Bacci et al., 2003) and ~50% of NGFCs in the hippocampus (Karayannis et al., 2010) display an autaptic current. In contrast, pyramidal cells in the visual cortex of adult cats have rarely been found to innervate themselves (Tamas et al., 1997). In addition, it was reported that basket cells and dendrite targeting interneurons in the neocortex have the highest percentage of autapses, whereas double-bouquet cells have a lower percentage, albeit more frequent than found in pyramidal cells (Tamas et al., 1997). Interestingly, the target sites of these autapses are often the same as the postsynaptic domains of other cells that they innervate and the kinetics of autaptic currents is also similar to postsynaptic currents (Karayannis et al., 2010), suggesting a precise rather than random phenomenon (Cobb et al., 1997; Tamas et al., 1997; Pawelzik et al., 2003).

But, what is the function of autapses? Autaptic current can be considered as a type of feedback inhibition and one function is to allow the rapid cessation of firing. This is important especially for PV-positive basket cells. As will be discussed in more detail later, PV-positive basket cells are thought to set the ‘tone’ for oscillatory activities in the hippocampus, and therefore it is important for them to have high temporal precision. Indeed, PV-positive basket cells have short membrane time constants, ultra-fast AMPA receptor conductance, rapid and reliable GABA transmission and a non-adapting high-frequency firing rate (Cardin et al., 2009; Sohal et al., 2009; Hu et al., 2010). Additionally,

the presence of an autaptic current would allow the cell to reset itself rapidly following excitation, increases temporal precision and shortens the time window for the integration of signals (Bacci and Huguenard, 2006). In contrast to excitatory neurons, inhibitory interneuron networks cannot generate canonic feedback inhibition. However, the presence of autaptic current allows fast feedback inhibition in inhibitory neuron networks, and provides fast self-inhibition that is crucial for the function of PV-positive basket cells (Deleuze et al., 2014).

Another function of autaptic currents is to maintain the reliability of interneuron networks. For example, PV cells form extensive reciprocal connections between them; this would lead to mutual silencing during period of sustained network activity. It has been demonstrated that autaptic current induced self-inhibition would prevent high-frequency bursts and disorganised mutual inhibition (Bacci and Huguenard, 2006). In addition, a modelling approach has reported that increases in the strength of autaptic current could shape its output frequency, allowing the modelled neuron to transition towards an oscillatory spiking regime without high-frequency bursts (White et al., 1998). The interneurons of the SLM have been shown to oscillate at the peak of theta from *in vivo* recording (Fuentealba et al., 2010) and the presence of autaptic currents in NGFCs may contribute to proper network function. Future computational modelling work may shed light on the role of NGFC-autaptic currents in the network.

1.3. Interneurons of the hippocampus

Interneurons play an important role in regulating information flow within the hippocampus. The hippocampus contains various interneuron types, in contrast to the relatively homogenous existence of glutamatergic neurons - such as pyramidal cells and granule cells. Different types of interneurons are involved in regulating each part of the circuit, which is required for proper functioning of the hippocampus. Interneurons provide important feedfoward, feedback and long range GABAergic inhibition on the soma, dendrites and axons of both pyramidal cells and other interneurons (Freund and Buzsáki, 1996). These interneurons are critical for overall network stability, the spatiotemporal flow of activity (Pouille and Scanziani, 2001), and for orchestrating the temporal dynamics of cellular ensembles (Klausberger and Somogyi, 2008).

Pyramidal cells of the hippocampus encode representations of spatial and other episodic memories. To perform this function, several types of GABAergic interneurons inhibit and regulate the relatively uniform pyramidal cells of the hippocampus. Interneurons are further recognised based on several criteria including firing patterns, molecular expression profiles, and innervations of the subcellular domains of pyramidal cells (Klausberger and Somogyi, 2008). There are at least 21 distinct types of interneurons (Figure 1.3.1) in the hippocampus, which begs the question of why such extensive diversity is required. There is no single answer to this question, although concepts relating to division of labour or functionality may best explain the apparent diversity.

A CA1 pyramidal cell receives about 30,000 synaptic inputs and extends several types of dendrite to provide a platform for synaptic integration. Remarkably, GABAergic synapses cover almost the entire membrane surface of pyramidal neurons, from the tip of distal dendrites to the initial axon segment (which is the site where an AP is usually

generated). These synapses on different domains of pyramidal cell membrane are mediated by distinct interneuron types, which serve specific functional roles in the regulation of principal cell activity and plasticity (Miles et al., 1996). For example, axo-axonic cells innervate exclusively the axon-initial segment; basket cells innervate the cell bodies and proximal dendrites; bistratified cells innervate the basal and oblique dendrites; oriens-lacunosum moleculare (O-LM) cells innervate the apical dendritic tuft, and NGFCs target the distal dendrites.

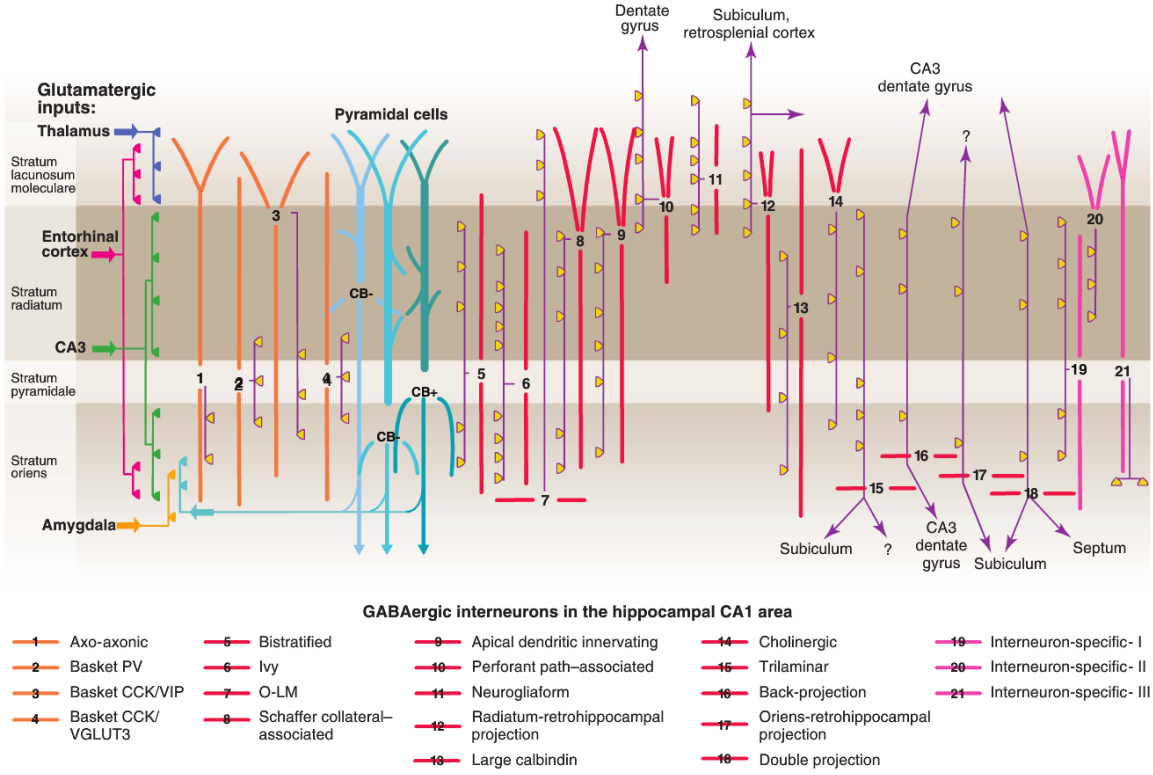

Figure 1.3.1 Diversity of GAbAergic interneurons in the CA1 area of the hippocampus

Three types of pyramidal cells (blue, cyan) are accompanied by at least 21 different types of GABAergic interneurons. The soma and dendrites of interneurons innervating pyramidal cells are shown in red or orange, and those innervating mainly other interneurons are pink. Axons are shown in purple and the main synaptic terminations are yellow. Perisomatic targeting interneurons are shown on the left side of pyramidal cells. Dendritic targeting interneurons or interneurons synapsing in Scaffer collateral or entorhinal pathway termination zones are shown on the right side. CB, calbindin; VIP, vasoactive intestinal polypeptide; O-LM, oriens lacunosum molecular, VGLUT, vesicular glutamate transporter.

Figure taken from Klausberger and Somogyi, 2008.

1.3.1. Perisomatic inhibition

There are three major types of interneuron assigned with this task of perisomatic inhibition: the PV- and cholecystokinin (CCK)-expressing basket cells, and PV-expressing axo-axonic cells. PV-containing basket cells are thought to function like clockwork for cortical network oscillations, whereas CCK-expressing cells operate as a plastic fine-tuning device. It is thought that a fast feedback loop is necessary for gamma oscillations and PV basket cells are able to respond rapidly and reliably to glutamatergic excitation as well as generate fast and precise inhibitory postsynaptic currents (IPSCs) that exhibit outward rectification (Hu et al., 2010). Experiments have shown that the selective optogenetic activation of neocortical PV basket cells strongly facilitates gamma-band oscillations (Cardin et al., 2009; Sohal et al., 2009), and selective suppression of GABA release from PV basket cells by μ opioid receptor agonists abolishes the pharmacologically-induced gamma oscillations in CA3 *in vitro* (Gulyás et al., 2010). The CCK-expressing interneurons, on the other hand, integrate both feedforward and feedback (from pyramidal cells) signals and fire later in a train (after pyramidal cells have been fired). Although both PV and CCK cells innervate overlapping territories of target pyramidal neurons, their intrinsic properties differ to allow for different and unique functions.

Morphologically, CCK cells express more types of receptors, such as 5-HT3, nicotinic receptors postsynaptically, and cannabinoid type 1 receptors (CB1R) presynaptically. In contrast, PV cells only possess a few receptor types for subcortical modulatory signals, such as μ opioid and muscarinic acetylcholine receptors, this is consistent with its 'oscillator' functionality (Freund and Katona, 2007). Both PV and CCK expressing cells have dendritic trees that span all layers and thus, are in principle activated by several overlapping inputs (Glickfeld and Scanziani, 2006). The mitigation of

this 'inconvenience' is thought to occur through the possession of multiple synaptic inputs: PV cells receive three times more asymmetrical glutamatergic inputs than CCK cells and stronger excitatory postsynaptic currents (EPSCs) (7 times larger compared to CCK cells) (Mátyás et al., 2004). In addition, CCK cells have a longer membrane time constant than PV cells, allowing them to integrate signals over a much greater time window than PV cells (Glickfeld and Scanziani, 2006). When Schaffer collaterals (SCs) are stimulated, PV cells discharge and drive feedfoward inhibition, integrating only over narrow time windows and thus accurately reporting the timing of ongoing hippocampal activity. However, because CCK cells receive much less glutamatergic inputs than PV cells, SCs stimulations may be insufficient to excite CCK cells. The stimulation of SCs will excite pyramidal cells which have feedback inputs to CCK cells, and since CCK cells have a longer summation window, they are able to integrate both the feedforward and feedback inputs and will only fire when local pyramidal cells are activated.

1.3.2. Dendritic inhibition

Conversely, other types of GABAergic interneurons are specialised to control the dendritic compartments of postsynaptic pyramidal cells. For example, O-LM cells, Ivy cells and NGFCs play critical roles in dendritic inhibition. NGFCs innervate the apical dendritic tuft of CA1 pyramidal cells, where the pyramidal cells also receive EC input. By contrast, Ivy cells, which are similar to NGFCs in morphology and molecular profile, innervate more proximal dendrites of the pyramidal cells, and are aligned with CA3 input. Interestingly, Ivy cells and NGFCs do not express PV or CCK, which are common markers for many interneuron types. Instead, they express nitric oxide synthase (NOS), reelin, COUP-TFII and neuropeptide Y (NPY) (Price et al., 2005a; Fuentealba et al., 2010). Both Ivy cells and NGFCs mediate a slow $GABA_A$ receptor mediated inhibition in the hippocampus (Price et al., 2005, Fuentealba et al., 2008), which is thought to occur through the unique spatiotemporal profile of their postsynaptic synapses (Karayannis et al., 2010). These cells modulate pre- and post- synaptic excitability at slower time scales and act more diffusely and less specifically on their targets – this communicative process is known as 'volume transmission' (Tamas et al., 2003, Olah et al., 2009). Their functional roles will be discussed in later chapters.

1.3.3. SLM interneurons

The SLM is the most superficial layer of the CA1 hippocampus and contains a relatively low density of neurons. This layer receives excitatory inputs from the EC and many other extrinsic inputs, and it is where distal dendrites of pyramidal cells terminate. Indeed, it has been reported that stimulation of the EC evokes EPSPs in CA1 pyramidal cells, but strong IPSPs are also detected, especially with low-frequency stimulation (< 0.1 Hz) (Soltesz and Deschenes, 1993). This is because the two cortical inputs from EC contact not only the DG or distal dendrites of CA1 pyramidal cells, but also interneurons of the SLM (Desmond et al., 1994), giving the strong IPSPs observed. There are a variety of different interneuron cell types found in the SLM (Klausberger, 2009; Capogna, 2011). These cell types include (defined with at least the soma in the SLM): the perforant pathway-associated (PPA) cells, the Schaffer collateral/commissural pathway-associated (SCA) cells, apical dendrite innervating cell, radiatum- and dentate-innervating (RADI) cell, basket cells and NGFCs (Figure 1.3.3.1).

Specifically, the SCA interneurons have their axonal branches in the SR, and occasionally in the SO, targeting the oblique and basal dendrites of pyramidal cells; the apical dendrites and SCA cells innervate target cells in the same fashion, but the former mostly targets the main apical shaft of CA1 pyramidal cells and expresses CCK, CB1R, vesicular glutamate transporter 3 (VGLUT3) and neurokinin 1 receptor; the PPA interneurons innervate the apical tuft of CA1 pyramidal cells and dendrites of granule cells of the DG, i.e. the target of perforant pathway, and its molecular profile includes CCK, calbindin or CB1R; RADI cells have been discovered recently (Fuentealba et al., 2010), these have pronounced innervations of granule cells and are immunopositive for CB1R, calbindin, neuropeptide precursor preprotachynin B (PPTB) and the transcription factor COUP-TFII; finally, basket cells are anatomically similar to those found in the SR

and SP, they target the soma of pyramidal cells and are immunopositive for CCK.

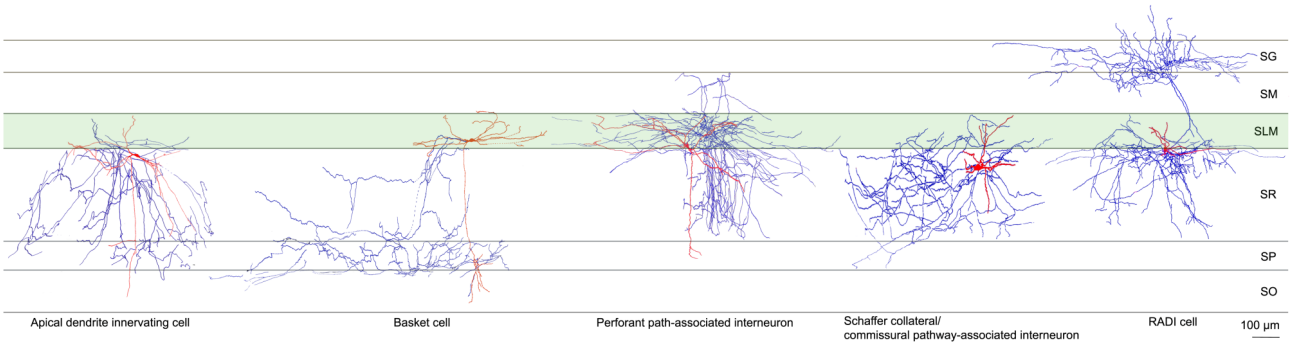

Figure 1.3.3.1 Diversity of SLM interneurons

This drawing shows examples of interneuron with the soma in the SLM or at the SR-SLM border. Soma and dendrites are shown in red; the axonal arborisation is shown in blue.

Figure taken from Capogna, 2011

1.3.4. Neurogliaform cells

NGFC is the one of the most interesting cell types found in the SLM region and they display certain unique characteristics. The NGFC is a very compact interneuron of the SLM; it has a relatively small and round soma, with dendrites arranged in a stellate fashion around it. The characteristic feature of NGFCs is its dense axonal arbour, which tends to be restricted to the SLM layer (Figure 1.3.4.1) (Price et al., 2005b; Fuentealba et al., 2010; Karayannis et al., 2010).

The NGFC receives monosynaptic and fast excitatory inputs from the TA pathway and from the SCs. These EPSCs can exhibit short-term facilitation or depression upon stimulation at theta frequency (Price et al., 2005), but long-term synaptic plasticity has not been reported thus far. Interestingly, in contrast to PV or CCK basket cells, CA1 pyramidal cells do not connect back to the NGFCs; therefore, NGFCs are unusual in their role as a 'pure' feedfoward interneuron (Alger and Nicoll, 1982). Although NGFCs receive inhibitory inputs from O-LM cells, the latter receive robust excitatory inputs from CA1 pyramidal cells, which allow the former to act as a feedback interneuron that shifts the balance between feedforward and feedback inhibition of CA1 pyramidal cells (Elfant et al., 2008). NGFCs have also been found to synaptically couple with each other and themselves (via autapse), and this indicates the possible formation of a specific interneuron network (Price et al., 2005). Moreover, because of their dense axonal arborisation and volume transmission (Ola et al., 2009), the probability of connectivity between NGFCs and a postsynaptic cell is very high; therefore, a single action potential evokes an unitary IPSC (uIPSC) with almost no failures and little peak amplitude variability is seen between trials (Szabadics et al., 2007; Karayannis et al., 2010).

The neuronal markers for NGFCs has been identified as NPY, neuronal nitric oxide synthase (nNOS, and enzyme that synthesises nitric oxide, NO), $GABA_A$ receptor

subunit α1 and δ, along with α-actinin2 and the transcription factor COUP-TFII (Price et al., 2005; Fuentealba et al., 2008, 2010). In addition, reelin expression has been reported in NGFCs but not Ivy cells (Fuentealba et al., 2008). Furthermore, mRNAs for CCK, SOM and calbindin has been found to be present on NGFCs as well as other interneurons of the SLM, albeit less frequently (< 50%) (Price et al., 2005). The variability in the neuronal marker expression of cells is partly due to their developmental origin. For example, nNOS-postive NGFCs and Ivy cells are derived from the medial ganglionic eminence progenitors through the control of the transcription factor, NKx2-1, while a subset of NGFCs that lacking nNOS are derived from caudal ganglionic eminence progenitors (Tricoire et al., 2010).

Another interesting property of NGFCs is its ability to display persistent firing. Since NGFCs form extensive interneuron networks with themselves as well as other interneurons in the SL via electrical synapses (Price et al., 2005; Zsiros and Maccaferri, 2005), the activation of island cell axons can evoke a depolarising response, which propagates through gap junctions that amplify this feedfoward inhibition (Kitamura et al., 2014). Furthermore, an interesting feature of SLM interneurons is that they can enter a state of continuous firing in the absence of input, called persistent firing, while application of a μ-opoiod receptor agonist can prevent cells from entering the persistent firing state (Krook-Magnuson et al., 2011). In particular, it has been reported that 80% of NGFCs and Ivy cells display persistent firing; by contrast, only 20% of other interneurons can display persistent firing (Krook-Magnuson et al., 2011). The high chance of NGFCs and Ivy cells to display persistent firing may be a result of the high frequency of gap junctions occurrence; gap junctions are formed not only within themselves but also with other interneurons (Simon et al., 2005; Zsiros and Maccaferri, 2005) - this may provide an explanation for the occasional persistent firing observed in other cell populations. The physiological role of persistent firing is not completely understood. One physiological

function could be its involvement in the generation of neuronal oscillations as persistent firing occurs at frequencies that match those commonly observed in network oscillations, such as beta and gamma rhythms (Sheffield et al., 2011b). Additionally, persistent firing could function as a mechanism for the storage of working memory (Egorov et al., 2002).

In addition, it is known that NGFC synapses are extremely use-dependent and repeated stimulation of NGFCs will quickly fatigue the IPSCs (Tamas et al., 2003; Price et al., 2005, 2008). Specifically, stimulation of a presynaptic NGFC at 5 Hz elicits a marked short-term depression that has been shown to be tightly regulated by presynaptic $GABA_B$ receptors (discussed in more detail in chapter 1.4.7). In addition to presynaptic $GABA_B$ receptors, slow presynaptic recycling of vesicles may also be a factor that contributes to the short-term depression observed (Hefft and Jonas, 2005).

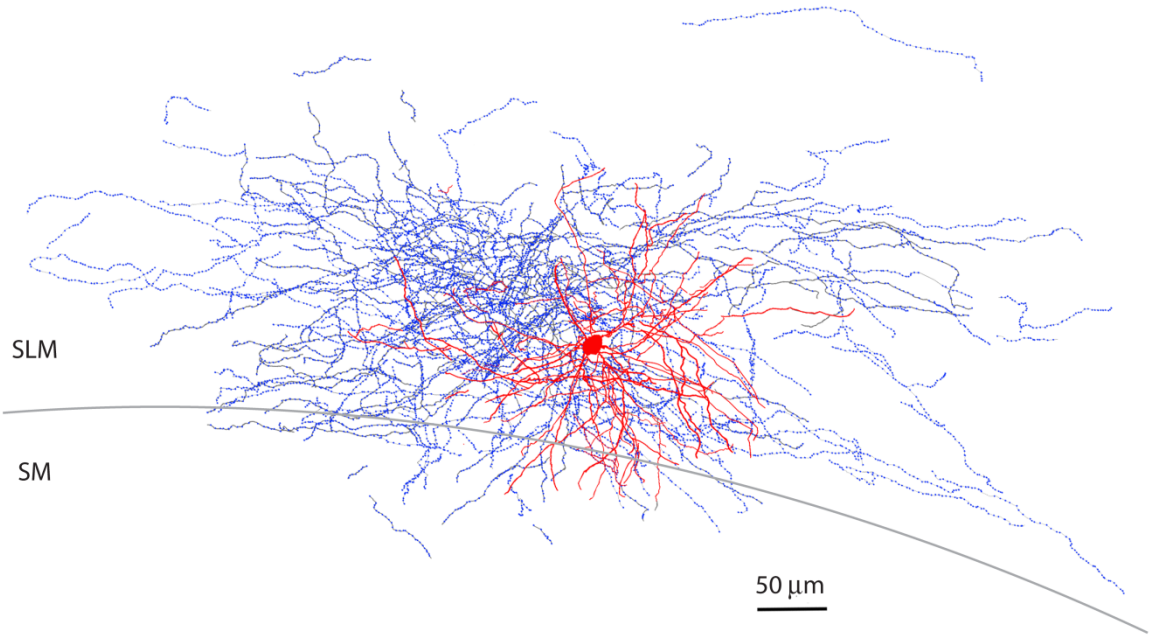

Figure 1.3.4.1 Example of a hippocampal neurogliaform Cell

Light microscopic reconstruction (x100) of a biocytin-labelled NGFC (soma and dendrites in red, axon in blue) in acute slice. The axonal arbor remains largely segregated within the stratum lacunosum-moleculare (SLM) but at some locations crosses the hippocampal fissure into the stratum moleculare. Note also that the axon overlaps extensively with the dendritic arbour forming putative autaptic contacts.

Figure taken from Karayannis et al., 2010

1.3.5. nNOS as a neuronal marker for NGFCs

A well-known neuronal marker for NGFC is the nNOS (Price et al., 2005). Other markers for NGFCs has also been identified, including NPY, $GABA_A$ receptor subunit α1 and δ, along with α-actinin2 and the transcription factor COUP-TFII (Price et al., 2005; Fuentealba et al., 2008, 2010). In addition, reelin expression has been reported in NGFCs but not Ivy cells (Fuentealba et al., 2008). Furthermore, mRNAs encoding CCK, SOM and calbindin has been found to be present on NGFCs and other interneurons of the SLM, albeit less frequently (< 50%) (Price et al., 2005). Although NGFCs are known to express nNOS, not all NGFCs express nNOS and this variability in neuronal marker expression of cells is partly due to their developmental origin. For example, nNOS-positive NGFCs and Ivy cells are derived from the medial ganglionic eminence progenitors through the control of the transcription factor, NKx2-1, while a subset of NGFCs that lack nNOS are derived from caudal ganglionic eminence progenitors (Tricoire et al., 2010).

NO is synthesised from L-arginine by nNOS following a rise in Ca^{2+} levels. NOS are complex proteins found to exist mainly in two isoforms, the neuronal (nNOS) and the endothelial (eNOS) type. There is a third type, inducible (iNOS) that is less frequently observed and is expressed when cells are subjected to immunological challenge. The nNOS is activated by Ca^{2+} complexed with calmodulin and has a wide distribution in the brain. In the hippocampus, nNOS is found on pyramidal cells, on both excitatory (Burette et al., 2002) and on the postsynaptic active zone of different GABAergic synapses located on soma, dendrite, and axon initial segment (Szabadits et al., 2007). In the excitatory synapse, the increase in local Ca^{2+} is maintained by synaptic NMDA receptors and other VGCCs (Bredt and Snyder, 1992). Whether this phenomenon also occurs in GABAergic synapses too is less clear. It has been suggested that L- and T-type calcium

channel activated by action potential backpropagation (bAP) may be sufficient to activate nNOS, as L- and T-type calcium channels are present around the GABAergic synapses in dendritic and perisomatic membranes (Magee, 1998). The presence of nNOS on postsynaptic GABAergic synapses at the soma, dendrites and axon initial segment suggests that nNOS is present in many interneuron types, as different domains of pyramidal cell are targeted by different interneurons. Specifically, a co-localisation study showed that nNOS is found in the synapses of PV- and CCK-positive terminals, as well as in CCK-negative terminals (Szabadits et al., 2007). In addition, it was also found that a good portion (> 50%) of non-NGFCs interneurons of the SLM also contain the nNOS mMRA (Price et al., 2005), suggesting nNOS is present in a wide range of interneurons.

After its production, NO may diffuse away from its production site. Since NO is a gaseous molecule that can freely cross membranes. However NO remains detectable only a few microns around its site of production (Namiki et al., 2005), and its deactivation occurs very quickly (Bellamy and Garthwaite, 2001), indicating that NO signalling is local and synapse specific. Although, it has also been reported that NO may be able to travel up to 100 µM (Lourenco et al., 2014). The receptor for NO is the heterodimeric enzyme nitric oxide sensitive soluble guanylyl cyclase (NOsGC), composed of two different subunits: $\alpha_{1\text{-}2}$ and $\beta_{1\text{-}2}$. Studies have demonstrated that α_1, α_2 and β_1 subunits are abundant, whereas β_2 subunits are rarely found (Gibb and Garthwaite, 2001). In addition, knocking out β_1 subunit results in a lethal phenotype (Friebe et al., 2007), indicating that there are only two kinds of functionally important subunit compositions of the NOsGC in the hippocampus: $\alpha_1\beta_1$ and $\alpha_2\beta_1$ complexes. The NOsGC is also found in several interneuron subtypes. Specifically, NOsGC α_1-positive cells have been found to be co-localised with ~68% of all CCK-positive cells, ~74% of all PV-positive cells, ~31% of all SOM-positive cells and ~20% of all nNOS-positive cells (Szabadits et al., 2007). After the activation of NOsGC by NO, cGMP is generated (Garthwaite and Boulton,

1995), and which mediates the main downstream effects of NO. However, studies on the effects of NO signalling have reported mixed results. For example, in subcortical areas, NO can either facilitate (Kraus and Prast, 2002) or depress (Ozaki et al., 2000) GABAergic signals. Since the molecular machinery for NO is present in the majority of hippocampal GABAergic synapses, it is important to study the functional role of NO in hippocampal interneurons.

1.3.6. GABAergic transmission by NGFCs

When GABA is released into the synapse, it diffuses across the synaptic cleft and activates postsynaptic GABA receptors to influence postsynaptic cell excitability. There are two types of GABA receptors, the ionotropic $GABA_A$ receptor and the metabotropic $GABA_B$ receptor. Classically, activation of $GABA_A$ receptors produces fast phasic IPSPs and tonic channel activity, whereas the activation of $GABA_B$ receptors produces slower IPSPs. NGFCs exhibit an unusual “slow” type of $GABA_A$ mediated transmission (Tamas et al, 2003; Price et al 2005) associated with $GABA_{A,slow}$ (Pearce, 1993). As the name suggests, the kinetics of $GABA_{A,slow}$ IPSP (with a decay time constant of 30 - 70ms) is slower than the classical phasic $GABA_A$ inhibition, but it is faster than the metabotropic $GABA_B$ inhibition (Figure 1.3.6.1). This unique response has been found in several brain regions such as the hippocampus (Pearce, 1993; Price et al., 2005), cerebellum (Rossi and Hamann, 1998) and isocortex (Tamas et al., 2003). Consistent with similar observations in the neocortex, it has been shown that NGFCs are the source of $GABA_{A,slow}$ in the hippocampus (Tamas et al., 2003; Price et al., 2005). Because of the slow kinetics, NGFC IPSCs have four times greater charge transfer than IPSCs that are evoked by a fast spiking basket cell (Szabadics et al., 2007).

The mechanisms underlying $GABA_{A,slow}$ has been debated. One possible explanation for the slow kinetics is that GABA vesicles are released asynchronously. Since there are many release sites on NGFCs (dense axons), it is conceivable that GABA would be released multiquantally and asynchronously, thus leading to slower kinetics (Hefft and Jonas, 2005). However, studies have demonstrated that altering the extracellular Ca^{2+} concentration and in turn the release probability, has no significant effects on the kinetics of $GABA_{A,slow}$, suggesting that the presynaptic release of vesicles is not asynchronous (Szabadics et al., 2007; Karayannis et al., 2010).

In contrast, the current data suggest that the slow kinetics most likely results from the unusually prolonged spatiotemporal profile of extracellular GABA that is released from the NGFCs (Capogna and Pearce, 2011). The GABA released by NGFCs is likely to activate the classical α1β2/3γ2 $GABA_A$ receptor, also the high-affinity $GABA_A$ receptors constitutes of the α5 subunit, as well as $GABA_A$ receptors that expresses the δ subunits (Szabadics et al., 2007). The observation that GABA Transporter 1 (GAT1) blockers, such as NO711 (Szabadics et al., 2007) and SKF89976A (Karayannis et al., 2010), significantly prolongs NGFC evoked IPSCs, but has little effect on IPSCs with conventional $GABA_{A,fast}$ kinetics supports the latter hypothesis. These data indicate that NGFC, but not interneurons eliciting fast IPSCs, generates a broad extracellular GABA transient. These results imply that the NGFC-IPSC rise time is not limited by the kinetics of $GABA_A$ receptors, but rather by the time of GABA exposure of the receptors. Secondly, the surprisingly distended NGFC synapses (1-5 μm), as compared to conventional synapses (10 - 20 nm) (Olah et al., 2009), favours voluminous GABA transmission at NGFC synapses unlike fast, conventional GABAergic synapses. This anatomical observation is consistent with the notion that the modulation of GABA uptake markedly prolongs $GABA_{A,slow}$. Thirdly, synapse-specific difference in $GABA_A$ receptor subtypes may also contribute partly to the slow kinetics of $GABA_{A,slow}$. Faster phasic inhibition is mediated by low affinity $GABA_A$ receptors located on postsynaptic sites and slower tonic inhibition is mediated by extrasynaptically located high affinity $GABA_A$ receptors. Since $GABA_{A,slow}$ displays intermediate kinetics, it is possible that it involves both low and high affinity $GABA_A$ receptors. Consistent with this notion, both pharmacological and genetic studies have found that both high and low affinity $GABA_A$ receptors subunits are expressed at connections formed by (Szabadics et al., 2007; Oláh et al., 2009; Zarnowska et al., 2009; Karayannis et al., 2010). Finally, the transient exposure of GABA at NGFC synapses has been demonstrated to be much longer than

observed with classical GABAergic synapses. Experimentally, a competitive antagonist with low affinity for the $GABA_A$ receptor and fast unbinding rate (~ 0.6 ms), significantly increased the rise time of NGFC-IPSCs, but not fast IPSCs (Karayannis et al., 2010). The increase in rise time is because GABA from NGFC synaptic cleft stays longer than the unbinding time of the antagonist. In addition, low affinity $GABA_A$ receptor antagonist has a greater inhibitory effect on NGFC-IPSCs than fast IPSCs.

The unique spatiotemporal profile of GABA released from NGFC by volume transmission allows longer time for GABA to act on target receptors, and this behaviour is likely to contribute to the slow kinetics of $GABA_{A,slow}$. Using computation modelling, it has been proposed that GABA released by NGFCs remain in the cleft over a prolonged period of time before approaching its minimum concentration (8-20 μM) (Karayannis et al., 2010). Normally, GABA released by other interneurons remain in the cleft for <1 ms within a concentration of ~1 mM (Karayannis et al., 2010). Thus, GABA released by NGFCs is able to remain elevated for more prolonged periods than observed in conventional synapses. However, it should be noted that NGFCs also appear to form conventional synapse (10-20 nm wide) (Tamas et al., 2003; Price et al., 2008), in addition to non-conventional synapses that are 1-5 μm away from target dendrites (Olah et al., 2009; Karayannis et al., 2010). How both types of connection (conventional and non-conventional synapses) invariably contribute to synaptic events with slow kinetics is not known. The current understanding on the roles of interneurons in the SLM and in particular, NGFCs, will be summarised in the following chapters.

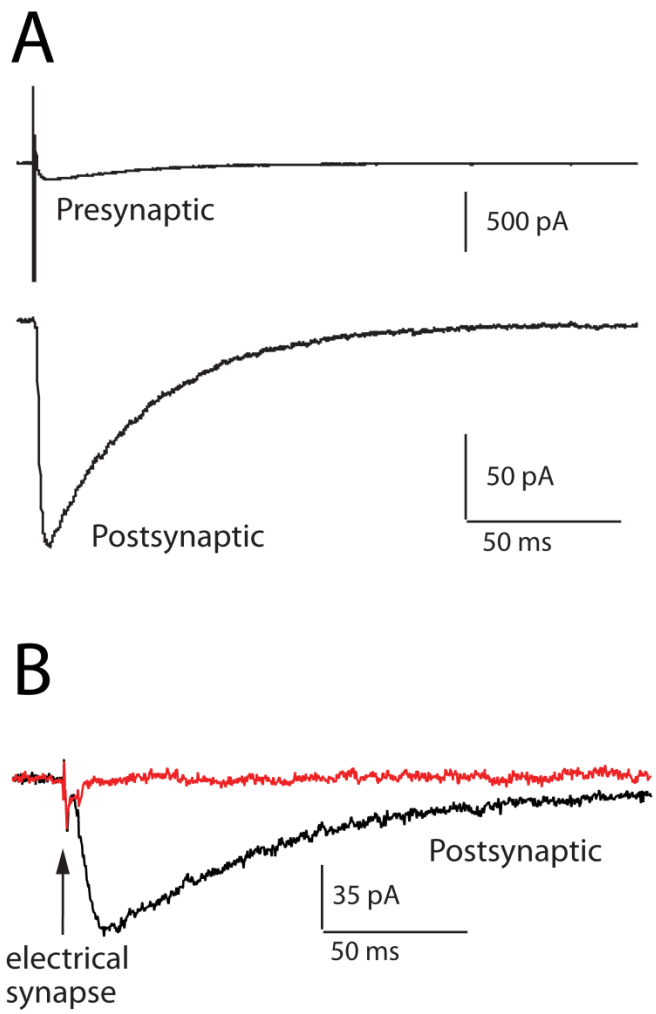

Figure 1.3.6.1 NGFC evokes slow synaptic and autaptic IPSCs in the hippocampus

A. A short square depolarising voltage pulse applied to a presynaptic NGFC elicited a fast initial action current (top trace), which in turn gave rise to a slow IPSC in a postsynaptic NGFC (bottom trace). **B.** Unitary NGFC-IPSCs in control conditions (black) and abolished by the $GABA_A$ receptor antagonist SR95531 (5 μM, red). Note that the presynaptic action is omitted, and the presence of a fast transient inward current (arrow) indicating the presence of an electrical connection.

Figure taken from Karayannis et al., 2010

1.3.7. Functional implications of NGFCs

As mentioned above, the SLM contains several types of interneurons and this heterogeneity is likely to be an indication of their functional diversity. Here I will briefly review physiological functions of interneurons in this region, in particular the NGFCs.

Networks of interneurons are critical in determining the temporal dynamics of neuronal ensembles (Chamberland and Topolnik, 2012). It is thought that interneurons in the SLM contribute to theta oscillation (Buzsáki, 2002; Capogna, 2011). Theta oscillations are observed during REM sleep, arousal, locomotion, and other voluntary behaviour; and they are also involved in memory formation and recall (Buzsáki, 2002). Theta oscillations have been found to be the largest in amplitude and most regular in frequency in the SLM region of the hippocampus (Bragin et al., 1995). *In vivo* recording of theta oscillations in non-anaesthetised rats demonstrated that the temporal delay between population activities in the EC and in the CA1 hippocampus was longer than if the delay was solely from axonal conduction velocities and passive synaptic integration (Mizuseki et al., 2009). In particular, as mentioned above, *in vivo* firing pattern of NGFCs is time-locked to the peak of the theta cycle, and the duration of inhibitory events mediated by NGFCs is approximately 125 ms, which is well adapted to ensure a firing frequency of no more than ~ 8 Hz. In addition, interneurons in the SLM such as NGFCs frequently forms electrical synapses (gap junctions), and It is thought that electrical coupling between interneurons is also critical in generating oscillations (Hestrin and Galarreta, 2005) or creating a low pass filter for incoming inputs (Karayannis et al., 2010)

A recent study has reported that a cluster of excitatory cells, called island cells, locates in layer II of EC (ECIIi) and directly projects to SLM and activates interneurons that target the distal dendrites of CA1 pyramidal neurons. The authors suggest that this circuit is crucial in controlling temporal association memory (Kitamura et al., 2014). As

mentioned previously, stimulation of EC activates SLM interneurons, albeit in an unspecific way. Kitamura et al. used optogenetics to selectively activate two different clusters of EC cells: the island cells, which target interneurons of stratum lacunosum (SL); and cells located in layer III of the medial EC (MECIII), which target interneurons of stratum moleculare (SM) and CA1 pyramidal cells. Island cells were found to target CA1 pyramidal cells, but only weakly, as repetitive photo-stimulation fail to trigger action potentials (Kitamura et al., 2014). The authors found that these island cells suppress the excitatory input from medial EC layer III through feedforward inhibition to control the strength and duration of temporal association. Specifically, inhibition of MECIII input or activation of ECIIi input impairs behavioural freezing in trace fear conditioning (Kitamura et al., 2014).

NGFC fire action potentials differentially phase-locked to various rhythmic activities of the hippocampus *in vivo*, such as theta, gamma or ripple oscillations. Specifically, *in vivo* recordings of CA1 NGFCs under anaesthesia have reported that NGFCs tend to fire close to the peak of the theta cycle and exhibit low frequency discharge rate (2–10 Hz) in the theta frequency range (Figure 1.3.7.1) (Fuentealba et al., 2010), which coincides with inputs from the EC (Buzsáki, 2002). NGFCs are most silent during sharp wave ripples and are phase coupled to local gamma oscillations (Fuentealba et al., 2010). On the contrary, *in vivo* recordings of Ivy cells from anaesthetised rats show a different preference for firing. Ivy cells tend to fire after the trough of the theta cycle (Fuentealba et al., 2008), which coincides with synaptic input from CA3 (Buzsáki, 2002). Similar to NGFCs, Ivy cells are also mostly silent during sharp wave ripples and when phase coupled to local gamma oscillations (Fuentealba et al., 2008). A recent study showed that the firing rate of Ivy cells is constant (~ 2.5 Hz) across all brain states, whereas basket cells change their firing rates during movement, sleep and quiet wakefulness. This result suggests that basket cells coordinate cell assemblies

in a behavioural state dependent manner, whereas Ivy cells are likely to control homeostasis of network excitability (Lapray et al., 2012).

Interestingly, despite tonic firing of NGFCs have been shown to be at theta frequency range in anaesthetised rat, the injection of the same firing pattern *in vitro* produced a type of synaptic depression called the 'mid-term depression' in either autaptic or postsynaptic NGFC-IPSCs (Figure 1.3.7.2) (Karayannis et al., 2010). This mid-term depression has a decay time constant around 0.3 s (the rapid phase) and a recovery time constant around 10 min, which is longer than short-term depression (recovers within seconds) but shorter than long-term depression (which may last indefinitely), and hence termed mid-term depression (Karayannis et al., 2010). This form of synaptic depression was reported to be specific for NGFC synapse, as it is not observed for uIPSCs from pairs of other interneurons of the SLM (~10% depression after the train) (Karayannis et al., 2010). However, it is puzzling why it is required for NGFCs to fire at such a frequency if their synaptic output is silenced for several minutes. Moreover, this mid-term depression that is achieved through injection of the *in vivo* firing pattern does not involve $GABA_B$ receptors, thus acting in contrast to the short-term depression achieved from stimulation at a frequency of 5 Hz described above (Price et al., 2005).

In addition, a slower train of stimulation (0.1 Hz) was also examined in NGFC-IPSCs. It has been suggested that low frequency stimulation help to minimise presynaptic factors that may contribute to depression (Rizzoli and Betz, 2005). Similar to the mid-term depression mentioned above, this protocol also elicited a robust but reversible depression of NGFC-IPSCs, in a $GABA_B$ receptor independent fashion (Karayannis et al., 2010). However, the elevation of ambient GABA in synaptic cleft by blocking the GAT-1 transporter or by applying exogenous GABA significantly enhanced the 0.1 Hz induced depression (Karayannis et al., 2010). By contrast, bath application of a competitive fast-dissociating $GABA_A$ receptor antagonist TPMPA slowed and reduced

this depression. These results suggest that a postsynaptic desensitisation mechanism may be a involved in generating the theta and 0.1 Hz evoked synaptic depression.

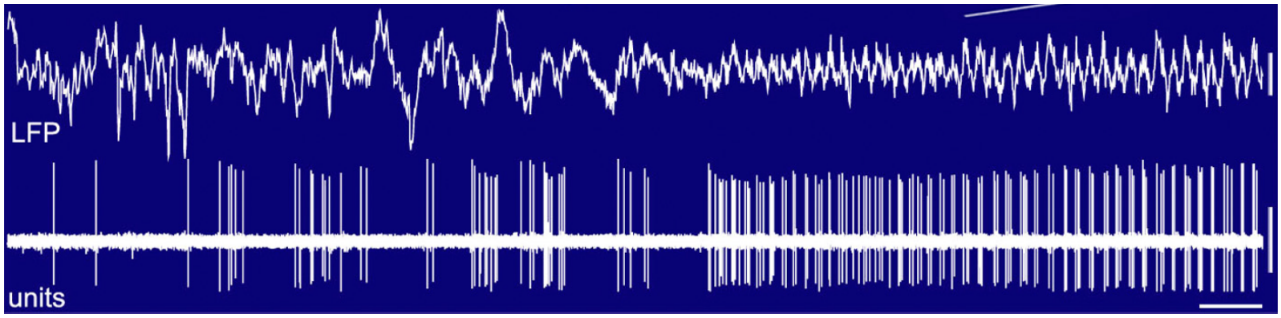

Figure 1.3.7.1 *In vivo* firing pattern of a NGFC

In vivo firing pattern of the cell during the transition from slow-wave oscillations to theta waves. Horizontal bar: 100 ms; vertical bar LFP: 1 mV; vertical bar units: 0.5 mV

Figure taken from Fuentealba et al., 2010

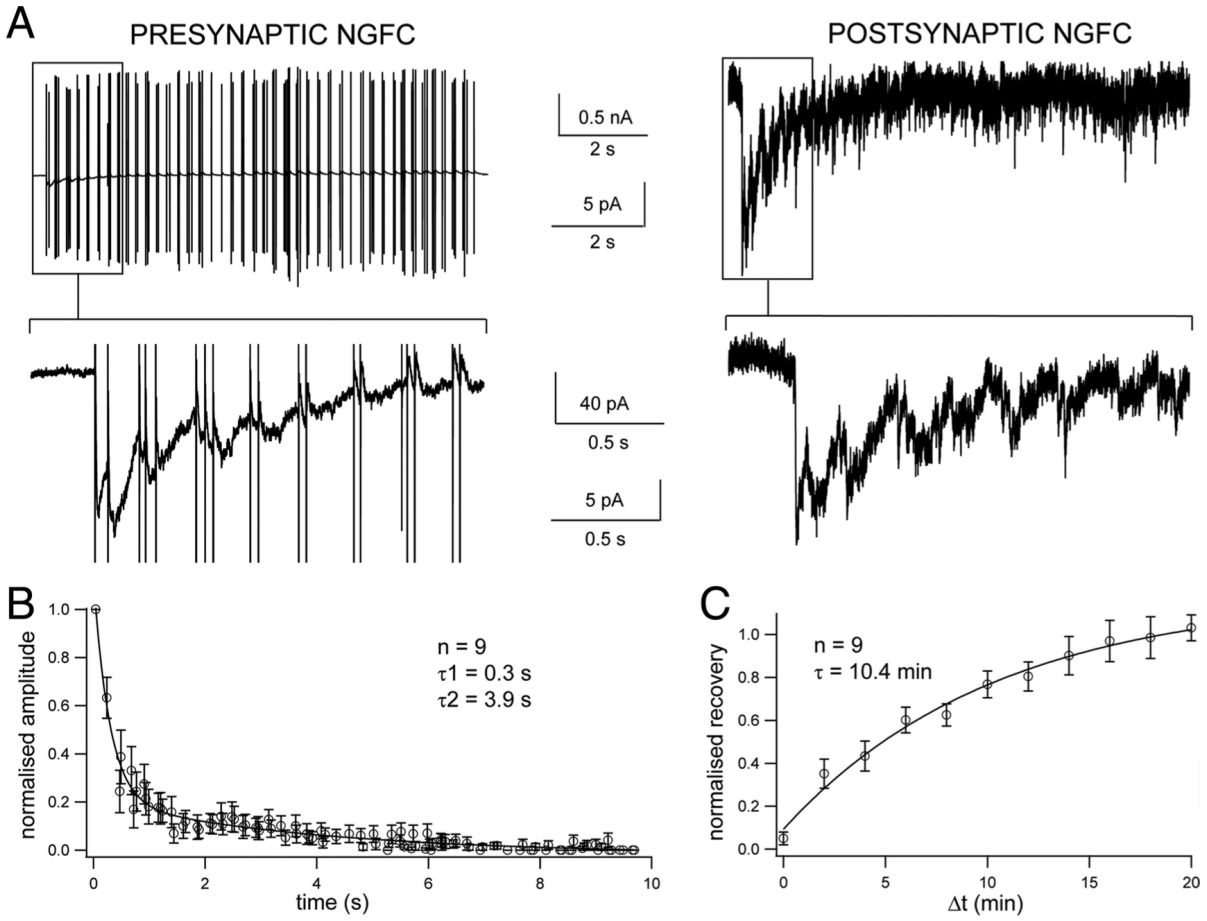

Figure 1.3.7.2 *In vivo* firing of NGFC during theta oscillations elicits mid-term synaptic depression of NGFC-IPSCs when the firing pattern was replayed in NGFCs *in vitro*

A. Responses of presynaptic (left) and postsynaptic (right) NGFC recorded in voltage clamp when the *in vivo* firing pattern was replayed *in vitro*. The presynaptic NGFC displayed autaptic (a)IPSCs (bottom left). Top left trace: the vertical bars represent a depolarising voltage pulses (100 stimuli, 1 ms each) used to evoke action currents that elicited aIPSCs and uIPSCs. The bottom traces show responses at the onset of the train (at expanded current and time scales). **B.** Normalised amplitude of the IPSC for each stimulus in the train (n = 9). The data were best fitted with double exponential function with decay time constants of 0.3 and 3.9 s. **C.** Summary graph showing normalised recovery from depression, with decay time constant 10.4 min.

Figure taken from Karayannis et al., 2010

1.4. Short-term synaptic plasticity

Synapses allow information to flow between neurons. However, synapses are more than just a medium to transmit information, they are equipped with numerous molecular machineries on either side of the synapse that can undergo activity dependent change. This process allows synapses to exhibit memory following activation, a phenomenon known as synaptic plasticity. In this way, synapses play a more active role in information processing.

Synaptic plasticity can be grouped into two major categories: 1) long-term plasticity, with timescale of hours to days or even longer, is thought to be key for learning and memory (Morris, 2003); 2) short-term plasticity, which is the main focus of this thesis, occurs over a much shorter timescale, ranging from milliseconds to minutes (Zucker and Regehr, 2002) and allows synapses to contribute to neuronal computation. These short-term changes in synaptic strength provide mechanisms for transient information storage, as well as for establishing neuronal networks that ultimately define longer-term changes in plasticity and brain oscillations associated with different brain functions. There are several forms of short-term synaptic plasticity that are part of the neuronal computation toolkit. For example, presynaptically, an increase in the number of vesicles of the presynaptic cell can leads to facilitation. On the other hand, postsynaptic receptors could be desensitised following a period of prolonged exposure to neurotransmitters, decreasing the ability of the postsynaptic cell to respond to presynaptic input and thus leading to depression. Often, the same synapse can subject to both facilitation and depression. Here I will review the function and mechanisms of various flavours of short-term synaptic depression with a focus on GABAergic synapses.

1.4.1. Short-term facilitation

Periods of elevated presynaptic activity can cause both increase or decrease in neurotransmitter release (Zucker and Regehr, 2002). Both facilitation and depression can occur at synapses and their relative weight depending on the initial level of release probability of neurotransmitters: facilitation reflects an increase in release probability and depression reflects a decrease in release probability, however a high initial level of release probability tends to generate depression and low initial level of release probability tends to induce facilitation following periods of sustained neuronal activity.

1.4.2. Short-term depression

In contrast to short-term facilitation, periods of elevated activity can also lead to a decrease in synaptic strength. There are many mechanisms associated with short-term depression. The most common mechanisms involves a presynaptic decrease in the release of neurotransmitters, that is likely to be a result from depletion of readily releasable pool of vesicles. Other mechanisms also exist; for example, postsynaptic properties such as desensitisation of ligand-gated receptors can reduce the responsiveness of target neurons to neurotransmitters. In addition, the release of neuromodulators from presynaptic cells, postsynaptic cells, or neighbouring cells may modulate synaptic strength as well.

1.4.3. Depletion models

Many synapses in the brain, such as the NGFC synapses mentioned above, are use-dependent. Higher levels of activity would gradually deplete the readily releasable pool of vesicles. Electron microscopy studies revealed that synapses usually contain hundreds of vesicles close to the release sites, but only a small set of these vesicles are in contact with the membrane. These vesicles constitute the readily releasable pool, and vesicles located further away that are unable to respond quickly are referred to as the reserve pool (Schneggenburger et al., 2002). In addition, the readily releasable pool also contains a set of docked vesicles (immediately releasable pool), one or a few docked and primed vesicles (ready to be released) and readily releasable vesicles. The concept of pools of vesicles in different compartment and accessibility suggests a plausible mechanism for synaptic depression (Zucker and Regehr, 2002) (Figure 1.4.3.1).

Repeated stimulation would result in the depletion of readily releasable pool, which in turn would lead to a decrease in the number of vesicles that could be released by presynaptic action potential. According to the depletion model, the magnitude of short-term depression is closely related to the number of vesicles in the reserve and readily releasable pools, as well as the transition rates between them. This is because the number of vesicles released by an action potential depends on the size of the readily releasable pool of vesicles, and the probability of release of the pool. If an action potential releases a large fraction of the readily releasable pool, subsequent action potential evoked before replenishment of the readily releasable pool would therefore release fewer vesicles (Zucker and Regehr, 2002). This model also suggest that the magnitude of depression will be larger if the initial release probability and frequency of presynaptic firing are higher, due to larger depletion of the ready-release pool. Indeed, several experiments have confirmed this phenomenon at different synapses such as

corticothalamic synapses and synapses in the auditory brainstem (Schneggenburger et al., 2002; Zucker and Regehr, 2002; Wang and Manis, 2008).

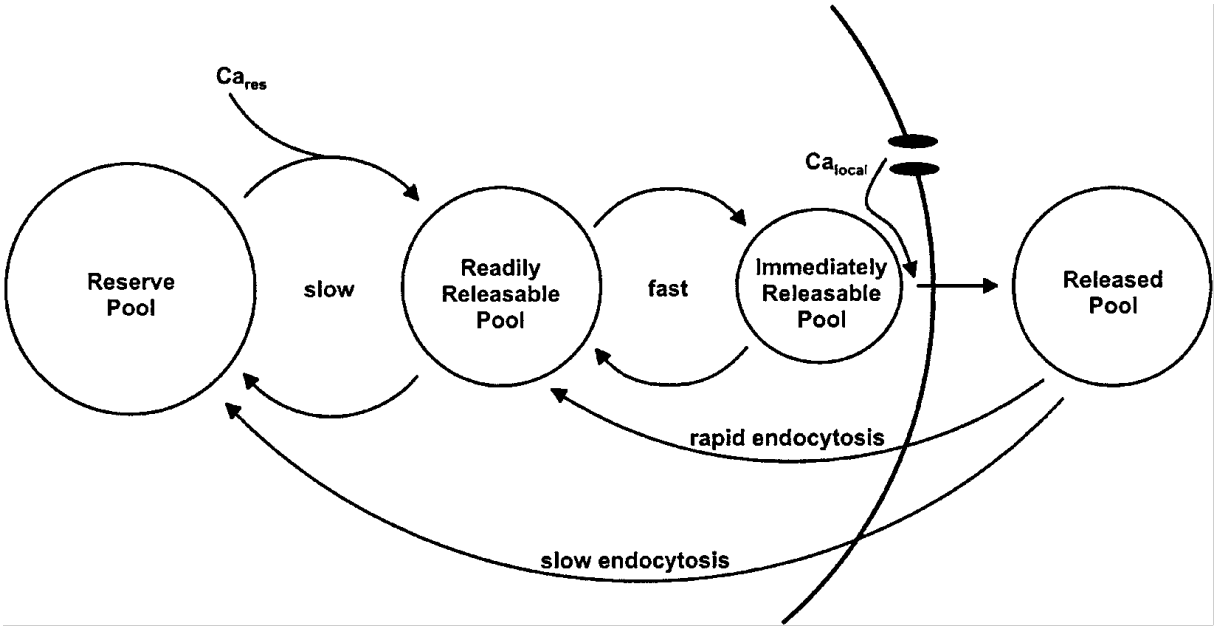

Figure 1.4.3.1 Scheme showing anatomy of an active zone

Each active zone contains contains one, or at most a few vesicles attached to release sites, these are docked and primed at the plasma membrane, readily releasable upon increase in local Ca^{2+} concentration from opening of VGCCs by action potential. These vesicles are rapidly replaced by other docked vesicles in a readily releasable pool. The majority of vesicles are stored in a large reserve cluster further away from the plasma membrane. The reserve pool can be used to refill the readily releasable pool after it is depleted in depression by a Ca^{2+} dependent process. Released vesicles are recovered by fast and slow endocytic processes into readily releasable and reserve pools.

Figure taken from Zucker and Regehr, 2002

1.4.5. Inactivation of release sites

In addition to the depletion model, fusion of a vesicle at a release site can inhibit subsequent fusion events at the same site, even if the readily releasable pool has been not been depleted (Neher and Sakaba, 2008). The mechanism behind this observation is thought to be a result of incorporation of vesicular membrane proteins during exocytosis. It takes time for the incorporated vesicular membrane proteins to be cleared away from the release sites by diffusion, in order to allow subsequent fusion of vesicles (Neher and Sakaba, 2008). Interestingly, in addition to diffusion, the speed at which active sites to recover from inactivation is also dependent on endocytosis. Study concerning the glutamergic synapse at the calyx of Held has shown that the presynaptic blockade of endocytosis reduces the recruitment of readily releasable vesicles and leads to increased depression during trains, suggesting endocytosis works as a mechanism to clear vesicular membrane proteins (Hosoi et al., 2009).

1.4.6. Desensitisation of postsynaptic receptors

Ligand-gated channels can exhibit a short period of inactivity following exposure to a ligand (known as the desensitised state), which can last from tens of milliseconds to minutes. In the case of $GABA_A$ receptors, a varying degree of desensitisation exists following repetitive simulation, and this may be influenced by subunit composition. For example, $GABA_A$ receptors with of the δ subunit show less desensitisation than $GABA_A$ receptors with the γ subunit (Bianchi and Macdonald, 2002). The subtypes of α subunit may also contribute to the rate and extent of receptor desensitisation. For example, receptors with α1βγ composition desensitises more rapidly than receptors expressing the α5 or α6 subunit (Caraiscos et al., 2004).

1.4.7. Presynaptic autoreceptors

The presynaptic release of neurotransmitters may also target receptors located on the presynaptic terminals, and thus regulating subsequent transmitter release. This has been demonstrated in the case of NGFCs, where stimulation at 5 Hz could elicit profound short-term depression in NGFCs (Price et al., 2005, 2008). This short-term depression can be significantly reduced by the application of a $GABA_B$ receptor antagonist CGP55845, and is likely to originate presynaptically since the effect of the $GABA_B$ receptor antagonist persisted when the postsynaptic cell was recorded with a patch pipette containing caesium (to block G-protein mediated signalling) (Price et al., 2005). This supports the idea that presynaptic $GABA_B$ autoreceptors is involved in the short-term depression in NGFCs seen with theta stimulation.

1.4.8. Endocannabinoid and depolarisation-induced suppression of inhibition

Presynaptic neurotransmitter release can be controlled by retrograde signalling mechanism. The endocannabinoid (eCB) dependent depolarisation-induced suppression of inhibition (DSI) is one of the most well-known and best characterised retrograde signalling systems (Alger et al., 1996; Kreitzer and Regehr, 2001; Wilson et al., 2001; Freund et al., 2003). Experimentally, if the postsynaptic cell is depolarised to 0 mV for a few seconds, there is a transient decrease in the inhibitory input onto the postsynaptic cell which was depolarised (Figure 1.4.8.1). This phenomenon was initially reported in the cerebellum, then in the hippocampus and in other brain areas (Freund et al., 2003). The locus of the effect appears to be presynaptic. This view is supported by experimental evidence showing that no decrease in miniature (m)IPSC amplitude is observed after

DSI. Furthermore, changes in postsynaptic $GABA_A$ receptor sensitivity have been excluded since the response to intophoretically-applied GABA does not change before and during DSI. Instead, the frequency of mIPSC is reduced; suggesting that this phenomenon involves presynaptic mechanisms (Alger et al., 1996). In addition, it was observed that DSI is reduced by 4-aminopyridine (4-AP) and veratridine, both acting on the presynaptic terminal (Alger et al., 1996). This effect is likely to be mediated by a G-protein coupled receptor since DSI was reported to be pertussis toxin sensitive in the hippocampus (Alger et al., 1996). Moreover, using minimal stimulation, DSI was found to increase the failure rate and affects different components of the IPSC (Alger et al., 1996). Thus, the evidence available indicates that DSI is due to a decrease in the presynaptic release of GABA.

The quest to identify the molecule responsible for DSI triggered intense investigation. The slow onset (~2–3 s to maximal effect), the requirement of persisting Ca^{2+} rise, and experiments data obtained using Ca^{2+} buffers indicate that DSI is carried by a hormone or peptide rather than classical vesicular neurotransmitter. In fact, Llano et al. hypothesised the involvement of retrograde signalling messenger 10 years before the discovery that eCB was responsible for DSI: "Ca^{2+} rise in the Purkinje cell leads to the production of a lipid-soluble second messenger" (Llano et al., 1991). Interestingly, the fast buffer BAPTA and the slow buffer EGTA both reduce DSI to a similar degree, suggesting that the site of Ca^{2+} entry (e.g. from voltage-dependent calcium channels) and the site of the action of Ca^{2+} are relatively far from each other (Lenz and Alger, 1999).

In the year of 2001, the discovery by Wilson and Nicoll, Ohno-Shosaku, and Kreitzer and Regehr ended a decade of long search for the molecule that is responsible for DSI (Kreitzer and Regehr, 2001; Ohno-Shosaku et al., 2001; Wilson and Nicoll, 2001). It was found that DSI is mediated by retrograde signalling via eCBs. Both receptor

localisation study and identification of the physiological actions of eCBs on synaptic transmission confirmed that eCBs act on presynaptic terminals, reducing transmitter release. During postsynaptic cell depolarisation, a rise in calcium level triggers eCB synthesis and release into the extracellular space. The eCBs then travels retrogradely to presynaptic terminals where CB1 receptors are located. The action of CB1 receptors then reduces neurotransmitter release. The level of calcium necessary for eCB production and release is thought to be in the micromolar range. For example, the concentration of calcium of 4 μM is required to induce a half-maximal effect in CA1 pyramidal cells of the hippocampus (Wang and Zucker, 2001), and higher (> 10 uM) in cerebellar Purkinje cells (Maejima et al., 2005).

The eCB system turns out to be very important in the CNS. First, the major type of eCB receptors, the CB1R, is expressed predominantly on axon terminals. Second, the pattern of eCB distribution is rather similar across species, indicating a conserved physiological function. Third, the density of cannabinoid receptors in the brain is comparable to the levels of glutamate, GABA, or striatal dopamine receptors (Herkenham et al. 1990), indicating its importance. Unlike traditional neurotransmitters, eCBs are not packaged and stored in vesicles before release. The eCBs are hydrophobic fatty acids that are produced on demand and released immediately upon synthesis (Piomelli, 2003). In addition to depolarisation of neurons and subsequent rise in calcium level, eCB production can also be induced by activation of metabotropic (m)GluR-1s and electrical stimulation. To summarise, according to the currently accepted model, depolarisation of the postsynaptic cell is thought to lead to the release of eCB, which activates presynaptic CB1Rs, which, in turn, suppresses GABA release from axon terminals to elicit DSI (Kreitzer and Regehr, 2001; Ohno-Shosaku et al., 2001; Wilson and Nicoll, 2001).

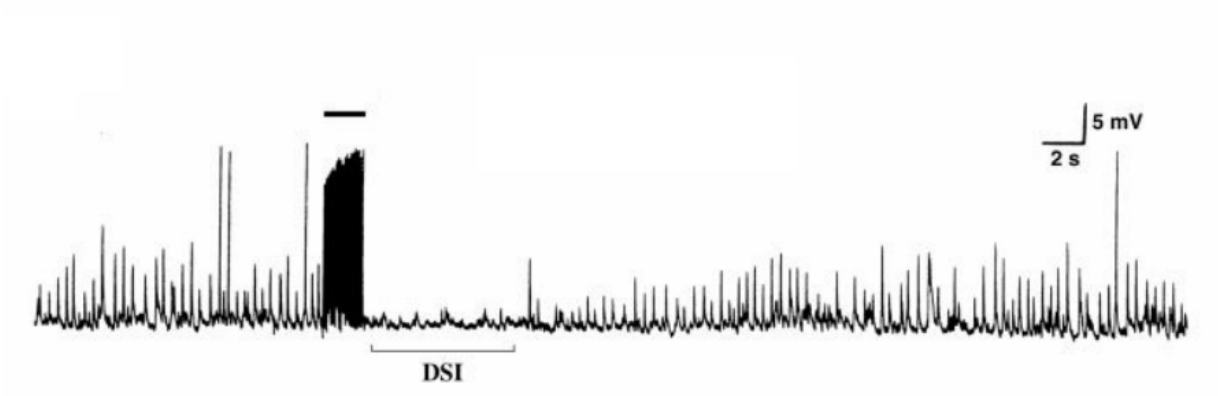

Figure 1.4.8.1 Example of Depolarisation Induced Suppression of Inhibition (DSI)

Intracellular recording from CA1 pyramidal cells (in the presence of ionotropic glutamate receptor antagonists) shows spontaneous inhibitory postsynaptic potential (depolarising) from activity of GABAergic interneurons. Following a brief train of postsynaptic action potentials (thick horizontal bar), spontaneous events are transiently suppressed (thin bracket labelled DSI).

Figure taken from Pitler and Alger, 1992

1.4.9. Nitric oxide as a retrograde signalling molecule

Numerous studies suggest a role for NO as a retrograde messenger. One example is represented by a NO-dependent LTP of inhibitory synapse (LTP-GABA) onto dopaminergic neurons in the ventral segmental area (VTA) (Nugent et al., 2007). This LTP-GABA has been found to be expressed presynaptically (as indicated from paired-pulse ratio), and blocked by the calcium chelator BAPTA. In addition, application of extracellular NO scavengers blocks LTP-GABA and application of NO donors trigger LTP-GABA. These results indicate the retrograde nature of NO signalling acting at this inhibitory synaptic site. Furthermore, NO signalling has been shown to be important for various behaviours, such as learning and memory. For example NO is involved in several forms of synaptic plasticity, including LTP and LTD (Garthwaite and Boulton, 1995; Edwards and Rickard, 2007); as well as sensory and motor function, such as the rhythmic swimming pattern associated with feeding (Moroz et al., 2004).

Interestingly, a study has reported that CB1-dependent DSI of cholinergically enhanced spontaneous IPSCs (sIPSCs) is blocked by inhibitors of NOS or nitric oxide sensitive guanylyl cyclase (NOsGC, the NO receptor), as well as by NO scavengers (Makara et al., 2007). Based on these results, NO and eCBs may cooperate under some circumstances to modulate GABA release from CCK basket terminals (Makara et al., 2007), whereas in PV cells which doest not contain CB1R, NO might able to function in a similar way as eCBs (Szabadits et al., 2007).

1.5. Functional roles of retrograde signalling systems

As described previously, different interneuron networks use various communication methods such as feedback, feedfoward and recurrent connections to achieve their function. How are the strengths of synapses controlled? Many neurons use retrograde signalling to control the strength of the synapses they receive. As the name suggests, when these signalling molecules are released, they act in a retrograde manner to regulate neurotransmitter release from presynaptic terminals. Typically, dedicated molecular machineries are devoted to synthesise and release the retrograde messenger located in the postsynaptic neuron. These molecular machineries are activated when the postsynaptic cell is active, for example, via depolarisation. In this way, retrograde signalling molecules are synthesised on demand. When this happens, the retrograde signalling molecule travels to presynaptic boutons by diffusion, and activates target cells to alter some aspect of synaptic transmission upon binding to appropriate receptors.

The molecular machinery possessed by various neuron types adds a degree of cell type specificity to retrograde signalling. For example, an important feature for CCK-expressing basket cells is that they express CB1Rs on their axon terminals, and CB1Rs are thought to exhibit high co-localisation with CCK (Katona et al., 1999). However, CCK (hence CB1R) are not found on PV cells or Ivy cells (Somogyi et al., 2012), and rarely found in interneurons of SLM (Price et al., 2005). Here I will review the functional relevance of the DSI system as an example of retrograde signalling mechanisms.

1.5.1. Functional roles of DSI

What are the functional roles of DSI? Study of the eCB system provided some insights. Administration of cannabinoid agonists such as delta-THC and HU210 impairs learning in the Morris water maze test (Ferrari et al., 1999; Varvel et al., 2001). In humans, marijuana (a source of cannabis) use can cause distorted perceptions, impaired coordination, and difficulty with problem solving. In addition, long-term or chronic use of this drug results in an adverse impact on learning and memory that can last days after withdrawing marijuana (Pope et al., 2001). However, the picture is not as straightforward. Pharmacological blockade of CB1R or using CB1R knock-out mice also impaired learning tasks such as reversal tasks (Varvel and Lichtman, 2002).

In the hippocampus, it is puzzling that CCK cells express CB1 receptors and are subjected to suppression of inhibition, whereas PV cells, that also target the soma of CA1 pyramidal cells, are not regulated by this process. Interestingly, evidence indicates that principal cells of the brain, such as granule cells in the DG, pyramidal cells in CA3 and CA1 hippocampus, pyramidal cells in layer II-III and V-VI of the neocortex are able to synthesise and release eCBs and thereby regulate incoming inhibition from cells that express CB1 receptors. On a system level, it has been proposed that eCB-mediated down-regulation of inhibition from the CCK GABAergic basket cells in hippocampus may enable CA1 pyramidal cells to dissociate their activity in time from the synchronous inhibitory activity during theta rhythm, and thus allow processing of specific information such as place field signals (O'Keefe and Recce, 1993; Freund and Katona, 2007). Indeed, retrograde signalling via eCB is well suited for this role. Depolarisation of pyramidal cells releases eCB which reduces the inhibitory input from interneurons, and in turn may temporally increase pyramidal cells firing.

Data obtained with *in vivo* recordings from the hippocampus have considerably

advanced the understanding of why the activity of a subset of interneurons, i.e. CCK cells, is suppressed. Evidence have showed that the large diversity of interneurons provide the components for shaping distinct network activities, in which interneuron subtypes with specific patterns of connectivity onto pyramidal cells exhibited distinct, phase-related firing patterns with respect on oscillations recorded from the extracellular field activity (Klausberger and Somogyi, 2008). In particular, CCK and PV basket cells were shown to fire differentially during neuronal oscillations (Klausberger et al., 2005), despite both CCK and PV cells target the same domain on pyramidal cells. Specifically, during theta oscillations, CCK cells fire at a phase when CA1 pyramidal cells start firing as the rat enters a spatial location - the place field of the cell; during gamma oscillation, CCK cells fire just before CA1 pyramidal cells. Because active pyramidal cells can release eCBs, which retrogradely activates CB1 receptors located on axonal terminals of CCK cells, this enables CA1 pyramidal cells to selectively reduce perisomatic inhibition from CCK expressing cells (DSI). The presence of these CB1 receptors helps to increase the contrast of pyramidal cells firing: the strongly active pyramidal cells receives less inhibition (via DSI), and weakly active or inactive pyramidal cells do not release eCBs and thus they are still inhibited by CCK interneurons. Thus DSI can be a way to support the implementation of sparse coding in cell ensembles, as DSI may able to increase the contrast of strongly active cells.

The cell type specific expression of CB1R also contributes to eCB function. By targeting only specific interneurons such as CCK basket cells, DSI effectively modulates only a specific subset of interneurons, and leaves others unaffected, such as PV and interneurons of the SLM. In addition, DSI is transient and local, as eCB travels to presynaptic terminals by diffusion. These features suggest that eCB might be able to selectively modulate gamma oscillations while preserving theta oscillations, and in turn altering the temporal output of the hippocampus.

1.6. Aim

The hippocampal GABAergic neuron type known as NGFC forms extensive networks with the same type as well as with other types of interneurons in the SLM region, but its role on the hippocampal circuitry is less well-known. The goal of this Thesis is to advance our understanding of the functional roles of NGFCs and connections they make. I will address the following questions:

1.6.1 What is the function of nNOS expressed by NGFCs?

GABAergic interneurons display a range of interesting molecular profiles, and the expression of enzymes and proteins is used as a method to distinguish neuron types. Despite we know many of the molecular profiles of different interneurons, the physiological role of interneuron markers is less understood. In particular, nNOS are very abundant in the hippocampus. The nNOS-expressing neurons comprise some CA1 pyramidal neurons and several types of interneurons including: NGFCs (Price et al., 2005), ivy cells (Fuentealba et al., 2008), interneuron-specific interneurons co-expressing the vasoactive intestinal peptide and calretinin, a subset of PV-expressing interneurons of the dentate gyrus, a subset of somatostatin-expressing interneurons, and projection cells with the soma close to the subiculum (Tricoire and Vitalis, 2012). In pyramidal cells, a previous study has suggested that NO plays a similar role as eCB and represent a retrograde signal that mediates DSI (Makara et al., 2007). However, the functional role of NO in nNOS-expressing hippocampal interneurons is not known. The presence of NOsGC in interneurons other than CCK-positive cells suggests NO may modulate GABAergic transmission. Interestingly, nNOS and CB1 have been reported to show no co-localisation (Szabadics et al., 2007). Therefore, one important aim was to

investigate the role of NO in NGFCs and other interneurons of the SLM.

1.6.2 What are the roles of NGFC tonic firing when the synaptic transmission is almost silenced?

In vivo recording in anaesthetised rats have shown that NGFCs exhibit theta frequency firing pattern, as shown in Figure 1.3.7.1 (Fuentealba et al., 2010). Interestingly, the output of NGFCs *in vitro* experiences a strong short-term depression when simulated at this frequency (Figure 1.3.7.2) (Karayannis et al., 2010). This raises the question that why NGFCs continue to fire at this frequency despite its synaptic transmission being almost silenced. One explanation could be that NGFCs fire at the theta frequency to silence themselves. However, there could be other explanations too. For example, NGFCs are known to express functional markers such as nNOS (Price et al., 2005) and insulin (Molnar et al., 2014). In particular, nNOS is a well-known neuronal marker for NGFCs and it is expressed in the axons, soma and dendrites of hippocampal interneurons (Szabadits et al., 2007). Therefore, the firing of NGFCs may be able to release other compounds such as NO in addition to GABA, in analogy to what has been recently demonstrate for insulin (Molnar et al., 2014). I plan to utilise the same *in vivo* firing pattern of NGFCs recorded in anaesthetised rats (Fuentealba et al., 2010) to explore this possibility.

NO has been demonstrated to function in retrograde signalling and has been implicated in the generation of LTP (Garthwaite, 2008). Hence, it will be interesting to see whether the *in vivo* firing patterns contribute to NO production. This is an important question because retrograde signalling is important for information processing in neuronal networks. By altering the neurotransmitter release of a presynaptic neuron,

retrograde signalling act to shape network activity in a use-dependent manner, which is essential to brain functions. A well-studied example is the DSI phenomenon which was elucidated by the eCB system. However, the expression of CB1 receptors is cell type specific and they are not found in many interneuron types. Therefore, a further aim of this project is to study retrograde signalling in cells that are thought to be eCB insensitive, such as interneurons of the SLM.

2. MATERIALS AND METHODS

2.1. Slice preparation

All procedures involving animals were performed using methods approved by the United Kingdom Home Office and according to The Animals (Scientific Procedures) Act (1986). Juvenile male and female rats (P15 – P22) or neuronal nitric oxide synthase (nNOS)-Cre-tdTomato male and female mice (P29 – P40) were anaesthetised with isoflurane and decapitated. The brain was carefully removed and mounted on the plate of a vibratome (Microm HM 650 V, Thermo Fisher Scientific Inc., Germany) in ice-cold ACSF containing (in millimolar, mM): 85 NaCl, 25 $NaHCO_3$, 2.5 KCl, 1.25 NaH_2PO_4, 0.5 $CaCl_2$, 7 $MgCl_2$, 10 glucose, 75 sucrose saturated with 95% O_2 and 5% CO_2, at pH ~7.3. Horizontal sections (thickness: 325 µm) consisting of the dorsal hippocampus and attached entorhinal cortex were prepared using a vibratome. During the initial period of slice storage (~20 min), the cutting solution was replaced with normal ACSF (containing in mM: 130 NaCl, 24 NaHCO3, 3.5 KCl, 1.25 NaH2PO4, 2.5 CaCl2, 1.5 MgSO4, 10 glucose saturated with 95% O2, 5% CO2, at pH 7.3). Slices were then maintained at room temperature (18-22˚C).

Acute slices were then placed in a recording chamber mounted on the stage of an upright microscope (Olympus BX 51WI or Axioscope, Zeiss) equipped with immersion differential interference contrast objectives (40x, 60x) coupled to an infrared camera system (Hamamatsu, Hamamatsu City, Japan), superfused at a rate of ~2 ml/min with oxygenated recording ACSF and maintained at a temperature of 33±1 ºC. Unless otherwise mentioned, experiment results are obtained from juvenile male or female rat.

2.2. Electrophysiology

2.2.1. Electrophysiology data acquisition

Whole-cell recordings were performed using EPC10/3 or EPC9/2 amplifiers (HEKA, Lambrecht, Germany). Rat interneurons with the soma in the SLM were identified based on soma shape, size and location under infra-red video microscopy. Mouse interneurons with the soma in the SLM expressing tdTomato under fluorescence illumination were also selectively recorded. Borosilicate patch pipettes were pulled (Zeitz puller – DMZ, Martinsried, Germany), and filled with a medium-high chloride internal solution except in dynamic clamp experiments. A medium-high chloride internal solution was used in order to increase the driving force for Cl^- ions (ECl^- = -11 mV) to the extent that the IPSC polarity was inward at the holding potential (Vh) of -65 mV. The medium-high chloride internal solution consisting of, in mM: 88 KCl, 42 K-gluconate, 10 HEPES, 10 Na_2Phosphocreatine, 4 Mg-ATP, 0.3 Na-GTP, pH 7.3 with KOH, osmolarity was 280-290 mOsmol. In dynamic clamp experiments performed in current clamp mode, a low chloride internal solution was used, which contained, in mM: 126 K-gluconate, 10 HEPES, 10 Na_2Phosphocreatine, 4 KCl, 4 Mg-ATP, 0.3 Na-GTP, pH 7.3 with KOH, the osmolarity was 270-280 mOsmol. Biocytin was added to the intracellular solutions before recording at a final concentration of 2-4 mg/ml. Pipettes had resistances of 5-6 MΩ when filled with internal solutions. Access resistance was always monitored to ensure the stability of recording conditions. Cells were only accepted for analysis if the initial series resistance was less than or equal to 20 MΩ and did not change by more than 20% throughout the recording period. No correction was made for the junction potential between the pipette and the ACSF, and therefore the recorded membrane potential, as calculated post-hoc using a junction potential calculator, was 16 mV and 11 mV more depolarised than the true membrane potential, for K-gluconate and high-Cl^- intracellular

solution, respectively.

Action currents or potentials were elicited in a presynaptic cell by using a short depolarising voltage step (from the holding potential of -68 mV to 0 ms, 3 ms) or a short depolarising current step (500-1000 pA x 3 ms, from –68 mV). The corresponding unitary inhibitory postsynaptic current (uIPSC) or unitary inhibitory postsynaptic potential (uIPSP) was recorded in a synaptically-coupled postsynaptic neuron or in the presynaptic neuron as an autaptic IPSC (aIPSC). Postsynaptic and autaptic currents were filtered at 3 kHz and recorded with a sampling rate of 5 kHz. Spontaneous inhibitory postsynaptic currents (sIPSCs) were also recorded at Vh = -65 mV filtered at 3 kHz with a sampling rate of 10 kHz for 120 s.

The *in vivo* firing sequence was recorded in an identified NGFC in an anesthetised rat with the juxtacellular/extracellular method during theta oscillations and previously published (Fuentealba et al., 2010). This firing sequence lasting 60 s was transformed as current steps (500-1000 pA, 1 ms each) using MATLAB (The MathWorks Inc., Natick, MA, USA) software, and injected as stimulus protocol to induce FSI into whole cell patch clamped cells in current clamp configuration using PatchMaster (HEKA) software (Figure 2.2.1.1). The stimuli evoked a train of action potentials *in vitro* that exactly matched the sequence of action potentials detected *in vivo*. A recorded pair was classified as having FSI if the uIPSC or uIPSP evoked 125 to 250 ms after the end of the stimulation protocol applied to the postsynaptic cell was decreased > 5% followed by full recovery of the peak amplitude of the response. In the majority of the cases the stimulation protocol was repeated several times (typically three times) for each experiment followed by at least two stimulations with recovery.

Synthetic (dynamic clamp) EPSPs (dEPSPs) were applied through the patch pipette using a synaptic module (SM-1) conductance injection amplifier (Cambridge

Conductance, Cambridge, UK). The dynamic conductance waveform for an EPSP was based on the magnitude, kinetics and reversal potential of the EPSC experimentally evoked by minimal stimulation in the same cell in voltage clamp prior to the dynamic clamp experiment (dEPSP peak conductance = 0.5 - 2 nS, 20 - 80% rise time = 0.6 – 0.7 ms, decay τ = 3 – 4 ms, reversal potential set at 0 mV). dEPSP data was analysed with scripts written in MATLAB. Ten dEPSPs were applied at 80 Hz and the peak amplitude of each dEPSP was calculated from its baseline before, during and after FSI. To obtain dEPSPs, minimal extracellular stimulation was conducted by applying rectangular pulses of current (0.4 ms width, intensity range: 10-15 μA) delivered through an isolation unit (A360 Stimulus Isolator, World Precision Instruments, Stevenage, UK) to a monopolar patch pipette filled with ACSF placed closed to the recorded cell (5 μM gabazine and 50 μM CGP35348 added to extracellular ACSF).

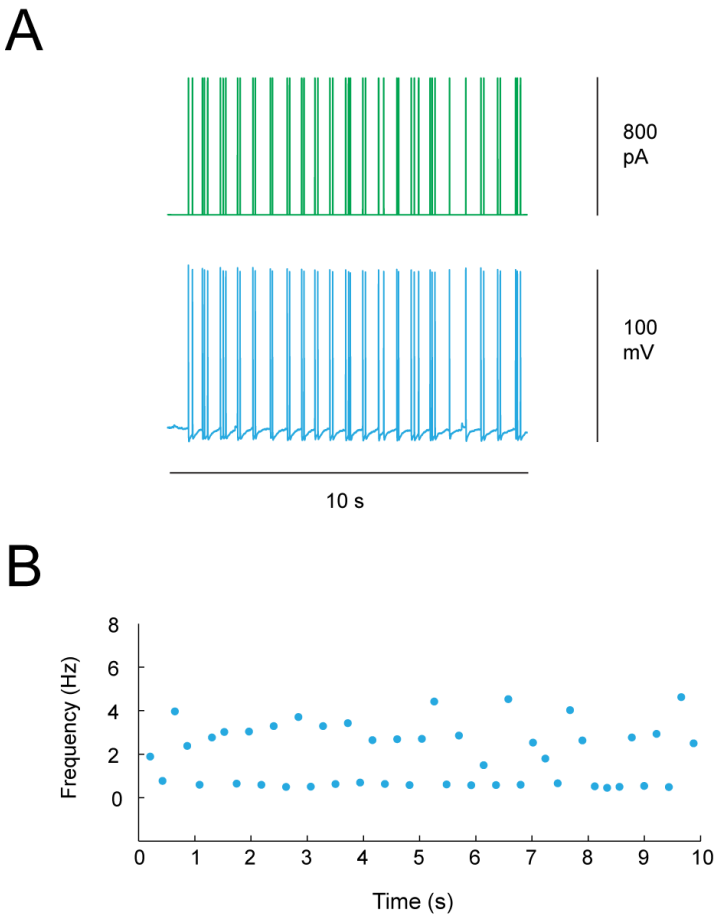

Figure 2.2.1.1 Example of the *in vivo* firing protocol used

A. Green trace, the first 10 s of current steps resembling the *in vivo* firing pattern (60 s) injected into the recorded cell *in vitro*. Blue trace, the membrane potential of the recorded cell in response to the current step injection. **B.** The instantaneous frequency graph of the firing pattern shown in A.

2.2.2 Electrophysiology data analysis

Electrophysiological data were analysed offline using custom made MATLAB software. All raw traces were smoothed before analysis to reduce noise. For FSI analysis, FSI amplitude was measured as: $1-\frac{IPSC(P)_{FSI}}{IPSC(P)_{baseline}}$, where $IPSC(P)_{FSI}$ is the amplitude of IPSC(P) 125 or 250 ms after the stimulus protocol, and $IPSC(P)_{baseline}$ is the average amplitude of three IPSC(P)s acquired before the stimulus protocol. For kinetics analysis, the 20% - 80% rise time and decay time constant (τ_{syn}) were calculated by fitting a single exponential for each trace. An example of electrophysiology data analysis is shown in Figure 2.2.2.1 The decay of the uIPSCs could also be fitted with a double exponential, and the weighted decay time constant was calculated using the following formula: $\tau_w = \tau_1 A_1 + \tau_2(1- A_1)$, where τ_w is the weighted decay time constant, τ_1 and τ_2 are the time constants of the first and second exponential functions, respectively, and A_1 is the proportion of the peak amplitude of the averaged uIPSC that is contributed by τ_1. For passive and active electrophysiological property analysis: the input resistance (R_{in}) was calculated as the inverse of the gradient of the linear fit from an I/V plot of the recorded cell (current injected against steady state voltage response); membrane time constant (τ_{mem}) was calculated by fitting a single exponential; membrane capacitance was calculated as τ_{mem}/R_{in}; the sag rectification ratio was calculated from the membrane potential at the end of 500 ms hyperpolarizing divided by the largest membrane potential change observed in response to a current step of -200 pA; and the adaptation index was defined as the interspike interval between the last versus the first action potential evoked by a depolarising current pulse lasting 500 ms. The peak amplitude and half-width were measured from the initial point of the rising phase of the action potential. The coefficient of variation (CV) for the stimulation protocol was calculated as the standard deviation of

interspike intervals/mean of interspike intervals.

Cumulative fraction of amplitude and inter-event intervals of sIPSCs were analysed using Mini Analysis (Synaptosoft Inc., Fort Lee, NJ, USA), using pre-set template and manually examining and removing error “peaks/events” after applying the template. Paired or un-paired Student’s t-tests, where appropriate, were performed with SPSS (Surrey, UK) or Prism 4.0 (Graphpad Software, La Jolla, CA, USA). When other statistical tests have been used then they have been specified in the text. Statistical significance was set at $p < 0.05$. Values presented in the text and in figures represent the mean ± SEM unless otherwise stated.

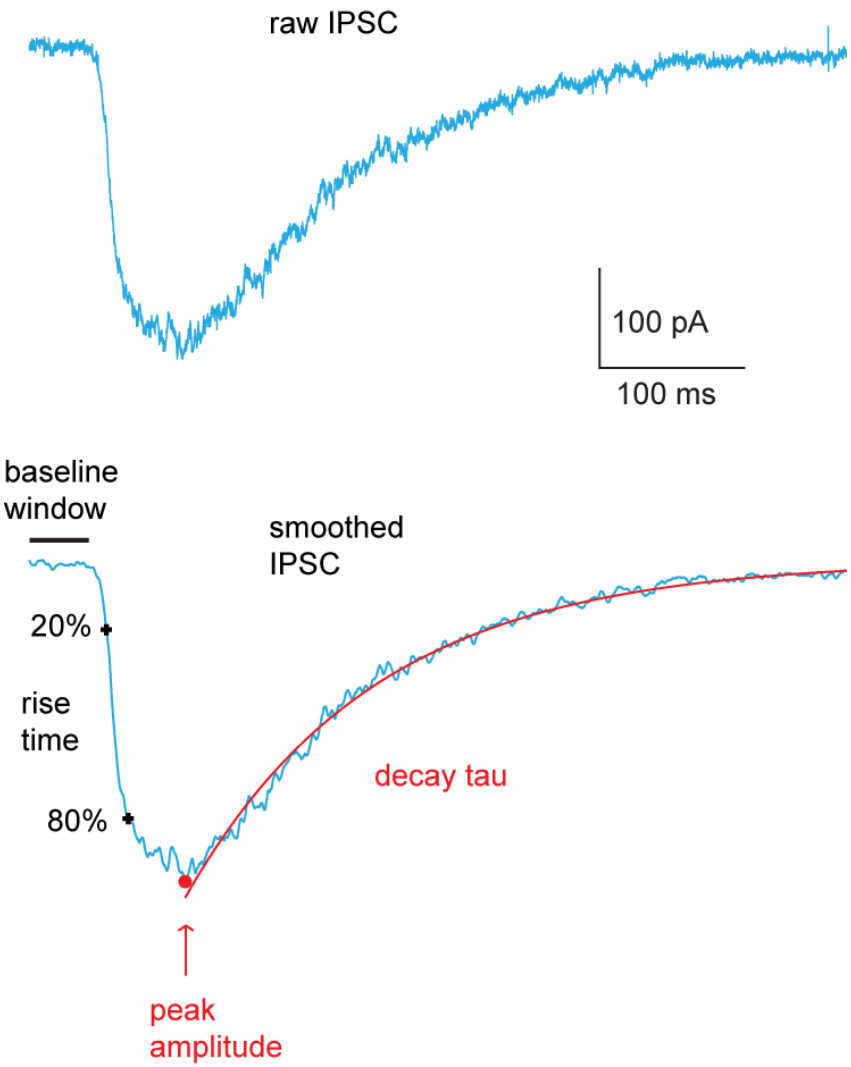

Figure 2.2.2.1 Example of IPSC analysis

Top panel, raw recording of an IPSC. Bottom panel, IPSC from top panel smoothed using moving average smoothing method. Black crosses denote the start and end point of 20% - 80% rise time. Red dot denotes local maximum which is the peak amplitude. Red curved line represents the decay tau, which is a single exponential fit from the peak amplitude to steady state. Black bar denotes the baseline window where baseline has been calculated from averaging.

2.3. Voltage sensitive dye and calcium Imaging

2.3.1. VSD and calcium imaging data acquisition

In voltage sensitive dye (VSD) and Ca^{2+} imaging experiments, a low chloride internal solution containing (in mM): 126 K-gluconate, 10 HEPES, 10 Na_2Phosphocreatine, 4 KCl, 4 Mg-ATP, 0.3 Na-GTP, pH 7.3 with KOH, the osmolarity was 270-280 mOsmol, was used. I have adopted the dye loading method described by Canepari et al. (Canepari et al., 2008). The dye (VSD JPW1114, 0.25-0.5 mg/ml of low chloride internal solution) was prepared in dark and loaded into the pipette. In particular the tip of the pipette was filled with dye-free internal solution to avoid spillage while approaching the cell. The dye loading procedure was similar to whole cell patch clamping method except a low air pressure (~5 millibar) was used initially while approaching the cell. When the pipette was in place, the air pressure was increased to the normal ~40 millibar a value typically used in standard electrophysiogy recordings. After whole-cell configuration was established, dye loading lasted 20–40 minutes (by passive diffusion), depending on the concentration of dye loaded, which was monitored continuously by exciting the dye with very low light intensity (0.01% of full power, full power = 300 mW). When this intensity reached an acceptable level, the patch pipette was removed slowly (>5 minutes) from the cell by forming an outside-out patch. The slow removal is very important to ensure the integrity of the cell membrane and recovery. The cell was then incubated for an additional 60–90 minutes to allow dye equilibration into dendrites and re-patched with a dye-free pipette containing the low chloride internal solution with biocytin (2-4 mg/ml). Voltage fluorescence was excited with a 532 nm 300 mW solid state laser (model MLL532; CNI, Changchun, China) as described previously (Canepari et al., 2010). For action potential acquisition, a high acquisition rate (5 kHz) and high excitation intensity (50% of full power) was used. Single acquisition usually lasted for ~10 ms to avoid phototoxicity and

bleaching.

In Ca^{2+} imaging experiments, the low-affinity indicators Oregon green 5N (OG5N) or Mag-Fura-2 (MF2) were added at 0.5 mM concentration to the internal solution and using similar dye loading method to VSD. Ca^{2+} fluorescence was excited with an OptoFlash (Cairn Research Ltd., Faversham, UK) using either a 470 nm LED (for OG5N) or a 385 nm LED (for MF2), mounted on the epifluorescence port of the microscope. The excitation light, either from the laser or the LED, was directed to a water immersion objective (Olympus 60x/1.1 NA). Fluorescent images, de-magnified by 0.25x or 0.38x, were visualised with a high speed CCD camera NeuroCCD-SM (RedShirtImaging LLC, Decatur, GA, USA) at a frame rate ranging between 125 Hz and 5 kHz. The corresponding electrophysiological signals from the soma were recorded at a frequency ranging between 8 kHz and 20 kHz. The CCD has 80 x 80 pixels covering an area of 125 µm x 125 µm with the 0.25x de-magnifier and 82 µm x 82 µm with the 38x de-magnifier. The area covered by a single pixel was 1.6 µm x 1.6 µm and 1 µm x 1µm with the 0.25x and 0.38x de-magnifiers respectively. The dendritic regions analysed in this study were within 20-120 µm from the soma.

2.3.1. VSD and calcium imaging data analysis

Both VSD and Ca^{2+} imaging data were analysed with dedicated software written in MATLAB. Optical signals were initially expressed as fractional changes of fluorescence averaged from 4x4 (16 pixels) regions of interest (ROIs) and obtained from averages of four trials unless otherwise mentioned. The fractional change of fluorescence was computed as the change of fluorescence of each individual frame from the initial fluorescence divided by the initial fluorescence. A bleaching sweep (without signal) was acquired and subtracted from the signal sweeps. For calibration of VSD signals, a "reference" signal associated with a long lasting hyperpolarizing current pulse (-50/-100 pA, 350 ms) was injected into the soma and recorded (400 ms x 9-16 sweeps) at low acquisition rate (typically 125 frames/s) using a moderate illumination (~ 10% of the full power) to minimise bleaching and phototoxicity. This signal should spread with minimal attenuation along the dendrites (Vetter et al., 2001) providing a uniform membrane potential change along the dendrite. Thus, because the VSD ΔF/F signal is linear with the membrane potential change, any ΔF/F can be converted into mV using the same procedure described elsewhere (Canepari and Vogt, 2008) for cerebellar Purkinje neurons. The amplitude of the images resulted from the average value ΔF/F during a steady state pulse (usually 50 ms) subtracted from ΔF/F value immediately before the onset of the pulse, baseline 10-20 ms ΔF/F mean value.

To calibrate fractional changes of OG5N fluorescence into changes of intracellular free Ca^{2+} ($\Delta[Ca^{2+}]$free), I have used the low-affinity indicator MF2 (Kd = 25 μM). When excited at 385 nm, this indicator exhibits a decrease in fluorescence associated with an increase in Ca^{2+} and the $\Delta[Ca^{2+}]$free can be estimated as Kd•(Fmin-F)/(F-Fmax), where Fmin and Fmax are the fluorescence at 0 and saturating Ca^{2+} respectively. This indicator has an excellent dynamic range and in Cueni et al. (Cueni et

al., 2008), in which at high concentrations (>0.5 mM), Fmin and Fmax can be approximated with the initial fluorescence and the slice autofluorescence respectively. In addition MF2 fluorescence is not excited at 470 nm, i.e. at the excitation wavelength of OG5N. Thus, in a series of calibration experiments, I added the two indicators together at 0.5 mM concentration in the patch pipette and monitored fluorescence signals associated with one to four action potentials to calibrate the OG5N fractional change of fluorescence into $\Delta[Ca^{2+}]$free.

2.4. Intracellular labelling and post-hoc visualisation of recorded cells

After recordings, the slices were immersed at 4° C for 12-24 hrs in a fixative solution containing: 4% paraformaldehyde, 15% (v/v) saturated picric acid and 0.1 M phosphate buffer (PB; pH 7.2-7.4). Then, gelatine-embedded slices were re-sectioned into 60 µm thick sections. Sections were then incubated with streptavidin-Cy3 solution (93% of 0.1 M phosphate buffer, 6% of Triton at 3% and 1% of Streptavidin-Cy3) overnight before mounting and imaging them under a fluorescent microscope. Pictures of the location and the dendritic/axonal patterns of the recorded neurons were performed and stored. After this step, some sections were further processed to reveal the fine details of the processes of the cells using the diaminobenzidine (DAB) staining method. In brief, sections containing biocytin-filled cells were incubated in avidin-biotinylated horseradish peroxidase complex (1:100 dilution; ABC Kit; Vector Laboratories, Burlingame, CA) followed by a peroxidase reaction using diaminobenzidine (DAB, Sigma-Aldrich; 0.05%) as the chromogen and 1% H_2O_2 as the substrate. Sections were then mounted on gelatine-coated slides, air-dried, immersed in xylene-based mounting medium (Entellan; Merck, Damstadt, Germany) and cover-slipped.

In addition, some recorded neurons were imaged under a confocal microscope (Zeiss LSM710 laser scanning microscope, Carl Zeiss Ltd, Cambridge, UK). Image stacks were acquired using a 40x 1.3 NA objective. Biocytin was visualised by steptavadin-Cy3, excited by a 543 nm laser; emission sampled from 550 nm to 680 nm. Lucifer Yellow was excited by a 405 nm laser; emission sampled from 510 nm to 680 nm. Projections were generated in ImageJ using the standard deviation method.

2.5. nNOS-Cre-tdTomato mouse

The nNOS-Cre-tdTomato mouse line was generated using methods described previously (Taniguchi et al., 2011). Tamoxifen administration was used to induce Cre activity in nNOS expressing neurons. Tamoxifen was administrated by intraperitoneal injection at 2-5 mg/dosage three times every other day from P21. When immunohistochemistry was performed on sections of nNOS-Cre-tdTomato mice, re-sectioned slices (50 μM) were incubated with a primary antibody raised against nNOS (1:500 goat ab1376, Abcam) and tdTomato (1:500 Rat RFP 5F8, Chromotek) overnight at 4° C in 0.3% Triton X-100 and 10% normal donkey serum containing PBS-azide buffer. The nNOS staining was revealed using AlexaFluor488-conjugated secondary antibody (1:500 donkey to goat, Invitrogen), and tdTomato staining was revealed using Cy3-conjugated secondary antibody (1:1000 donkey to rat, Jackson Immunoresearch).

For cell counting experiments, re-sectioned slices of nNOS-Cre-tdTomato mice were visualised under a confocal microscope (Zeiss LSM 710). Images were acquired using the acquire SRS image stack workflow function in StereoInvestigator (MBF Bioscience), in which the whole hippocampus was included. Cell counting (interneurons and pyramidal cells) was carried out offline: the digital copy of each section was opened in StereoInvestigator, the guard zone was 2 μm and the probe length was 10 μm, only cells with soma in the probe zone were counted.

2.6. Chemicals and drugs

All drugs were applied to the recording preparation through the bath. Salts used in the preparation of the intracellular recording solution and ACSF were obtained from either BDH Laboratory Supplies or Sigma (Poole, UK). Kynurenic acid, biocytin was purchased from Sigma (Poole, UK), 6-Imino-3-(4-methoxyphenyl)-1(6H)-pyridazinebutanoic acid hydrobromide (SR95531), CGP35348, 1H-[1,2,4]Oxadiazolo[4,3-a]quinoxalin-1-one (ODQ), NG-Nitro-L-arginine methyl ester hydrochloride (L-NAME), L-arginine, nimodipine, ryanodine, U73122, 4-aminopyridine (4-AP), tetraethylammonium (TEA), tetrodotoxin (TTX) were purchased from Tocris Cookson (Bristol, UK).

3. RESULT

3.1. *in vivo* firing induces a transient suppression of synaptic inhibition

I have recorded the unitary inhibitory postsynaptic potentials (uIPSPs) or currents (uIPSCs) from synaptically-coupled putative NGFCs or other interneurons with the soma in the SLM of the rat hippocampus *in vitro*. Neurons were recorded with a high chloride internal solution to increase the signal of these events and as a result these events were depolarising potentials (current clamp recordings at -68 ± 2 mV) or inward currents (voltage clamp recordings at -68 ± 2 mV). A firing sequence (60 s duration, average frequency and CV values: 8.3 Hz, 0.75; stimulation protocol) was recorded in a rat NGFC *in vivo* during theta oscillations (Fuentealba et al., 2010) and which was injected in current clamp configuration in a postsynaptic interneuron of the SLM *in vitro*. I have found that shortly after (125 or 250 ms) the firing of the postsynaptic cell from the *in vivo* sequence, there was a transient decrease in the amplitude of the uIPSPs recorded in current clamp (75 ± 1.4% of control, $p < 0.001$, 23/70 cell pairs, Figure 3.1.1A, C). In addition, the stimulation protocol elicited a transient decrease in the amplitude of the uIPSCs recorded in voltage clamp configuration as well (72.6 ± 2.1% of control, $p < 0.001$, 25/54 cell pairs, Figure 3.1.1B, C). Thus, this use-dependent effect of synaptic modulation by *in vivo* cells' firing was present in about 30% of cell pairs tested.

The kinetics of baseline and decreased uIPSCs evoked before and immediately after the stimulation protocol was similar (Figure 3.1.1B, inset, showing scaled traces) (rise-time was 97 ± 4% of control, $p > 0.1$; weighted decay time constant was 98 ± 12%

of control, $p > 0.1$, $n = 9$), suggesting that presynaptic mechanisms were more likely than postsynaptic mechanisms to be responsible for the decrease in the synaptic response. After 60 seconds from the end of the stimulation protocol the uIPSPs or uIPSCs returned to control level and remained stable (inter-stimulus interval = 60 s). Therefore, it was possible to induce several transient depressions of the uIPSPs or uIPSCs by repeating cycles of the stimulation protocol followed by low frequency stimulations in the same cell pair (Figure 3.1.1C). I have termed this transient depression of the uIPSPs or uIPSCs as "firing induced suppression of inhibition" (FSI). On average, I have found that the FSI of the uIPSP peak amplitude recorded in current clamp was not significantly different from the FSI of the uIPSCs recorded in voltage clamp ($p > 0.1$, Figure 3.1.1D). Additionally, the number of FSI cell pairs between current clamp and voltage clamp configuration did not significantly differ (23/70 vs. 25/54, $p > 0.1$, Chi-squared test). Therefore, data obtained from both recording modes were pooled and will be presented together in the following sections. In addition, I have found that most of the presynaptic neurons displayed autaptic(a) IPSCs, a synaptic event detected from the NGFC type in the SLM of the hippocampus (Karayannis et al., 2010). Interestingly, the stimulation protocol also induced FSI on aIPSP/Cs (autapse formed on presynaptic cell) in 6/30 cell pairs that also showed FSI regulation of uIPSP/Cs (postsynaptic signals). However, this transient depression on aIPSP/Cs was mild (92.5 ± 1.8% of control, $p < 0.05$, Figure 3.1.2) in comparison with FSI on uIPSP/Cs (~ 70%, Figure 3.1.1).

In summary, I have found that *in vivo* NGFC firing during hippocampal theta rhythm induces a DSI-like event (FSI) recorded from pairs of interneurons with the soma in the SLM. The following experiments have been designed to study the cell types and mechanisms involved in this phenomenon.

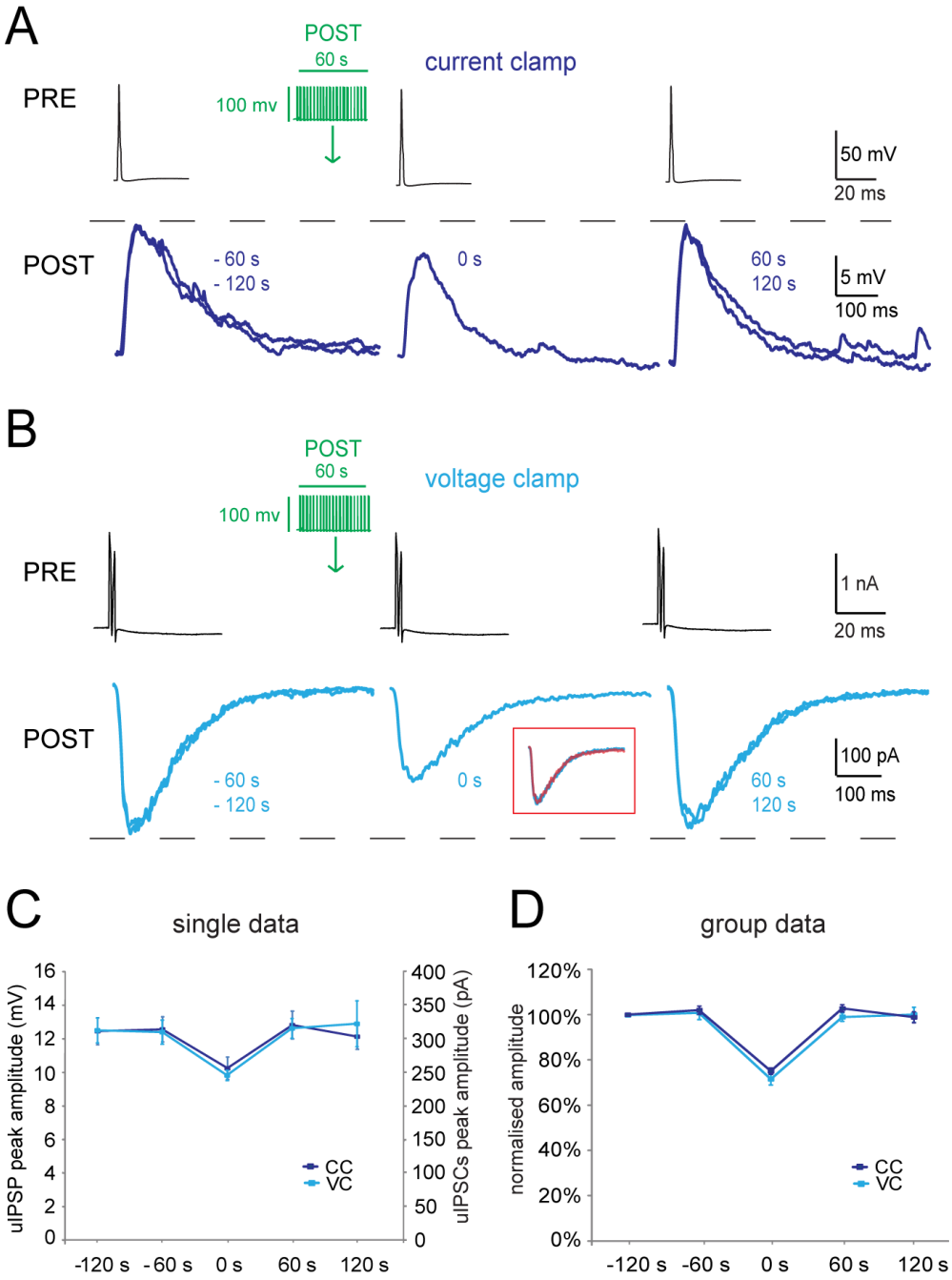
A
POST
60 s
current clamp
PRE
100 mv
50 mV
20 ms
POST
- 60 s
- 120 s
0 s
60 s
120 s
5 mV
100 ms
B
POST
60 s
voltage clamp
100 mv
PRE
1 nA
20 ms
POST
- 60 s
- 120 s
0 s
60 s
120 s
100 pA
100 ms
C
single data
uIPSP peak amplitude (mV)
uIPSCs peak amplitude (pA)
CC
VC
-120 s
-60 s
0 s
60 s
120 s
D
group data
normalised amplitude
CC
VC
-120 s
-60 s
0 s
60 s
120 s

Figure 3.1.1 NGFC *in vivo* firing pattern induces a transient suppression of synaptic inhibition

A, NGFC paired recording *in vitro*, current clamp mode, presynaptic action potentials (PRE, black traces) evoked depolarising uIPSPs in a postsynaptic cell recorded with an electrode filled with 84 mM Cl- solution (POST, left dark blue traces superimposed recorded 120 s or 60 s before the stimulation protocol). Injection of firing recorded *in vivo* from an NGFC for 60 s (stimulation protocol) in the postsynaptic NGFC recorded *in vitro* induced a transient decrease of the amplitude of the uIPSP (POST, middle trace), that returned to the baseline level 60 s and 120 s after the end of the stimulation protocol (right traces superimposed). **B**, NGFC paired recording, voltage clamp mode, presynaptic action currents (PRE, black traces) evoked inward uIPSCs in a postsynaptic cell recorded with an electrode filled with 84 mM Cl- solution (POST, left light blue traces superimposed recorded 120 s or 60 s before the stimulation protocol). Injection of *in vivo* NGFC firing for 60 s (stimulation protocol) in the postsynaptic NGFC induced a transient decrease of the amplitude of the uIPSC (middle trace), that returned to the baseline level 60 s and 120 s after the end of the stimulation protocol (right traces superimposed). Inset, scaled traces show no changes in the kinetics of the uIPSCs before and during FSI. **C**, mean uIPSP (CC, current clamp) or uIPSC (VC, voltage clamp) peak amplitude before and after the stimulation protocol (repeated sequentially three times) for the cell pairs shown in A and B; error bars are SEM. **D**, summary of normalised peak amplitudes of uIPSPs (CC, current clamp) or uIPSCs (VC, voltage clamp) before and after the stimulation protocol in all pairs showing FSI, error bars are SEM ($p < 0.001$, $n = 23$ for CC data, $n = 25$ for VC data). In the graphs of panels C and D of this and subsequent figures, 0 s indicates mean uIPSP or uIPSC amplitude detected 125 or 250 ms after the end of the stimulus protocol.

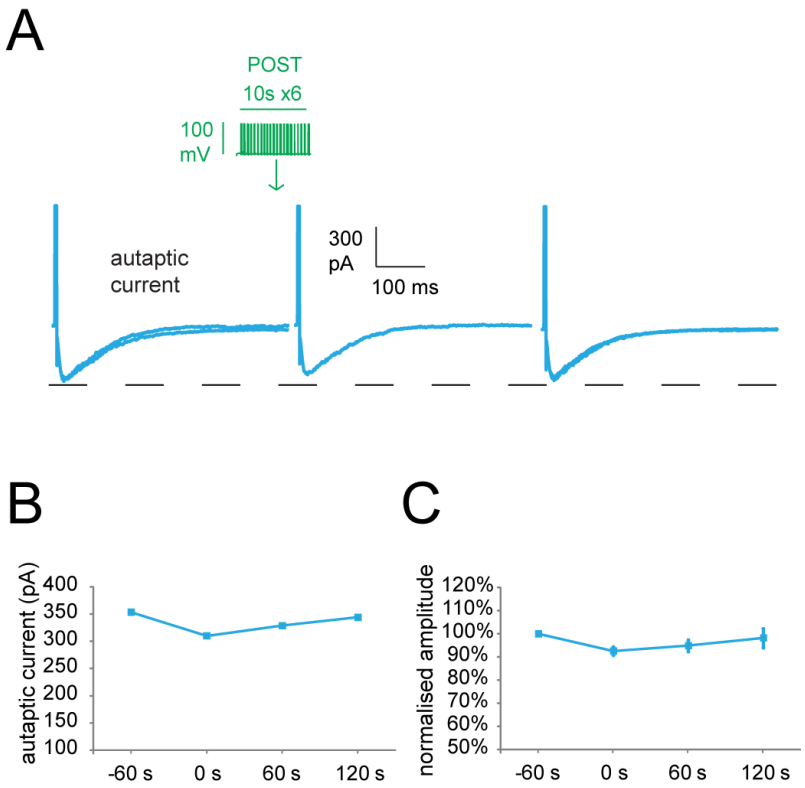

Figure 3.1.2 *in vivo* firing pattern also induces FSI in autaptic IPSC (aIPSC)

A, NGFC paired recording *in vitro*, presynaptic action potentials evoked depolarising aIPSCs in the same presynaptic cell (autaptic current) recorded with an electrode filled with 84 mM Cl- solution (left traces superimposed, baseline). Injection of the *in vivo* firing pattern (stimulation protocol) in the postsynaptic NGFC recorded *in vitro* induced a transient decrease of the amplitude of the aIPSC (middle trace), that returned to the baseline level 60 s and 120 s after the end of the stimulation protocol (right traces superimposed). **B**, mean aIPSC peak amplitude before and after the stimulation protocol for the cell pairs shown in A. **C**, summary of normalise peak amplitudes of aIPSCs before and after the stimulation protocol in all pairs showing FSI, error bars are SEM (FSI for aIPSCs was 92.5% $p < 0.05$, $n = 6$).

3.2. Anatomical examination of cell pairs recorded

Next I aimed to confirm that the recorded neurons in the SLM were NGFCs, and also to test the anatomical identity of the recorded neurons, since this layer of the hippocampus contains the soma of several other interneuron types (Vida et al., 1998; Klausberger, 2009; Capogna, 2011). Neurons were identified as NGFCs by three criteria. First, the recorded neurons were tested for the presence of aIPSPs or aIPSCs occurring as a depolarising potential (current clamp mode) or an inward current (voltage clamp mode) immediately after an action potential or current, the autaptic response being a feature of NGFCs (Karayannis et al., 2010). Second, the kinetics of the postsynaptic uIPSCs were analysed; when the rise-time was > 3 ms and the decay time constant > 60 ms, the presynaptic neuron was considered as an NGFC. This was based on previous observations establishing that NGFCs mediate slow IPSPs in the hippocampus (Price et al., 2005; Karayannis et al., 2010; Capogna and Pearce, 2011). Third, all recorded neurons were filled with biocytin for subsequent analysis of the dendritic and axonal patterns; NGFCs were expected to display stellate dendrite and dense axonal aborisation.

Based on these three criteria combined, I found that 41/48 presynaptic neurons displaying FSI were NGFCs, characterised by round somata, short, highly arborising dendrites close to the soma and an axon which profusely arborised to cover the dendritic tree (Figure 3.2.1). However, I also found that five presynaptic cells were other types of interneurons including two putative perforant path-associated interneurons, identified by the axonal branches segregated within the hippocampal fissure, and three putative cholecystokinin (CCK)-expressing basket neurons, characterised by the flask-like shape of their soma. Two presynaptic interneurons could not be identified.

I have also recovered the dendritic and axonal processes of 21 postsynaptic

neurons showing FSI. Of which, 17 cells were identified as NGFCs, three cells as putative perforant path-associated interneurons, and one cell was classified as a putative CCK-expressing basket cell. The NGFCs (Figure 3.2.1) and few other interneurons of the SLM included in this study exhibited firing patterns and intrinsic electrophysiological responses consistent with previous reports e.g. (Elfant et al., 2008).

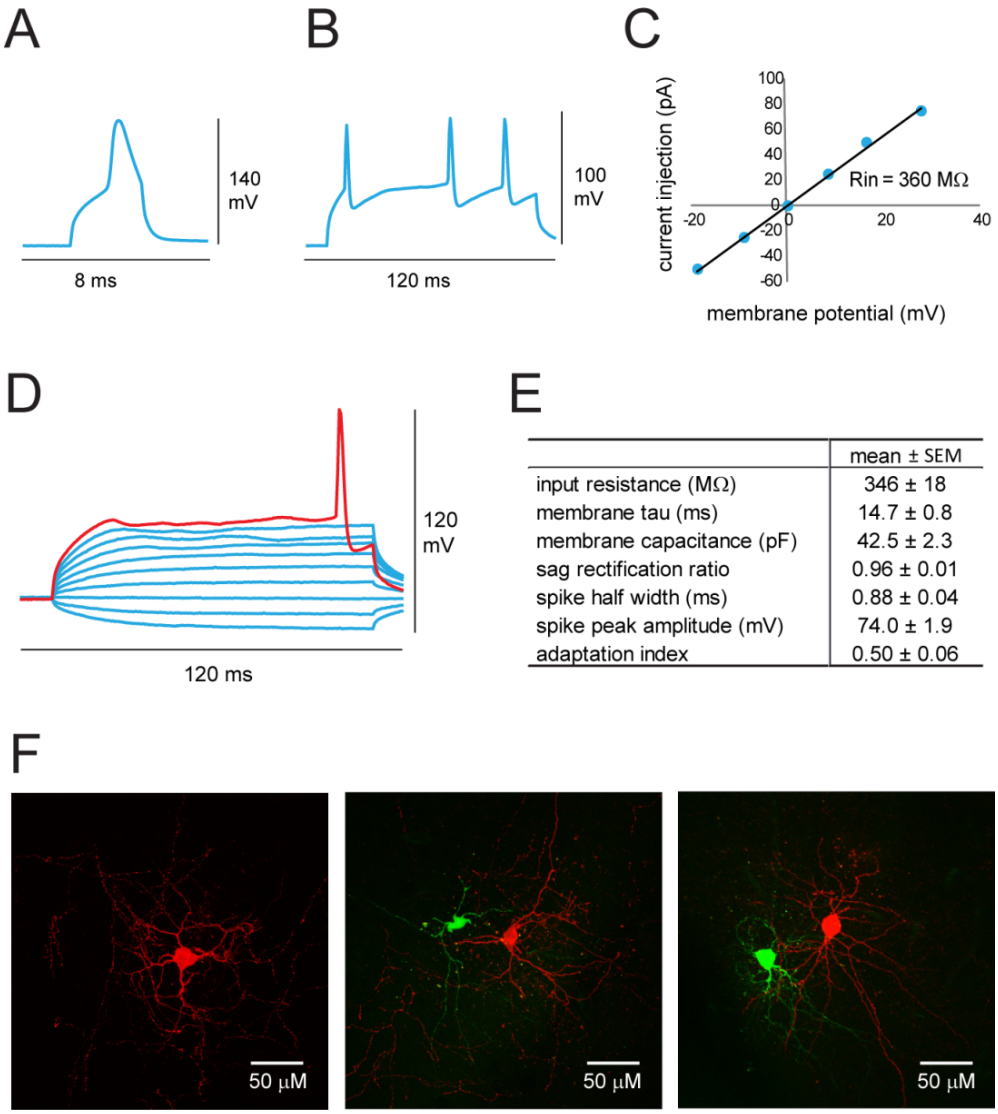

Figure 3.2.1 NGFC intrinsic electrophysiology properties and fluorescent images

A, NGFC single action potential (3 ms, 800 pA depolarisation). **B**, NGFC firing pattern (100 ms, 200 pA depolarisation). **C**, IV graph of a typical NGFC. **D**, IV of a typical NGFC (current injection at 25 pA per increment from -75 pA), note the characteristic delayed AP firing (red). **E**, summary of NGFC electrophysiological properties (n = 22). **F**, examples of NGFC fluorescent images. Left panel, single NGFC filled with biocytin (visualised with streptavadin Cy3); middle panel, NGFC pair (green cell filled with lucifer yellow, red cell filled with biocytin); right panel, a NGFC (green cell filled with lucifer yellow) and a non-NGFC interneuron of the SLM (red cell filled with biocytin).

3.3. What triggers FSI in the postsynaptic neuron?

Before studying the mechanisms of FSI, I have performed two control experiments to rule out some unspecific factors underlying FSI. First, I have ruled out that FSI was simply due to a transient and unspecific change in the postsynaptic membrane conductance during the conditioning protocol in current clamp mode. I have found that an unspecific transient change in the postsynaptic cell input resistance was not responsible for FSI. Experimentally, the application of a hyperpolarising current pulse (-150 pA, 350 ms) into the postsynaptic cell before and immediately after the stimulation protocol did not modify the cells' membrane input resistance (97.3 ± 1.9% of control after the train, $p > 0.05$, $n = 18$, Figure 3.3.1). Together with observing FSI in voltage clamp mode, this result suggests that a change in membrane conductance did not account for the decrease in the amplitude of the synaptic responses observed. Secondly, I have found that FSI was not affected by the application of a $GABA_B$ receptor antagonist (CGP35348, 50 µM, $p > 0.5$, $n = 4$, Figure 3.3.2). This indicates that, although presynaptic $GABA_B$ receptors tightly control axonal GABA release from NGFCs (Price et al., 2005; Price et al., 2008), $GABA_B$ receptor activation is not involved in FSI.

The data illustrated so far indicate that FSI was not caused neither by an unspecific increase in membrane conductance nor by the activation of $GABA_B$ receptors. So what triggers FSI? In the case of DSI, as discussed in the introduction, this phenomenon is due to eCB retrograde signalling triggered by postsynaptic cell depolarisation. According to this idea, the *in vivo* firing protocol could be the trigger for FSI. Thus, I will aim to study what happens to the postsynaptic cell during the *in vivo* firing protocol.

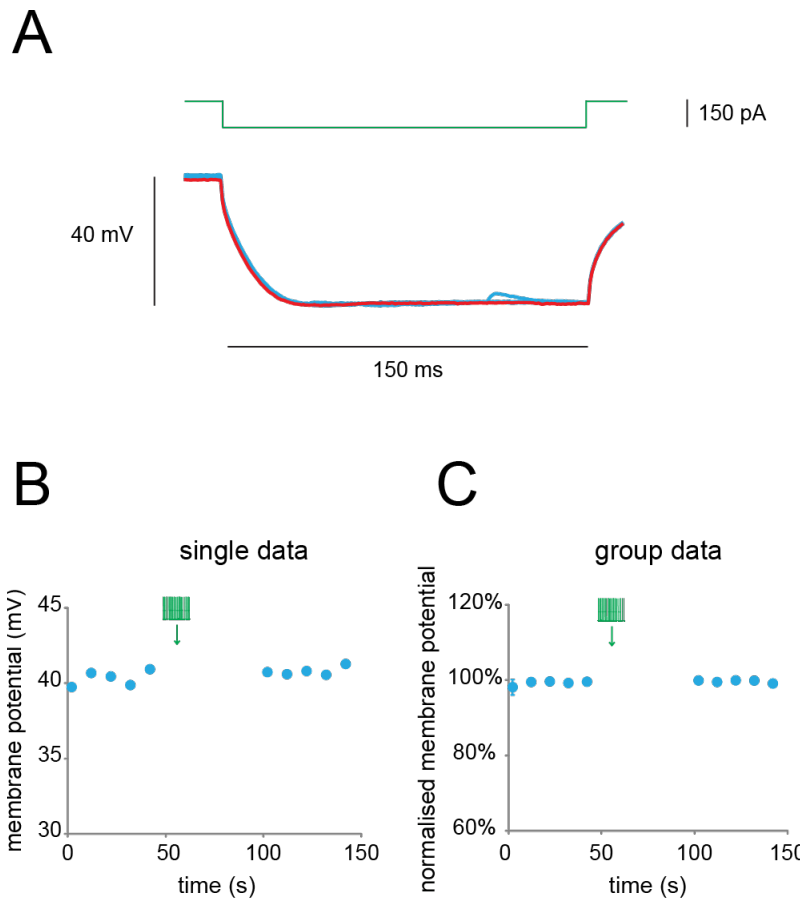

Figure 3.3.1 Membrane conductances was not changed followed by the stimulus protocol

A, Injection of a long hyperpolarising current pulse (-150 pA, 150 ms, green trace) into the postsynaptic cell hyperpolarised the membrane potential. The passive response of membrane potential to the long hyperpolarising current pulse shortly after the conditioning protocol (red trace) was similar to baseline and recovery (blue traces superimposed). **B**, quantification of changes in membrane potential for the data shown in A. **C**, normalised data (mean and SEM) for membrane potential change studied with this protocol (membrane potential was 97.3 ± 1.9% of control after the conditioning protocol, $p > 0.05$, $n = 18$).

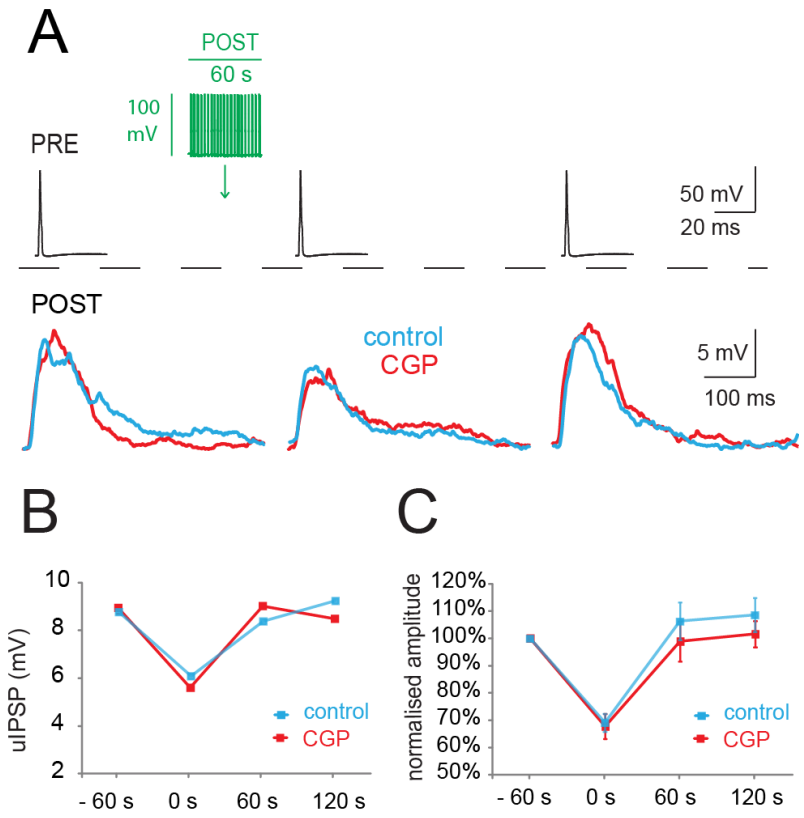

Figure 3.3.2 $GABA_B$ receptor antagonist was unable to block FSI

A, Presynaptic action currents (PRE, black traces) evoked inward uIPSPs in a postsynaptic NGFC recorded with an electrode filled with 84 mM Cl- solution (POST, blue traces). Injection of the stimulation protocol in the postsynaptic cell induced a transient depression of the uIPSC amplitude (middle blue trace), that returned to control level 60 s after the end of the stimulation protocol (right blue trace). Application of the $GABA_B$ receptor antagonist CGP35348 (50 µM) had no effect on FSI (red traces). **B**, quantification of the uIPSP peak amplitude that occurred before or in the presence of CGP35348 for the data shown in A. **C**, normalised data (mean and SEM) for all uIPSPs or uIPSCs studied with this protocol (FSI control was 68.7 ± 3.4%, in the presence of CGP35348 FSI was 67.7 ± 4.6%, $p > 0.5$, $n = 4$).

3.4. What happens to the postsynaptic neuron during the *in vivo* firing protocol?

FSI is temporally-correlated with the postsynaptic firing, but is postsynaptic cell firing required for FSI? I have studied this question by using a subthreshold protocol. First, I injected the control stimulation protocol to induce FSI, and then I have applied subthreshold depolarising current pulses (75 pA x 1 ms) with the same temporal pattern of the *in vivo* action potentials. I have found that a subthreshold protocol was unable to induce FSI in all cell pairs tested (97.4 ± 2.5% of control, $p > 0.5$, $n = 11$, Figure 3.4.1). This result suggests that FSI was initiated by the postsynaptic neuron firing, indicating that active processes were likely to be involved. According to this result, AP backpropagation (bAP) could be one of the active processes that occur, namely bAP travels along the postsynaptic dendrites in order to trigger FSI. To test this hypothesis, I have visualised bAPs in 24 interneurons of the SLM by using single cell voltage imaging as described in the Methods (Figure 3.4.2A). I have analysed ΔF/F signals at various dendritic locations associated with a somatic AP evoked by intracellular current injection. The cells tested with this protocol included NGFCs ($n = 9$), but also other interneurons of the SLM such as putative perforant path associated and CCK-expressing basket cells ($n = 15$). I have observed a ΔF/F signal with an AP shape at all dendritic locations and in all interneurons studied (Fig. 3.4.2C).

Since the amount of dye distributed along the dendritic axis may vary (different diffusion rate of the dye due to different internal structures of dendrites), I performed a calibration protocol of ΔF/F signals using the injection of a long-lasting hyperpolarising current pulse into the soma as described in the Methods. The calibration procedure is shown in Figure 3.4.2B. Using this procedure, I have observed robust bAPs along the dendrites of NGFCs and other hippocampal interneurons of the SLM without significant

decrement ($p > 0.5$, $n = 24$). A summary of the quantification of the bAP along the dendrites of all interneurons studied with VSD is shown in Figure 3.4.2C. Interestingly, I have also found that NGFCs have more robust bAP than other interneurons of the SLM ($p < 0.05$, 9 NGFCs, 15 non-NGFC interneurons of the SLM, two-sample t-test assuming equal variances, Figure 3.4.2D). Optically-recorded bAP events were always associated with somatic APs, and both signals were abolished by the application of tetrodotoxin (TTX, 1 μM, Figure 3.4.2E).

Using VSD, it was also possible to study the kinetics of APs after applying the *in vivo* firing pattern (stimulus protocol). I have analysed the kinetics of the optical AP 125 ms after the condition protocol (test AP) versus a single optical AP evoked alone. The 20-80% rise time between control and the test AP was similar ($p > 0.5$, $n = 14$). However, the half-width of test AP increased slightly (18% ± 5.0%, $p < 0.05$, $n = 14$, Figure 4.4) compared with control. It is known that dendritic expression of K^+ channels could control bAP, and various types of interneurons express different types and distribution of K^+ channels (Goldberg et al., 2003). Therefore, the increase in the half-width of test AP I have observed could be explained by the desensitisation of K^+ channels. Indeed, I have found that application of K^+ channel blockers could increase the half-width of bAP. Specifically, 4-aminopyridine (4-AP, 1 mM), which targets both Kv3 and Ia-type K^+ channel (Kirsch et al., 1993), had larger effect than tetraethylammonium (TEA, 1 mM), which target Kv3 but not Ia-type K^+ channel at 1 mM (Lien et al., 2002), on the half-width of AP. Quantitatively, 4-AP increased somatic (electrophysiological recording) and dendritic (VSD) AP width-half by ~60% and ~65%, respectively, in two putative NGFCs (Figure 3.4.4). In contrast, TEA had little effects (<10%) on the half-width of soma and dendritic APs (not shown).

Thus, my result showed that APs backpropagated along the dendrites of NGFCs and other interneurons of the SLM, and this event is likely to initiate FSI.

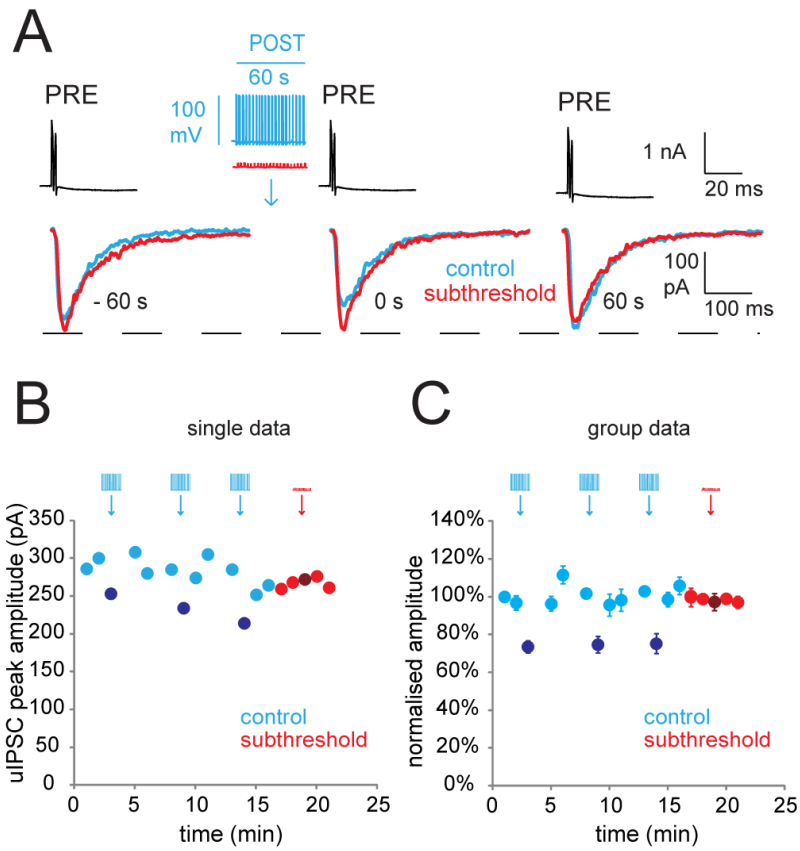

Figure 3.4.1 Stimulation protocol of weak subthreshold depolarising current pulses does not elicit FSI

A, stimulation protocol (60 s, blue) applied to a postsynaptic NGFC (POST) elicited FSI of uIPSC peak amplitude (blue middle trace) recorded with an electrode filled with 84 mM Cl^- solution and evoked by presynaptic action currents (PRE, black traces). In contrast, subsequent injection of weak subthreshold depolarising current pulses (75 pA x 1 ms) (red) did not evoke FSI (red middle trace). Left and right traces show uIPSCs before and after FSI. **B**, mean uIPSCs peak amplitude before and after firing or subthreshold stimulation protocol for the data shown in A (dark symbols denote values immediately after stimulation protocol). **C**, normalised data (mean and SEM) for all cell pairs studied with this protocol (FSI control was 76.8 ± 2.7% and 97.4 ± 2.5% with subthreshold pulses, n = 11).

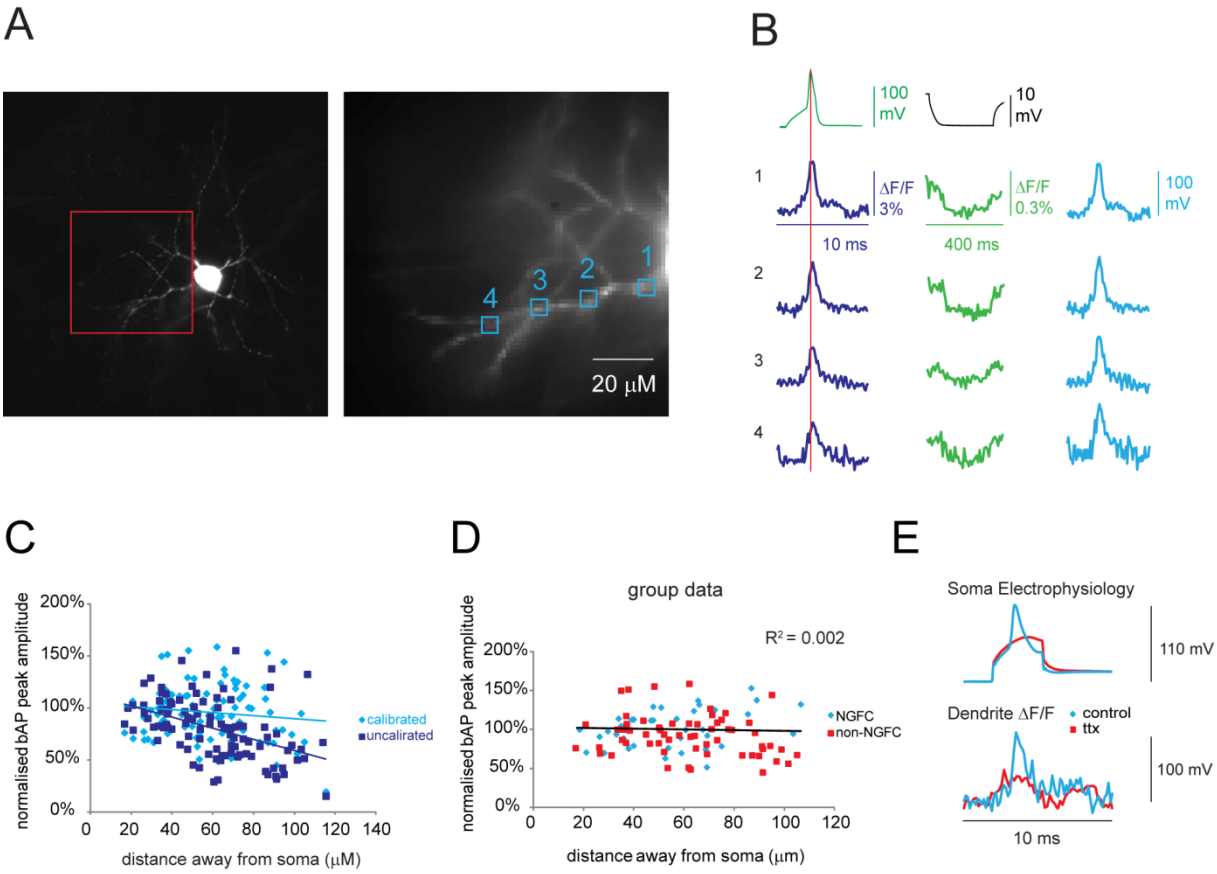
A
B
100 mV
10 mV
ΔF/F 3%
ΔF/F 0.3%
100 mV
10 ms
400 ms
1
2
3
4
20 μM
C
normalised bAP peak amplitude
200%
150%
100%
50%
0%
0 20 40 60 80 100 120 140
distance away from soma (μM)
calibrated
uncalirated
D
group data
R² = 0.002
normalised bAP peak amplitude
200%
150%
100%
50%
0%
0 20 40 60 80 100 120
distance away from soma (μm)
NGFC
non-NGFC
E
Soma Electrophysiology
110 mV
Dendrite ΔF/F
control
ttx
100 mV
10 ms

Figure 3.4.2 bAP along the dendrites of NGFCs or other interneurons of the SLM

A, Right image, NGFC (filled with biocytin, visualised after biocytin-streptoavidin-Cy3 reaction) showing characteristic stellate dendrites (objective x20). Left image, the same neuron in A, which was loaded with JPW-1114 and voltage imaging was performed from dendritic sites included in the red box; in particular, ΔF/F signals at the sites indicated (1-4, 4x4 pixels) were analysed. **B**, Left, A depolarising current pulse (800 pA, 3 ms) induced a somatic action potential (AP) recorded in current clamp (green trace) and the corresponding ΔF/F signals from the site 1-4 in A are illustrated. The red vertical bar denotes the AP peak recorded from the soma. **B**, Middle traces, fractional changes of voltage fluorescence (ΔF/F) in response to a ~ 10 mV membrane potential hyperpolarisation lasting 350 ms (average of 9 traces) injected into the soma and recorded from sites 1-4 of the dendrites; somatic current clamp recording is illustrated on the top. Right traces, ΔF/F of the bAPs peak amplitude calibrated with the corresponding ΔF/F induced by the hyperpolarising current pulse recorded from regions 1-4 of the dendrites. **C**, summary graph showing bAP peak amplitude recorded at different dendritic sites normalised to the bAP amplitude recorded at 20-30 μm (shortest distance) from the soma (light blue, calibrated; dark blue, uncalibrated; n = 24). **D**, group data of calibrated bAP peak amplitude shown in C. Note that bAPs occurs in NGFCs and in other interneurons of the SLM (non-NGFC) without any significant decrement (bAP peak amplitude detected at dendrites >70 μm or ~20 μm away from the soma was not significantly different, $p > 0.5$, n = 24). **E,** Top trace, effect of 1 μM TTX on an AP recorded in current clamp evoked by a depolarising current pulse (800 pA x 3 ms, top traces). Bottom trace, effect of 1 μM TTX on ΔF/F bAP recorded from a dendrite of an NGFC. Blue traces, control; Red traces, TTX. Note that TTX blocks the ΔF/F of the bAP, whereas it spares ΔF/F of the subthreshold depolarisation evoked by the somatic subthreshold depolarising pulse.

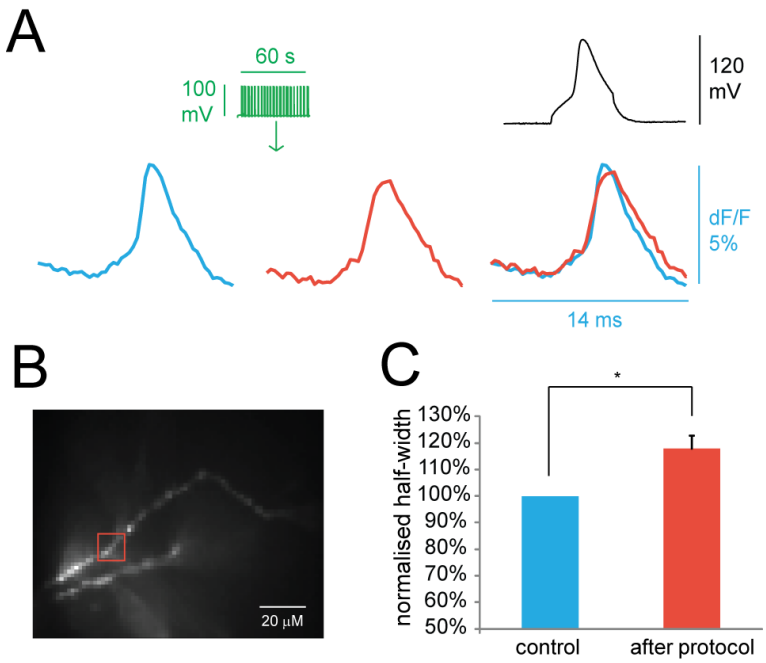

Figure 3.4.3 The half-width of test AP increased slightly after the stimulus protocol compared to control AP

A, NGFC bAP recorded with voltage imaging methods in vitro (blue, control; red, after conditioning protocol, black, AP from the same cell recorded with electrophysiology). **B**, red square showing the region of interest where ΔF/F in A was obtained. **C**, a summary histogram showing normalised half-width of interneurons recorded (n = 14, half-width after conditioning protocol was 118% ± 5.0% of control)

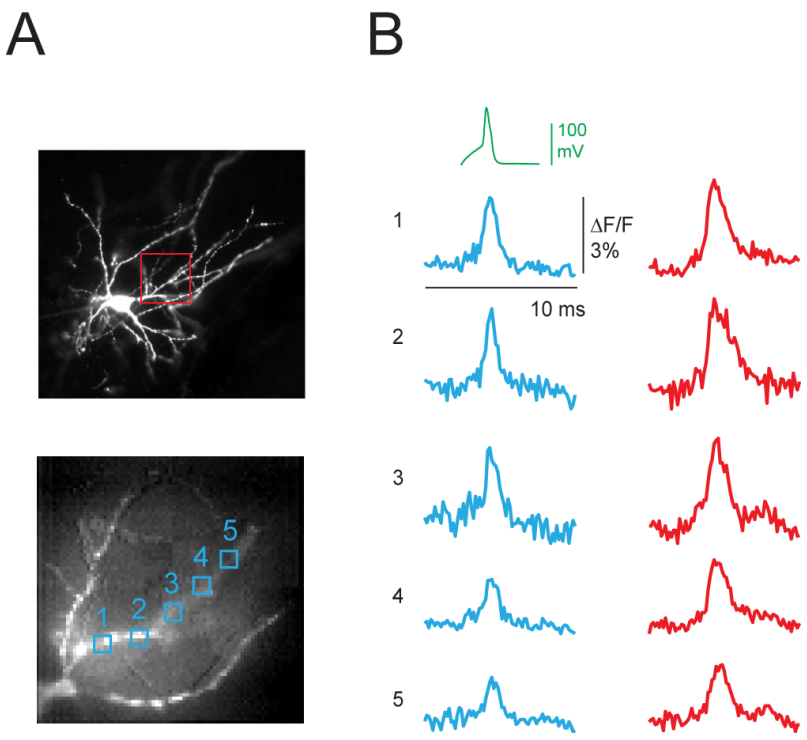

Figure 3.4.4 Application of K^+ channel blocker increases AP half-width

A, Top image, NGFC (filled with biocytin, visualised after biocytin-streptoavidin-Cy3 reaction) showing characteristic stellate dendrites (objective x20). Bottom image, the same neuron in A, which was loaded with JPW-1114 and voltage imaging was performed from dendritic sites included in the blue box; in particular, ΔF/F signals at the sites indicated (1-5, 4x4 pixels) were analysed. **B**, ΔF/F of bAP recorded from NGFC shown in A, the half-width of bAP increased after application of a K^+ channel blocker. Blue trace, control; red trace, in the presence of 1 mM 4-AP (n = 2).

3.5. What does AP backpropagation do?

A possible function for bAP is to activate downstream enzymes that are responsible for the synthesis of retrograde signalling molecules. It has been reported that rise in Ca^{2+} level are associated in retrograde messenger release such as cannabinoid (Nyilas et al., 2008). According to this idea, I have tested the hypothesis that the postsynaptic bAPs may elicit an increase in the dendritic Ca^{2+} concentration. First, I have recorded postsynaptic neurons with a high chloride internal solution containing the Ca^{2+} chelator BAPTA (10 mM). In these experiments, only pairs showing FSI immediately after the formation of whole-cell patch clamp recording were tested. In the presence of BAPTA, FSI was gradually attenuated (FSI was 69.7 ± 4.6% of control at the onset of the recording and 86.7 ± 3.0% of control after 8 ± 2 min., $p < 0.05$, $n = 4$, Figure 3.5.1), consistent with the delayed action of BAPTA at the distal dendritic sites of the recorded interneurons. Second, I have investigated the source of dendritic Ca^{2+} leading to FSI. To test the involvement of intracellular Ca^{2+} stores (Collin et al., 2005), I have included ryanodine (200 µm) and U73122 (3 µm) in the patch pipette of postsynaptic cells to inhibit Ca^{2+} release from the endoplasmic reticulum and phospholipase C (PLC), an important component of the Ca^{2+} signalling cascade, respectively. However, these Ca^{2+} store blockers in the postsynaptic cell did not alter FSI. The amplitude of FSI was initially 83.5 ± 6.2% of the baseline, and 78.9 ± 7.4% after 18 min of recording ($p > 0.1$, $n = 3$, Figure 3.5.2). This result rules out that the Ca^{2+} stores are involved in FSI induction. As a positive control, I have observed that the insertion of ryanodine (200 µm) and U73122 (3 µm) in the presynaptic cell gradually inhibited the uIPSCs in experiments lasting ~ 20 min (not shown).

Alternatively, the rise in dendritic calcium level may due to calcium entering through dendritic L-type Ca^{2+} channels, and this could trigger FSI. In addition, L-type

Ca^{2+} channels has been shown to be involved in short-term plasticity, but does not affect the baseline GABAergic transmission at low frequency (Jensen and Mody, 2001). Therefore, it is suitable to use a bath applied L-type Ca^{2+} channel blocker to test its involvement. I have found that bath applied nimodipine (10 μm), a L-type Ca^{2+} channel blocker, inhibited FSI without affecting the size of uIPSCs evoked by low frequency of stimulation. On average, FSI was 70.6 ± 4.8% of control at the onset of the recording and 94.8 ± 6.3% of control after 20 min of nimodipine application ($p < 0.01$, $n = 5$) (Figure 3.5.3). Taken together, these results suggest that L-type Ca^{2+} channels, but not Ca^{2+} stores, are involved in FSI induction.

Next, to directly measure Ca^{2+} signals associated with the stimulation firing protocol, I have performed Ca^{2+} imaging experiments of NGFC dendrites using the low-affinity indicator OG5N (0.5 mM) to minimise the physiological perturbation of the Ca^{2+} homeostasis. First, I have measured the dendritic Ca^{2+} signal associated with a single AP (Figure 3.5.4A) and with a train of ten APs at 100 Hz (Figure 3.5.4B). As shown in the figure, the Ca^{2+} transient associated with the AP train had a slower decay time compared to that associated with a single AP. Then, I have measured the Ca^{2+} signal associated with the stimulation protocol and compared it with the linear sum of a single AP response template. As expected from the previous series of experiments, the Ca^{2+} signal associated with the stimulation protocol was larger than that obtained by summation of template signals. Importantly, this supralinear Ca^{2+} summation, as quantified by the difference of the Ca^{2+} signal 10 s after the onset and at the end of the stimulation protocol, was significantly larger in the postsynaptic neurons showing FSI than in the postsynaptic cells that did not display FSI (Figure 3.5.4C, D, $n = 6$ each group, $p < 0.05$).

In order to estimate the change in dendritic free Ca^{2+} concentration associated with an action potential and with the stimulation protocol, I have performed a series of calibration experiments using both OG5N and MF2 in the patch pipette. Comparison of ΔF/F signals

associated with three different stimulation protocols (5, 10 or 20 APs at 100 Hz) gave a conversion factor of ~2.5 for OG5N (Figure 3.5.4E) indicating that ΔF/F=1% corresponded approximately to a free Ca^{2+} concentration change of 100 nM for this indicator, assuming a K_d = 25 μM for MF2 (Cueni et al., 2008). I conclude that a sustained elevation of free Ca^{2+} in the dendrites of the postsynaptic neuron (typically > 1 μM) is associated with the stimulation protocol that induces FSI. Such prolonged increase in dendritic Ca^{2+} could lead to the release of a chemical messenger.

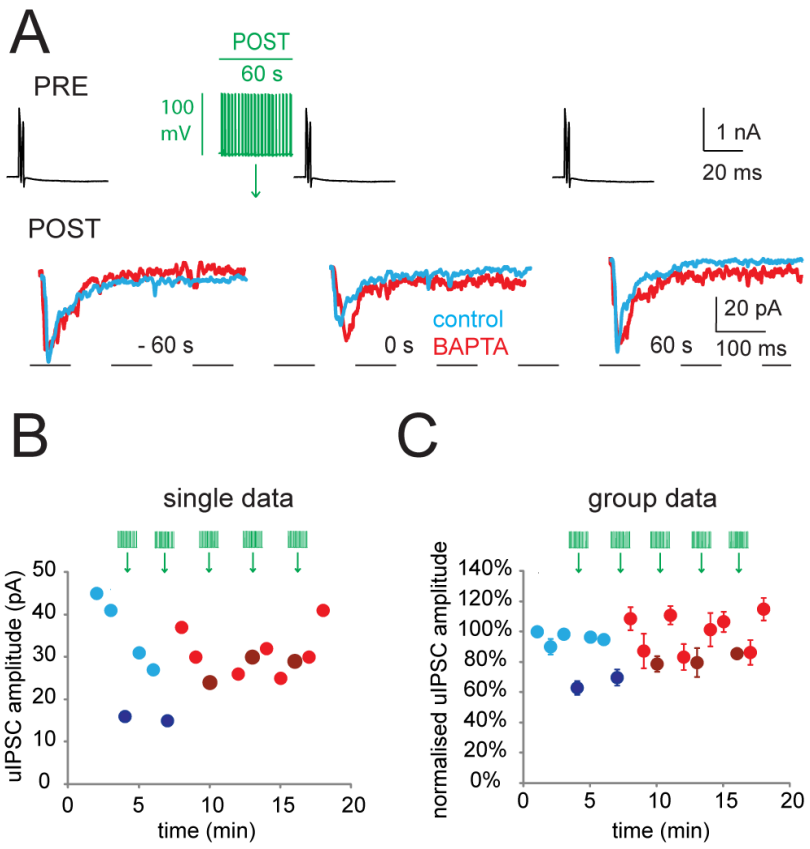

Figure 3.5.1 The Ca^{2+} buffer BAPTA attenuates FSI

A, Presynaptic action currents (PRE, black traces) evoked inward uIPSCs in a postsynaptic NGFC recorded with an electrode filled with 84 mM Cl^- solution (POST, blue traces). Injection of the stimulation protocol in the postsynaptic cell induced a transient depression of the uIPSC amplitude (middle blue trace), that returned to control level 60 s after the end of the stimulation protocol (right blue trace). Application of the Ca^{2+} chealator BAPTA (10 mM) attenuated FSI (red traces). **B**, quantification of the uIPSC peak amplitude that occurred before or during the bath application of nimodipine for the data shown in A (dark symbols denote values immediately after stimulation protocol). **C**, normalised data (mean and SEM) for all uIPSCs studied with this protocol (FSI control was 69.7 ± 4.6% and 86.7 ± 3.0% with BAPTA, $p < 0.05$, $n = 4$).

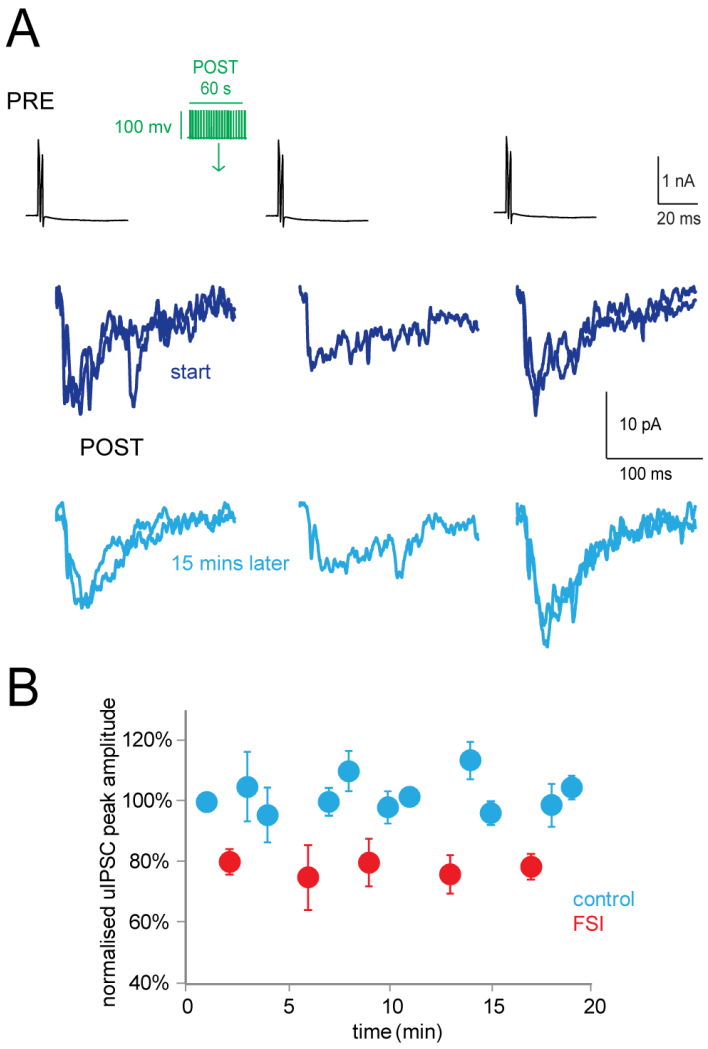

Figure 3.5.2 Blocking internal Ca^{2+} stores does not inhibit FSI

A, NGFC paired recording *in vitro*, voltage clamp mode, presynaptic action potentials (PRE, black traces) evoked depolarising uIPSCs in a postsynaptic cell recorded with an electrode filled with 84 mM Cl- solution (POST, left traces superimposed recorded 120 s or 60 s before the stimulation protocol, dark blue: control, light blue: ryanodine). Injection of the stimulation protocol in the postsynaptic cell induced a transient depression of the uIPSC amplitude (middle dark blue: control, middle light blue: ryanodine), that returned to control level 60 s after the end of the stimulation protocol (right traces superimposed recorded for 60 s or 120 s after the stimulation protocol, dark blue: control, light blue: ryanodine). **B**, normalised data (mean and SEM) for all uIPSCs studied with this protocol (FSI control was 83.6 ± 6.2% and 78.9 ± 7.4% with ryanodine after 18 min., $p > 0.1$, $n = 3$).

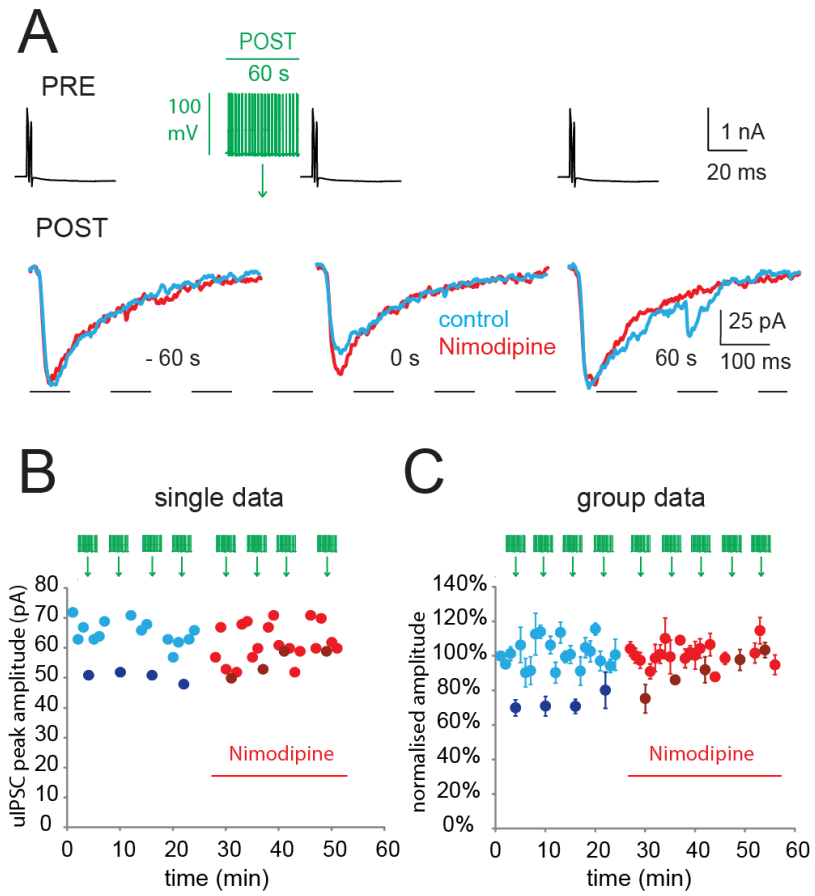

Figure 3.5.3 The L-type Ca^{2+} blocker nimodipine inhibits FSI

A, Presynaptic action currents (PRE, black traces) evoked inward uIPSCs in a postsynaptic NGFC recorded with an electrode filled with 84 mM Cl^- solution (POST, blue traces). Injection of the stimulation protocol in the postsynaptic cell induced a transient depression of the uIPSC amplitude (middle blue trace), that returned to control level 60 s after the end of the stimulation protocol (right blue trace). Application of the L-type Ca^{2+} channel blocker nimodipine (10 µM) inhibited FSI (red traces). **B**, quantification of the uIPSC peak amplitude that occurred before or during the bath application of nimodipine for the data shown in A (dark symbols denote values immediately after stimulation protocol). **C**, normalised data (mean and SEM) for all uIPSCs studied with this protocol (FSI control was 70.9 ± 6.0% and 96.7 ± 3.5% with nimodipine, $p < 0.01$, $n = 4$).

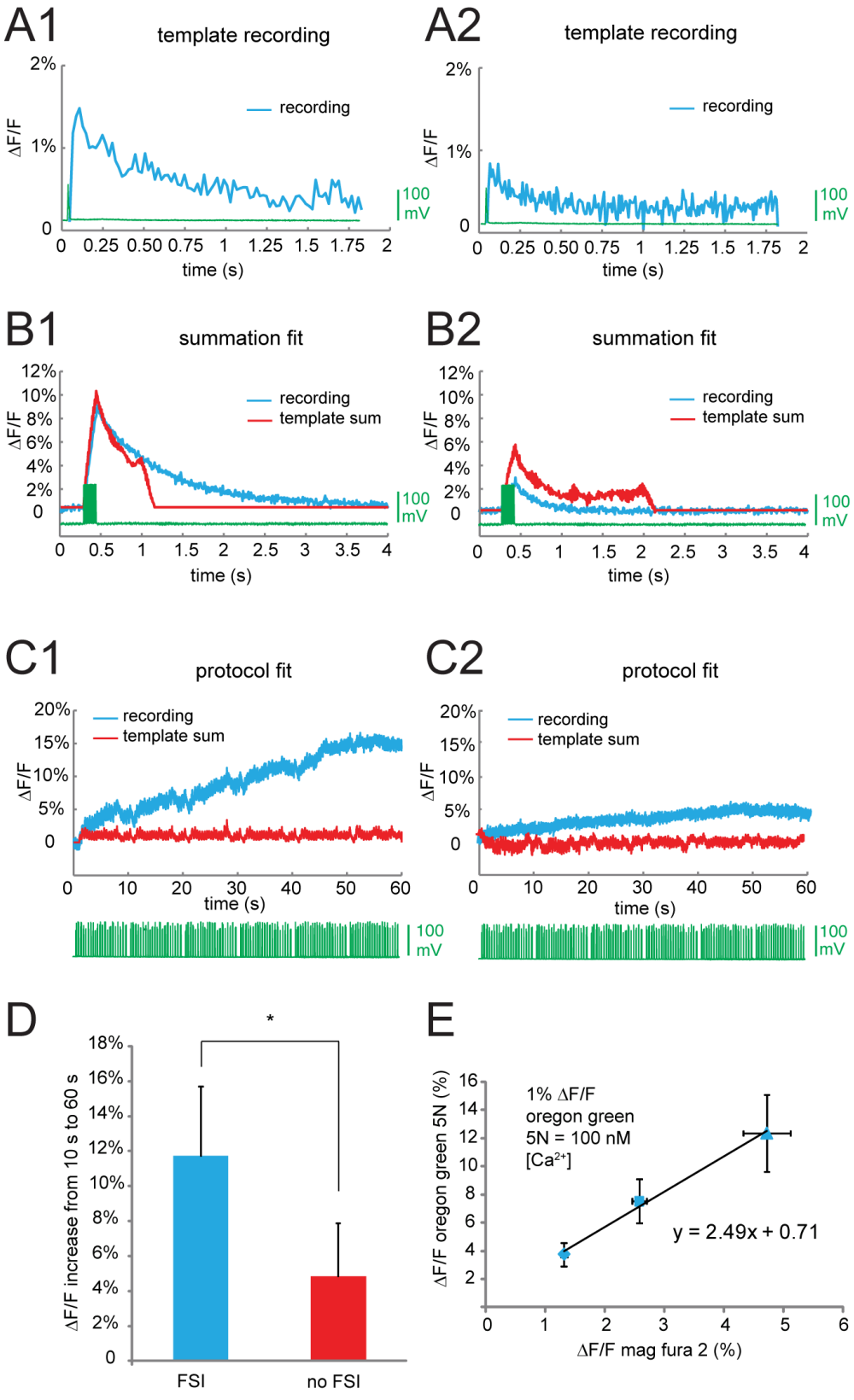
A1
template recording
recording
ΔF/F
2%
1%
0
100 mV
0 0.25 0.50 0.75 1 1.25 1.5 1.75 2
time (s)
A2
template recording
recording
ΔF/F
2%
1%
0
100 mV
0 0.25 0.50 0.75 1 1.25 1.5 1.75 2
time (s)
B1
summation fit
recording
template sum
ΔF/F
12%
10%
8%
6%
4%
2%
0
100 mV
0 0.5 1 1.5 2 2.5 3 3.5 4
time (s)
B2
summation fit
recording
template sum
ΔF/F
12%
10%
8%
6%
4%
2%
0
100 mV
0 0.5 1 1.5 2 2.5 3 3.5 4
time (s)
C1
protocol fit
recording
template sum
ΔF/F
20%
15%
10%
5%
0
0 10 20 30 40 50 60
time (s)
100 mV
C2
protocol fit
recording
template sum
ΔF/F
20%
15%
10%
5%
0
0 10 20 30 40 50 60
time (s)
100 mV
D
*
ΔF/F increase from 10 s to 60 s
18%
16%
14%
12%
10%
8%
6%
4%
2%
0
FSI
no FSI
E
1% ΔF/F
oregon green
5N = 100 nM
[Ca2+]
y = 2.49x + 0.71
ΔF/F oregon green 5N (%)
16
14
12
10
8
6
4
2
0 1 2 3 4 5 6
ΔF/F mag fura 2 (%)

Figure 3.5.4 Sustained elevation of Ca^{2+} in the dendrites of postsynaptic interneurons triggers FSI

A, ΔF/F Ca^{2+} signal from an NGFC with FSI (A1) or without FSI (A2) filled with OG5N (blue trace) associated with an AP (green trace, single trial). **B**, Same as A (in the same neurons) but for a train of ten APs at 100 Hz (single trial); note the increased decay time compared to the calcium signal associated with single AP; the red trace is the summation of 10 template ΔF/F Ca^{2+} signals associated with the single AP (note the faster decay time). **C,** ΔF/F Ca^{2+} signals (blue traces) associated with the stimulation protocol (green traces, single trial) from the dendrites of two NGFC cells, one exhibiting FSI (C1) and the other not showing FSI (C2); the red traces are again the linear summation of single AP template ΔF/F Ca^{2+} signals; note the larger supralinear summation of ΔF/F Ca^{2+} signals in the cell exhibiting FSI. **D**, Columns and error bars are the mean and the SEM of the difference of ΔF/F dendritic Ca^{2+} signal occurring 60 s and 10 s after the onset of the stimulation protocols in postsynaptic neurons with FSI (blue column) and in cells without FSI (red column); this value in the two populations of neurons was significantly different ($n = 6$, $p < 0.05$). **E**, calibration of OG5N ΔF/F Ca^{2+} signal in terms of MF2 ΔF/F Ca^{2+} signal: plot of OG5N ΔF/F peak vs. MF2 ΔF/F peak associated with different protocols (spade, 5 APs at 100 Hz; square, 10 APs at 100 Hz; triangle, 20 APs at 100 Hz, $n = 6$) in the same cells. The linear fit gives a conversion factor of 2.5; given that 1% for MF2 corresponds to ~250 nM, 1% for OG5N corresponds to ~100 nM.

3.6. What messenger(s) is responsible for FSI?

What messenger triggers FSI? A well-known molecular marker for NGFCs of the SLM is nNOS. Indeed, it has been reported that nNOS is expresses by several hippocampal interneurons. Major cell types including both PV-positive and CCK-positive basket cells, PV-positive axo-axonic cells, Ivy cells and NGFCs (Price et al., 2005; Tricoire et al., 2010; Tricoire and Vitalis, 2012). In addition, the NO receptor NOsGC has been detected in the axon terminals and in the soma-dendritic compartment of various interneurons in all layers of the hippocampus (Szabadits et al., 2007). It seems NOsGC are present in several types of interneurons as NOsGC subunits were found to co-localise with many major neuronal markers such as CCK, PV, nNOS and SOM, although no correlation between the signal intensity of NOsGC and specific neuronal markers were found (Szabadits et al., 2007). Both NOS and NOsGC signals are abundant in the SLM of the hippocampus (Szabadits et al., 2007). Therefore, NO can be a possible candidate to be responsible for FSI, in which NO could be released from the dendrites of NGFCs and other interneuron types of the SLM, diffuses retrogradely, and inhibits the release of GABA from other interneurons.

I have tested this hypothesis by studying the action of the nNOS inhibitor L-NAME (200 µM) on FSI. I started by injecting the stimulation protocol in a postsynaptic neuron to induce FSI (76.7 ± 2.5%, $p < 0.001$, $n = 11$). Then I have applied the nNOS inhibitor L-NAME (200 µM) for at least 10 minutes and the stimulation protocol was repeated. I have found that in the presence of L-NAME, FSI was abolished in 10/11 cell pairs (95.1 ± 2.4%, $p < 0.001$, $n = 10/11$, Figure 3.6.1). It is worth noting that I have found no significant effect of 200 µM L-NAME on spontaneous (s)IPSCs (in the presence of 3 mM kynurenic acid to block sEPSCs, $n = 3$, Figure 3.6.2). Both amplitude and inter-events distributions of sIPSCs were not significantly different in control and in the

presence of L-NAME ($p > 0.1$ Kolmogorov-Smirnov test for each cell), suggesting that the intracellular NO level is low under baseline conditions. Moreover, L-NAME did not affect the peak amplitude or the kinetics of single VSD-recorded bAP elicited 125 ms after 60 s stimulation firing - the bAP peak amplitude and the half width was not changed by L-NAME ($p > 0.1$, $n = 10$, Figure 3.6.3), suggesting that L-NAME does not affect bAP and that NO is released downstream of the bAP along the dendrites of the interneurons.

Further experiments confirmed the involvement of NO as a signal mediating FSI. First, I have investigated whether blocking the NOsGC receptor, the main effector of NO, abolished FSI. Similar to the nNOS inhibitor, bath application of ODQ (10 μM), a NOsGC receptor antagonist, applied for at least 10 minutes, blocked FSI that was successfully induced before the application of the drug in each cell tested (Figure 3.6.4) (FSI control was 71.1 ± 3.7% and during ODQ was 96.8 ± 2.3%, $p < 0.01$, $n = 8$). Second, the application of the NO precursor L-arginine (1 mM, $n = 5$) (Palmer et al., 1988) potentiated FSI (FSI control was 73.1 ± 4.4% and during L-arginine was 62.4 ± 6.1%, $p < 0.05$, $n = 5$, not shown). Third, the application of the NO donor SNP (200 μM) occluded FSI, consistent with the idea that this agent would saturate NO receptors and with the action of this drug on NO-mediated modulation of excitatory synaptic events (Makara et al., 2007). FSI was 72.4 ± 5.6% before and 96.5 ± 6.3% in the presence of SNP, $n = 6$, $p < 0.05$, Figure 3.6.5). Interestingly, I have also found that sometimes SNP was able to reduce the amplitude of uIPSCs (Figure 3.6.5A, top traces), often in younger animals, consistent with data from a previous study (Makara et al., 2007).

In addition, the likelihood of FSI detection was enhanced when synaptically-coupled pairs of tdTomato-labelled nNOS neurons were recorded in a nNOS-Cre-tdTomato mouse line, in which nNOS expressing neurons were visible (Figure 3.6.6). In these experiments 7 out of 9 cell pairs tested showed a robust FSI (69.4 ± 2.6%, $p < 0.001$) induced by the stimulation protocol. This frequency of occurrence of FSI was

significantly higher than the probability of FSI occurrence in pairs recorded from control rats (78% versus 39% FSI detection, $p < 0.01$, chi square test, Figure 3.6.6D). In the two cell pairs that did not show FSI, it might be that the presynaptic cell does not contain NOsGC. The FSI observed when recording from tdTomato-labelled nNOS neurons was blocked by 200 µM L-NAME or 10 µM ODQ (n = 3, data not shown). Control analysis showed that the nNOS-CreER driver correctly labelled nNOS positive neurons. To this end, three tdTomato mice (n = 3) have been perfused, their brain fixed and tested for a specific antibody against nNOS. The great majority of tdTomato expressing hippocampal neurons from these mice were immunolabelled for nNOS (98 out of 104 of counted cells, Figure 3.6.6E, F).

Taken together, my data suggest that NO is a signal that responsible for FSI. It is likely that NO is released from the dendrites of NGFCs, diffuses retrogradely, binds to specific presynaptic receptors and inhibits the release of GABA from other NGFCs.

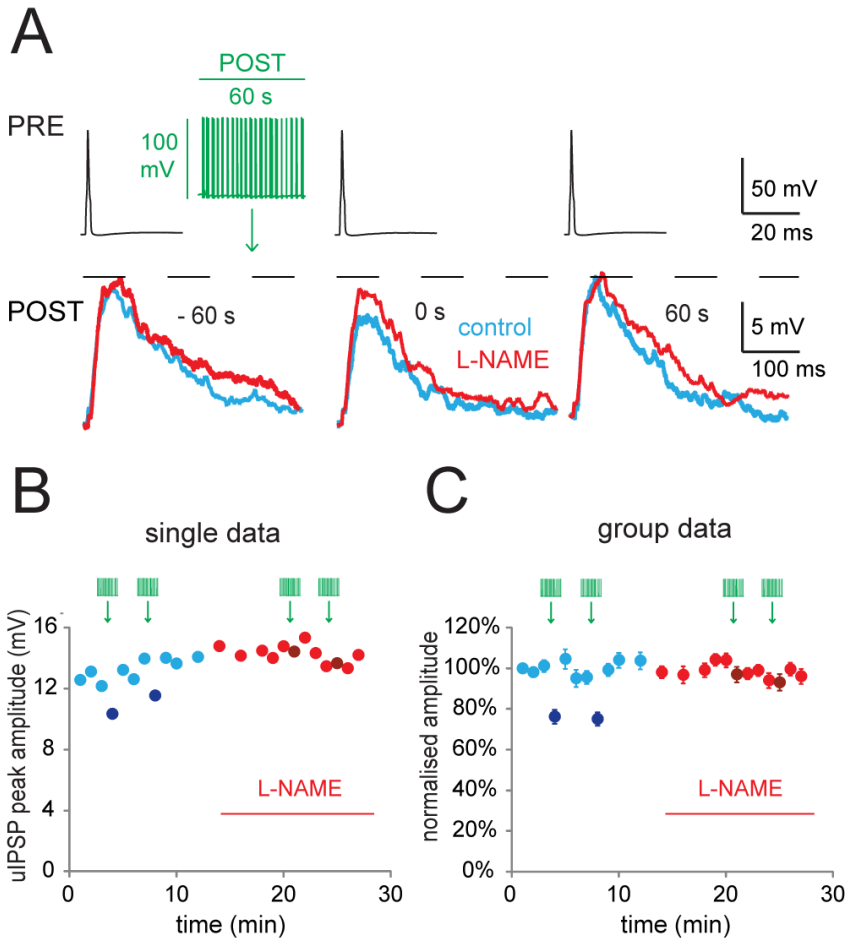

Figure 3.6.1 The nNOS inhibitor L-NAME blocks FSI

A, Presynaptic APs (PRE, black traces) elicited depolarising uIPSPs (control, left traces superimposed) recorded with an electrode filled with 84 mM Cl^- solution showing FSI immediately after stimulation protocol applied to a postsynaptic NGFC (control, blue middle trace). The uIPSP recovered 60 s after the stimulation protocol (blue trace, right). Application of the nNOS inhibitor L-NAME (200 µM) blocked FSI (red traces). **B**, quantification of the uIPSP peak amplitude that occurred before or after the stimulation protocol (dark symbols) in control and in the presence of L-NAME for the data shown in A. **C**, normalised data (mean and SEM, shaded areas) for all uIPSPs or uIPSCs studied with this protocol (FSI control was 76.6 ± 2.5% and 95.1 ± 2.4% with L-NAME, $p < 0.001$, $n = 10$).

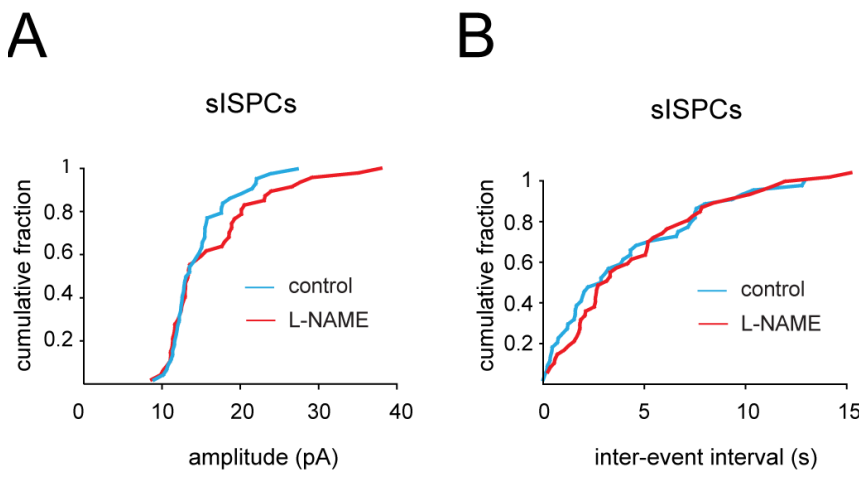

Figure 3.6.2 L-NAME has no effect on kinetics of sIPSCs

A, sIPSCs recorded with an electrode filled with 84 mM Cl^- solution in the presence of 3 mM kynurenic acid**.** The cumulative fraction of sIPSC amplitude in control condition (blue) and in the presence 200 µM L-NAME were similar (KS $p > 0.1$, $n = 3$). **B**, analysis of inter-event intervals of the cells shown in A. There were no significant difference for sIPSCs recorded in control condition and in the presence of 200 μM L-NAME (KS $p > 0.1$, $n = 3$).

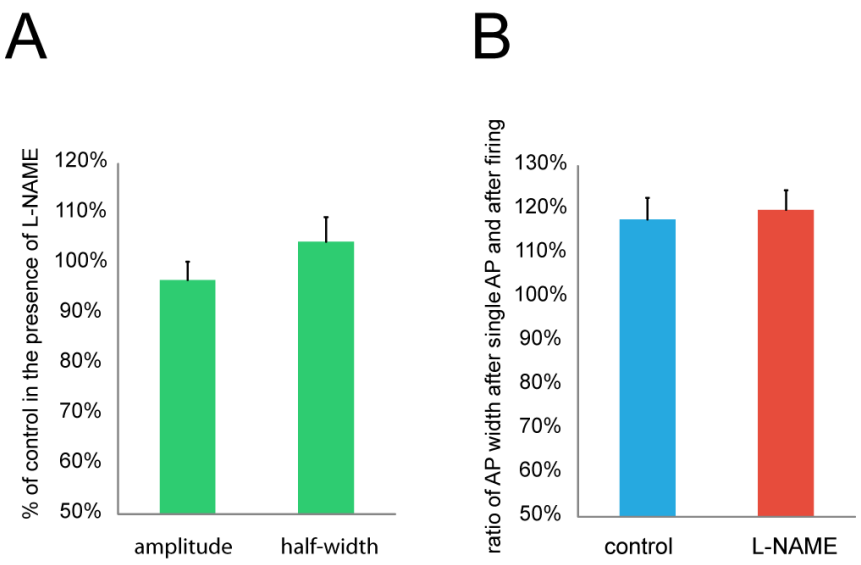

Figure 3.6.3 L-NAME has no effect on the kinetics of bAPs

A, summary histogram showing amplitude and half-width of bAPs in the presence of 200 μM L-NAME as a percentage of control, there were no significant differences ($p > 0.1$, $n = 10$). **B**, summary histogram showing the ratio of between test AP and control AP half-width in control condition or in the presence of 200 μM L-NAME, there were no significant differences ($p > 0.1$, $n = 10$).

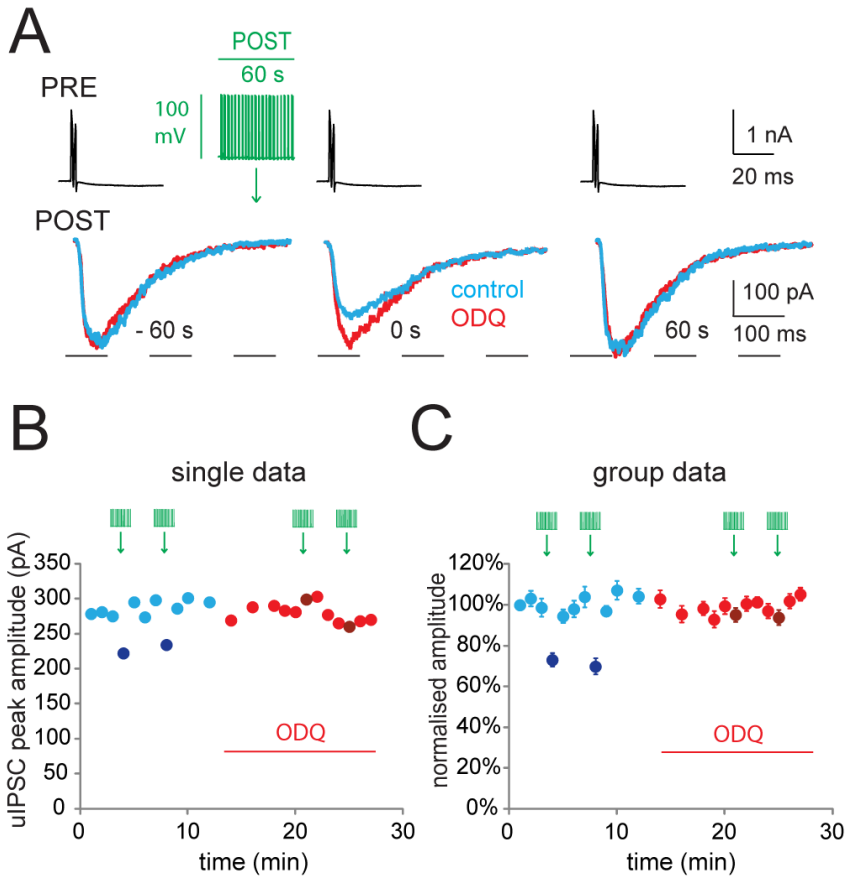

Figure 3.6.4 The NO receptor antagonist ODQ blocks FSI

A, Presynaptic action currents (PRE, black traces) evoked inward uIPSCs in a postsynaptic NGFC recorded with an electrode filled with 84 mM Cl^- solution (POST, blue traces). Injection of the stimulation protocol in the postsynaptic cell induced a transient depression of the uIPSC amplitude (middle blue trace), that returned to control level 60 s after the end of the stimulation protocol (right blue trace). Application of the NO receptor antagonist ODQ (10 µM) blocked FSI (red traces). **B**, quantification of the uIPSC peak amplitude that occurred before or in the presence of ODQ for the data shown in A (dark symbols denote values immediately after stimulation protocol). **C**, normalised data (mean and SEM) for all uIPSPs or uIPSCs studied with this protocol (FSI control was 71.1 ± 3.7% and 96.8 ± 2.3% with ODQ, $p < 0.01$, $n = 8$).

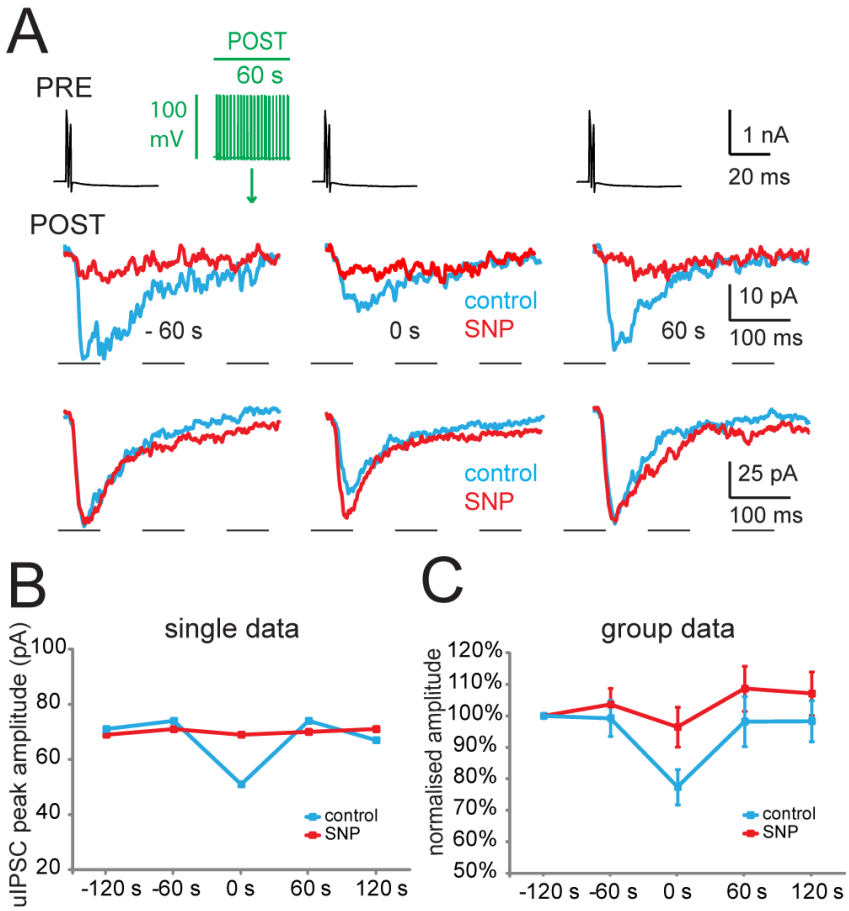

Figure 3.6.5 The NO donor SNP occluded FSI

A, Presynaptic APs (PRE, black traces) elicited depolarising uIPSPs (control, left traces superimposed) recorded with an electrode filled with 84 mM Cl^- solution showing FSI immediately after stimulation protocol applied to a postsynaptic NGFC (control, blue middle trace). The uIPSP recovered 60 s after the stimulation protocol (blue trace, right). Application of the NO donor SNP (200 µM) occluded FSI (red traces). Note that top traces showing SNP reduced uIPSC peak amplitude and in bottom traces SNP did not reduce uIPSC peak amplitude. **B**, quantification of the uIPSC peak amplitude in bottom traces of A. **C**, normalised data (mean and SEM, shaded areas) for all uIPSPs or uIPSCs studied with this protocol (72.4 ± 5.6% before and 96.5 ± 6.3% in the presence of SNP, $n = 6$, $p < 0.05$).

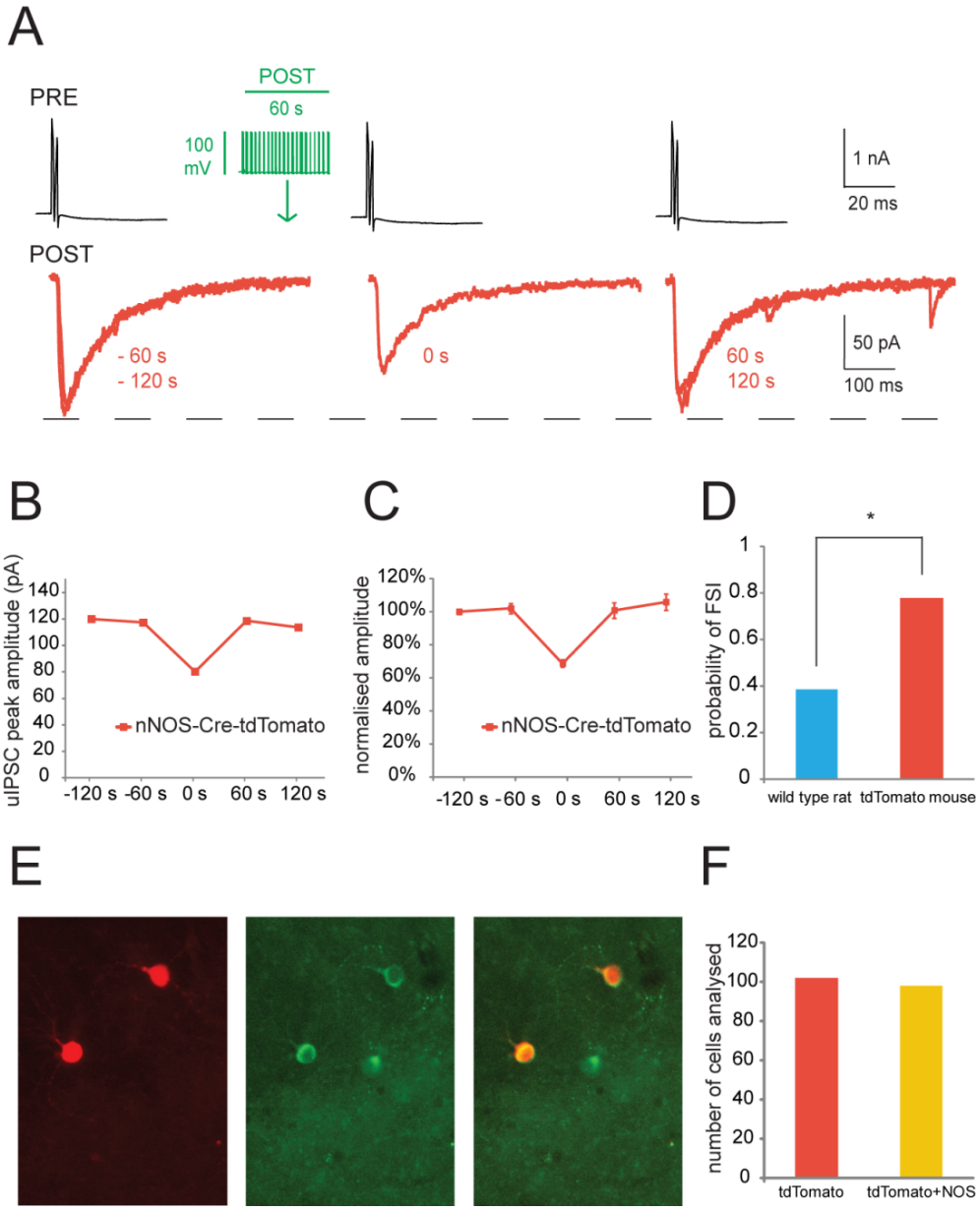
A
PRE
POST
60 s
100 mV
1 nA
20 ms
POST
- 60 s
- 120 s
0 s
60 s
120 s
50 pA
100 ms
B
uIPSC peak amplitude (pA)
140
120
100
80
60
40
20
0
-120 s -60 s 0 s 60 s 120 s
nNOS-Cre-tdTomato
C
normalised amplitude
120%
100%
80%
60%
40%
20%
0%
-120 s -60 s 0 s 60 s 120 s
nNOS-Cre-tdTomato
D
*
probability of FSI
1
0.8
0.6
0.4
0.2
0
wild type rat
tdTomato mouse
E
F
number of cells analysed
120
100
80
60
40
20
0
tdTomato
tdTomato+NOS

Figure 3.6.6 FSI occurs frequently in pairs of neurons expressing nNOS-Cre-tdTomato.

A, NGFC paired recording, voltage clamp mode, a presynaptic action current (PRE, black trace) evoked an inward uIPSC in a postsynaptic NGFC recorded with an electrode filled with 84 mM Cl^- solution (POST, red traces superimposed). Injection of the stimulation protocol in the postsynaptic cell induced a transient depression of the uIPSC amplitude (middle trace), that returned to control level 60 s and 120 s after the stimulation protocol (right traces superimposed). **B,** uIPSC mean peak amplitude before and after the stimulation protocol for the data shown in A. **C**, summary of mean and SEM peak amplitudes of uIPSCs before and after the stimulation protocol in all pairs recorded (FSI = 69.4 ± 2.6%, $p < 0.001$, $n = 7$). **D**, bar graphs that the probability to observe FSI was significantly higher when pairs of tdTomato neurons were recorded compared to pairs recorded in wild type rats (78% versus 39% FSI detection, $p < 0.01$, chi square test). **E**, Examples of two tdTomato expressing neurons of the hippocampal SLM (left), also immunopositive for nNOS (middle); a merged picture is shown on the right. An nNOS immunopositive cell not expressing tdTomato is also visible. **F**, summary data, 98 out of 104 tdTomato expressing neurons also expressed nNOS.

3.7. Involvement of cannabinoid in FSI

Given the importance of eCB in DSI, it is logical to test whether it is also involved in FSI. I have used the CB1R blocker AM251 to study this issue, and I had mixed results. I have found that AM251 (2 μM) abolished FSI in 6/9 pairs (73.7 ± 2.6% of control before and 95.7 ± 1.3% of control, $p < 0.001$) (Figure 3.7.1). In contrast, AM251 did not alter FSI in another three cell pairs; in these pairs, the subsequent bath application of L-NAME abolished FSI (FSI was 74.1 ± 6.1% in control, 77.9 ± 5.3% in the presence of AM-251, $p > 0.05$, and 97.4 ± 3.9% after addition of L-NAME, $p < 0.05$, $n = 3$, Figure 3.7.2). In another cell pair, FSI was only partially blocked by AM251 and then it was fully blocked after by the subsequent addition of L-NAME. My results also indicate that the CB1R is likely to be present at least in the terminals of NGFC subpopulations. This is because AM251 was able to successfully block FSI in 6/9 cell pairs in which the presynaptic cell is likely to be NGFCs, as they exhibited $GABA_{A,slow}$ kinetics and autpatic currents. However, my data does not allow a firm conclusion of whether there is a functional interaction or a parallel effect downstream the activation of CB1 and NO receptors, as well as if they occur in the same or in different pairs of neurons.

As a matter of fact, cell types studied in these experiments included both NGFCs as well as other interneuron of the SLM. Specifically, for cell pairs that responded to AM251, all presynaptic cells were identified as NGFCs or putative NGFCs, two postsynaptic cell was identified to be NGFC, but all the other postsynaptic cells could not be identified. In the three cell pairs that AM251 did not work, all presynaptic cells were identified as NGFCs, however, I was unable to identify the postsynaptic cells for technical reasons.

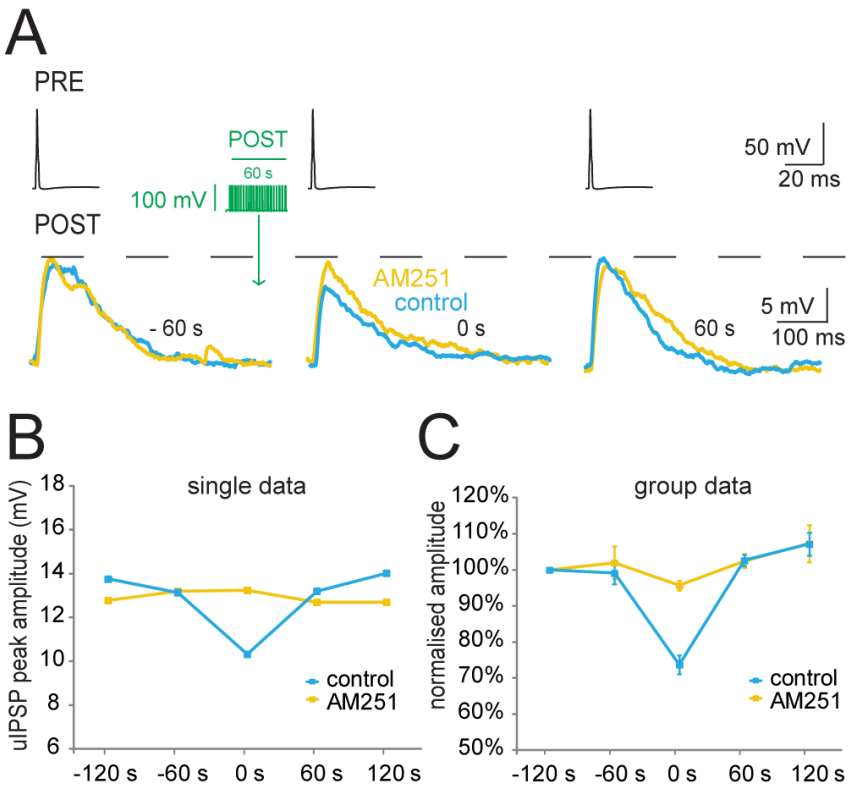

Figure 3.7.1 The CB1R antagonist AM251 blocks FSI

A, Presynaptic APs (PRE, black traces) elicited depolarising uIPSPs recorded with an electrode filled with 84 mM Cl^- solution showing FSI immediately after stimulation protocol applied to a postsynaptic NGFC (control, blue middle trace). The uIPSP recovered 60 s after the stimulation protocol (blue trace, right). Application of the CB1R blocker AM251 blocked FSI (yellow traces). **B**, quantification of the uIPSP peak amplitude that occurred before or after the stimulation protocol in control and in the presence of AM251 for the data shown in A. **C**, normalised data (mean and SEM, shaded areas) for all uIPSPs or uIPSCs studied with this protocol (FSI control was 73.7 ± 2.6% and 95.7 ± 1.3% with AM251, $p < 0.001$, $n = 6$).

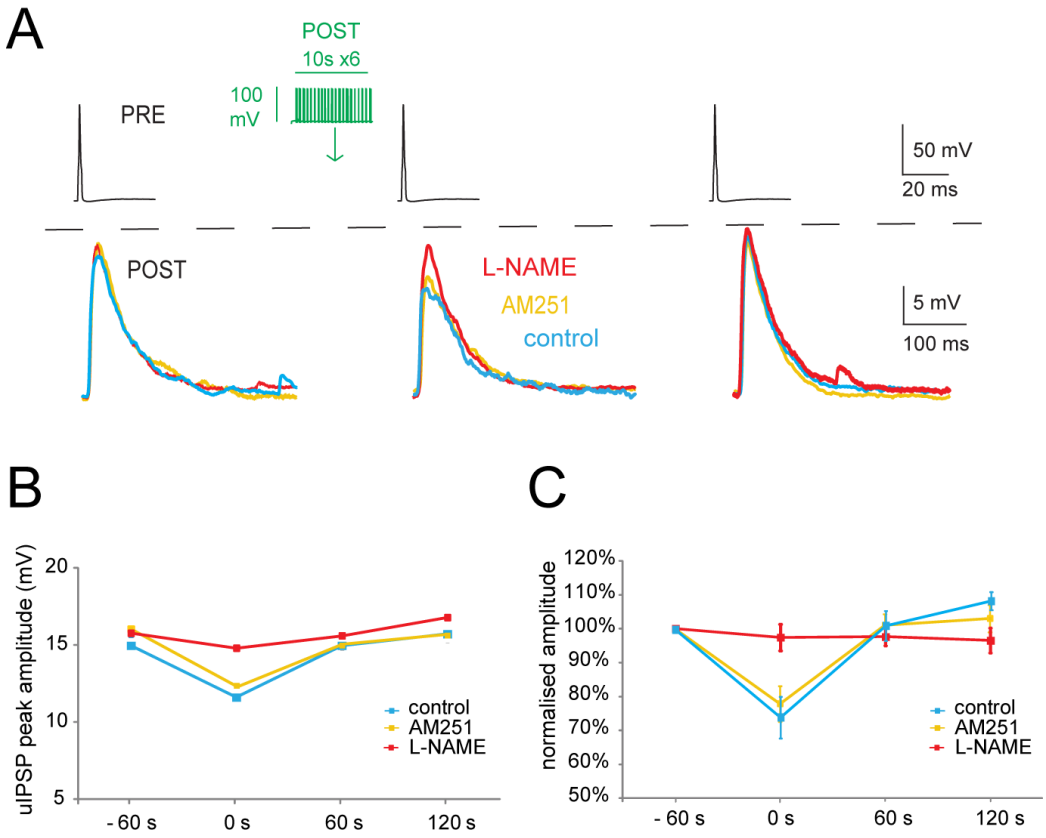

Figure 3.7.2 L-NAME blocks FSI in cell pairs that are not affected by AM251

A, Presynaptic APs (PRE, black traces) elicited depolarising uIPSPs recorded with an electrode filled with 84 mM Cl^- solution showing FSI immediately after stimulation protocol applied to a postsynaptic NGFC (control, blue middle trace). The uIPSP recovered 60 s after the stimulation protocol (blue trace, right). Application of the CB1R blocker AM251 did not block FSI (yellow traces), application of nNOS inhibitor L-NAME (200 μM) in the same cell pair blocked FSI (red traces) **B**, quantification of the uIPSP peak amplitude that occurred before or after the stimulation protocol in control for the data shown in A. **C**, normalised data (mean and SEM, shaded areas) for all uIPSPs or uIPSCs studied with this protocol (FSI was 74.1 ± 6.1% in control, 77.9 ± 5.3% in the presence of AM-251, $p > 0.05$, and 97.4 ± 3.9% after addition of L-NAME, $p < 0.05$, $n = 3$).

3.8. Physiological implications of FSI

To test the physiological role of FSI on single cell integration, I recorded putative unitary EPSPs in NGFCs evoked by the minimal stimulation of the SLM at gamma frequency in the presence of 5 mM gabazine and 50 mM CGP35348 to block synaptic inhibition. This stimulation evoked short-term EPSP facilitation followed by depression, as previously reported (Price et al., 2005). Of note, I found that the stimulation protocol (*in vivo* firing pattern) did not evoke any significant change in the amplitude of these EPSPs, excluding a retrograde modulation of excitatory synapses (the EPSPs immediately after the firing protocol were 95.8 ± 7.0% of control, $p > 0.5$, $n = 3$, Figure 3.8.1). Next, I injected a train of EPSPs as synaptic conductance by using dynamic clamp (dEPSPs) in postsynaptic NGFCs (Figure 3.8.2A). Since NGFCs have short dendrites and are biophysically compact, the somatic injection of unitary dEPSPs should represent a realistic representation of EPSPs evoked by stimulation of one or a few fibres present in the SLM, such as the perforant path from the EC. At the same time as dEPSPs injection, an action potential in a presynaptic NGFC was also evoked, and this elicited a hyperpolarising uIPSP in the postsynaptic NGFC. Next, the stimulation protocol (*in vivo* firing pattern) was applied to the postsynaptic NGFC, to induce FSI and transiently reduce the size of the uIPSP (69.4 ± 10.6% of control, $p < 0.05$, $n = 8$). I observed that when FSI occurred, the amplitude of the dEPSPs was significantly increased ($p < 0.05$ for the first three dEPSPs of the train, $n = 8$, Figure 3.8.2C) compared to dEPSPs elicited in the presence of control synaptic inhibition before or after FSI. Remarkably, this affected several sequential dEPSPs, consistent with the long-lasting duration of NGFC-evoked uIPSPs (Tamas et al., 2003; Price et al., 2005).

Thus, FSI transiently increased the size of the dEPSPs thereby promoting the temporal/spatial integration of the uEPSPs elicited by stimulation of perforant path/other

excitatory fibres present in the SLM.

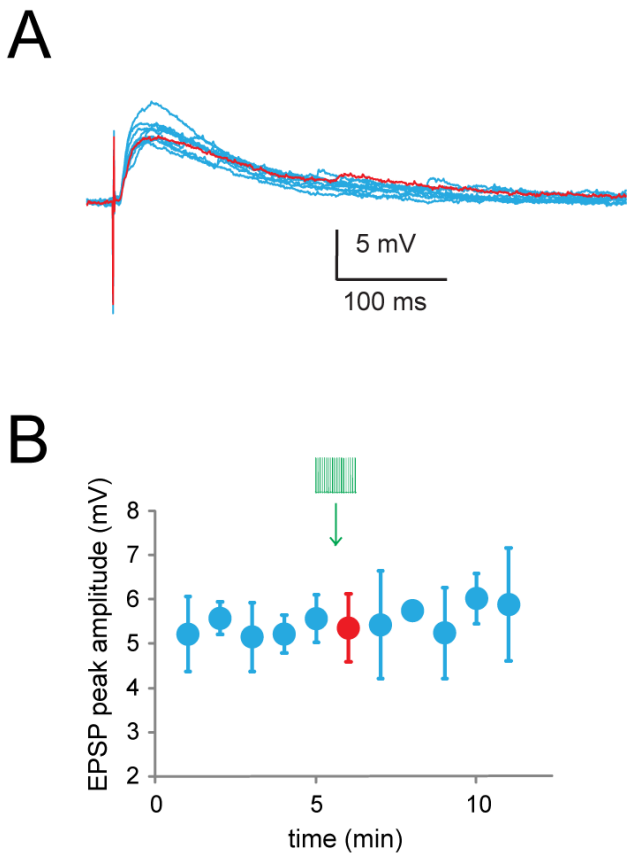

Figure 3.8.1 Injection of *in vivo* firing pattern does not affect EPSPs

A, single NGFC recording *in vitro*, current clamp mode, extracellular stimulation in regions close to the recording cell evoked steady EPSPs. The EPSP amplitude from extracellular stimulation shortly after injection of the stimulation protocol (red trace) is similar to control EPSPs (blue traces superimposed, baseline and recovery). **B**, summary graph (EPSPs immediately after the firing protocol were 95.8 ± 7.0% of control, $p > 0.5$, $n = 3$).

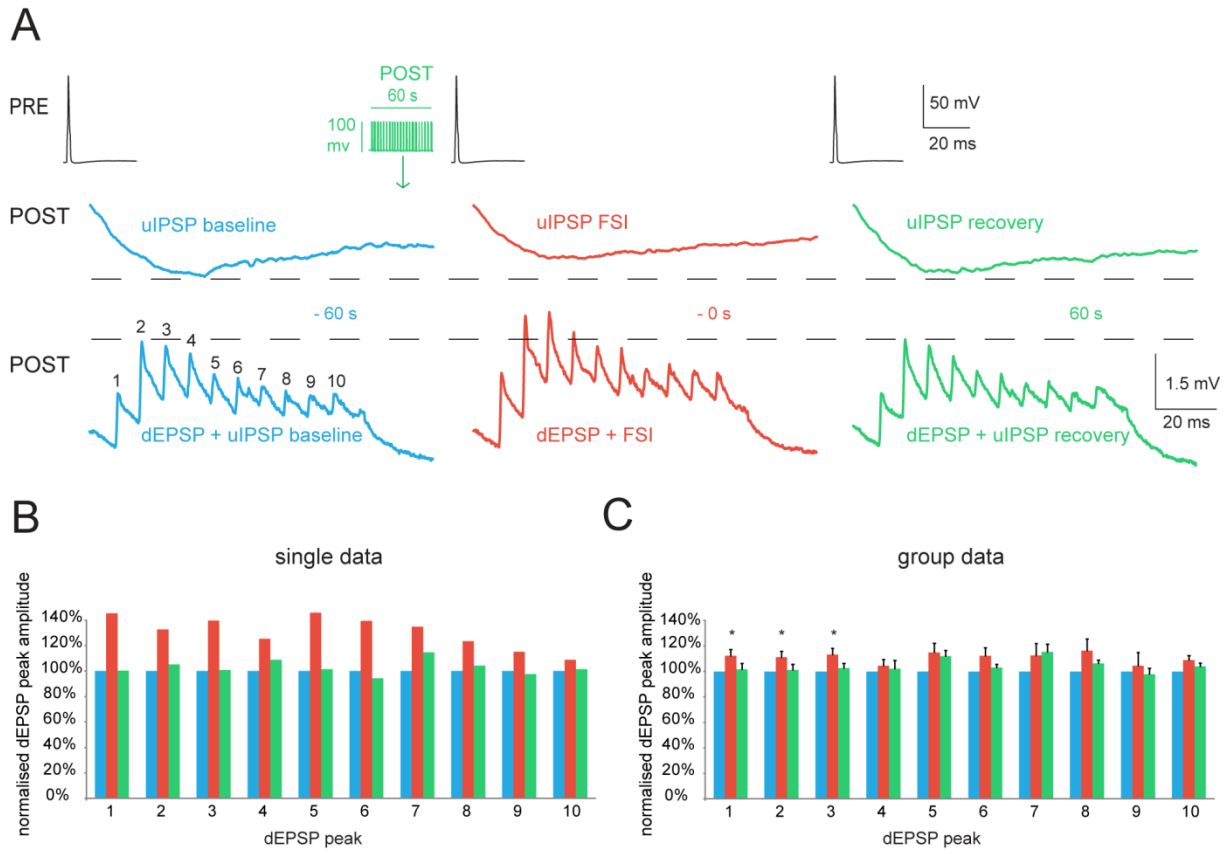

Figure 3.8.2 FSI transiently modulates EPSPs impinging onto NGFCs

A, An EPSP train was injected as synaptic conductance using dynamic clamp (POST, dEPSPs, blue trace, - 60 s) in a postsynaptic NGFC while an action potential in a presynaptic NGFC (PRE, black trace) elicited a coincident uIPSP. Application of the stimulation protocol in the postsynaptic cell evoked a transient, smaller uIPSP (FSI). As a result, a significant enhanced depolarisation level was reached by several dEPSPs of the train (red trace), the depolarisation level of the EPSPs returned to the baseline 60 s after FSI (green trace, 60 s). **B**, **C**, normalised values of the dEPSPs amplitude during FSI (red bars) or 60 s after FSI (recovery, green bars) versus before FSI (blue histograms), for the events shown above (B) or for all recorded cell pairs (C). In the presence of FSI, the first three dEPSPs had significantly larger amplitude than before FSI ($p < 0.05$, $n = 8$).

4. DISCUSSION

The data suggest novel physiological roles for the rhythmic firing of hippocampal NGFCs during theta oscillations and for the presence of NO in this interneuron type. Specifically, NO acts as a transmitter, likely released by the dendrites and possibly acting at presynaptic site, to modulate the strength of local inhibitory circuits, an event I referred to as FSI. In addition, I have also showed that FSI transiently modifies the strength of incoming EPSPs onto interneurons.

4.1. *in vivo* firing pattern induces FSI

The FSI plastic event reported here resembles the classical DSI phenomenon consisting of postsynaptic depolarisation-induced suppression of synaptic inhibition (Alger, 2012). However I triggered FSI through the injection of a firing sequence recorded *in vivo* during theta oscillations (Fuentealba et al., 2010) and replayed in the same cell type *in vitro*. In contrast, DSI is usually triggered by a prolonged steady depolarisation of the postsynaptic neuron (Regehr et al., 2009). Here I used an *in vivo* firing sequence during theta oscillations because this rhythm is physiologically relevant and it is prominent in the SLM (Buzsáki, 2002).

Importantly, the choice of firing pattern was based on a previous study in our laboratory, which showed that such patterns could trigger a mid-term depression of NGFC-evoked unitary IPSCs (Karayannis et al., 2010). This *in vivo* firing pattern of NGFC was recorded in anaesthetised rats during the transition from slow-wave oscillation to theta oscillations and thus offers physiological relevance (Figure 1.3.7.1). The *in vivo* firing pattern of two NGFCs were recorded in the Fuentealba et al. study, and

both cells showed a clear phase preferences for theta oscillations and is less inclined towards other brain states such as ripples (Fuentealba et al., 2010). The firing pattern used in this study is derived the NGFC that discharged more frequently during theta oscillations as a higher frequency may indicate the cell is more active. In fact, theta oscillations are most regular in frequency, and have the largest amplitude, in the SLM of CA1 (Bragin et al., 1995) where NGFCs are located. During theta oscillations, the firing of NGFCs is time-locked to the peak of the theta cycle, fires just after the peak of the cycles corresponding to the local field activity recorded in stratum pyramidale (Fuentealba et al., 2010). However, the firing of NGFCs during other brain episodes remained mostly silent (Fuentealba et al., 2010). The timing of NGFCs firing pattern is interesting: NGFCs release GABA when the stratum pyramidale local field potential is most positive (when distal dendrites are most depolarised), and at the same time EC glutamatergic volley to SLM is presumably most active (Buzsáki, 2002). This specific timing of inhibition by the dendritic targeting NGFCs to the pyramidal cells is a striking example of the temporal complementarities of neuronal circuitry, delivered by distinct types of interneurons (Somogyi and Klausberger, 2005).

In vitro, NGFCs evoke uIPSCs with duration close to a single theta cycle (Karayannis et al., 2010). A classical model of hippocampal theta rhythm includes two phasic dipoles: an extrinsic input from the EC, and another dipole from the medial septum via local interneurons targeting the soma of pyramidal cells (Holsheimer et al. 1982). It has been suggested that NGFCs activity links these two dipoles by providing simultaneous inhibition to dendrites of pyramidal cells and local interneurons (Capogna and Pearce, 2011). However, *in vitro,* NGFCs exhibit short-term synaptic depression when stimulated at 5 Hz, and this short-term plasticity is subjected to tight regulation by presynaptic $GABA_B$ receptors (Price et al., 2005, 2008). When the same *in vivo* firing pattern was replayed in NGFCs *in vitro* it evokes an even stronger and longer lasting

synaptic depression, with recovery time constant around 10 mins that occurs independently of $GABA_B$ receptors (Karayannis et al. 2010). This strong synaptic depression is specific to NGFC-IPSCs as it does not occur with uIPSCs from other types of interneurons of the SLM (Karayannis et al. 2010). This observation suggests that the inhibitory input of NGFCs onto the distal dendrites of pyramidal cells, as well as surrounding interneurons, are temporally silenced following the theta frequency firing. The physiological function for this is not clear, and also it is not known whether a similar synaptic depression also occurs *in vivo* when NGFCs undergoes this firing pattern (Fuentealba et al., 2010).

I have injected the *in vivo* firing pattern throughout a 60s duration as shorter firing sequences (10 - 30s) produced less robust and reliable FSI than when applied for 60s (data not shown). However, I have not systematically addressed the issue of the optimal firing duration needed to induce FSI. A recent study reported that *in vitro* replay of place-cell firing (recorded *in vivo*) in pyramidal cells elicits the eCB-dependent transient depression of GABA release (Dubruc et al., 2013). Furthermore, this study found that the presence of DSI is critically dependent on the number of APs replayed in the postsynaptic neuron. Specifically, injection of a lower number of APs does not elicit DSI, whereas injection of a higher number of APs (> 29) elicits DSI of similar magnitude within a 10-250 Hz range (Dubruc et al., 2013). In contrast, an earlier study failed to elicit DSI in vitro by using trains of APs recorded *in vivo*, likely due to the low number of APs injected (Hampson et al., 2003).

Prior to the investigation of the mechanisms underlying FSI, it was important to ascertain whether this phenomenon did not simply result from an unspecific change in the membrane conductance of the postsynaptic recorded neurons. In the current clamp experiments, the application of a stimulus protocol of the prolonged train of APs could

have elicited a slow and persistent increase in the membrane conductance of the neurons that overlap the IPSC and are evoked shortly after (125-250 ms) the end of the firing. However, this was not the case as my data demonstrated that the application of a hyperpolarising current pulse into the postsynaptic cell before and immediately after the stimulation protocol did not modify the cells' membrane input resistance. In addition, the observation of FSI in voltage clamp mode further suggests that a change in membrane conductance was irrelevant to my observations.

Furthermore, a well-known mechanism of use-dependent plasticity of inhibitory synapses is mediated by presynaptic $GABA_B$ receptors (Scanziani, 2000). This mechanism appears to be particularly prominent at NGFCs synapses, since the stimulation of this neuron type at 5 Hz elicits a profound short-term depression, which is tightly regulated by presynaptic $GABA_B$ receptors (Price et al., 2005, 2008). However, my preliminary experiments excluded a $GABA_B$ receptor-mediated involvement in FSI. This is because the application of a $GABA_B$ receptor antagonist CGP35348 had no effect on FSI.

It is interesting to note that FSI was not only observed when both cells of the pair were reciprocally synaptically-coupled, but also in other circumstances (i.e. unidirectional connection), suggesting that the axon terminals of the postsynaptic cell were likely to be further away from the presynaptic cell membrane than the membrane of the postsynaptic cell in relation to the presynaptic terminals. This renders it likely that a retrograde messenger was released from the dendrites, but not the axon terminals of the postsynaptic cell that are likely to be more distant than dendrites from the presynaptic cell membrane.

4.2. Cell types involved in FSI

What cell types of the hippocampal SLM are involved in FSI? The great majority of anatomically identified recorded pairs exhibiting FSI were identified as NGFCs. This cell type expresses nNOS together with several other markers such as COUP TFII, reelin and NPY in the rodent hippocampus (Price et al., 2005; Fuentealba et al., 2010). NGFCs are closely related to Ivy cells in terms of their electrophysiological and morphological features. Unlike NGFCs, Ivy cells do not express reelin, and they are located near SP and target the proximal instead of the distal dendrites of pyramidal cells (Fuentealba et al., 2008, 2010). NGFCs and Ivy cell family are the most abundant interneuron class in the CA1 hippocampus, comprising ~ 37% of all GABAergic cells (Fuentealba et al., 2008). Fate-mapping analysis shows that hippocampal NGFCs derived from the median ganglionic eminence express nNOS, whereas NGFCs originating in the caudal ganglionic eminence are nNOS-negative (Tricoire et al., 2010; Tricoire and Vitalis, 2012). My data demonstrate a selective influence of nNOS-expressing NGFCs on local synaptic activity. Moreover, a small percentage of cell pairs displaying FSI were likely to be perforant path-associated or CCK basket interneurons. This latter interneuron type is well-known to express the CB1R (Katona et al., 2001; Nyiri et al., 2005), but it was previously observed that CCK could co-localise with nNOS in a single-cell PCR analysis of SLM interneurons (Price et al., 2005). I cannot exclude that other types of interneurons from the SLM, including Schaffer collateral associated cells, could also be involved in FSI, because of incomplete sampling or non-recovery in some of my recorded cells.

The NGFCs receive excitatory input from both CA3 and EC (and possibly other extra-hippocampal sources), and provide feedfoward inhibition to CA1 pyramidal cells (Capogna, 2011). On a network level, phasic EC activity evokes feedfoward inhibition in

pyramidal cells (Empson and Heinemann, 1995) through the activation of interneurons of the SLM such as NGFCs (Remondes and Schuman, 2002), which also rhythmically inhibit perisomatic targeting interneurons at theta frequency (Banks et al., 2000). The temporal delays between population activities in the EC and in the CA1 hippocampus were found to be longer (by half a theta cycle) than expected from purely velocity of axonal conduction and passive synaptic integration of feed-forward excitatory inputs. It has been suggested that this delay is due to local computations done by the interneurons of the SLM (Mizuseki et al., 2009). Since FSI controls the strength of inhibitory networks in the SLM is likely to contribute to such local computations.

In addition to employing FSI as a method to control the synaptic activity of interneurons of the SLM, pyramidal cells can also indirectly exert modulatory control over them. It is known that pyramidal cell uses eCB dependent DSI to regulate perisomatic inhibition. In contrast, virtually no information is available regarding the existence of regulatory mechanisms on dendritic feedfoward inhibitory inputs and its mechanism of action. Interestingly, NGFCs and interneuron of the SLM not only form a local inhibitory network, but also receive inhibitory input from interneurons located in other hippocampal layers, such as in SO (Elfant et al., 2008). Specifically, anatomical and physiological properties of inhibitory connections from O-LM cells onto various types of interneurons of the SLM, including NGFCs, have been reported (Elfant et al., 2008). Moreover, it has been reported that during a period of high pyramidal cell activity, for example, at 25 – 100 Hz, these neurons preferentially recruit interneurons of the SO (Pouille and Scanziani, 2004). When activated by pyramidal cells, O-LM cells are able to shift the balance from feedforward to feedback inhibition of CA1 pyramidal cells by silencing interneurons of the SLM (Elfant et al., 2008). Another interesting property of the NGFC family is their ability to display persistent firing (cells continue to fire in the absence of the stimulus, such as a depolarising current), resulting in the occurrence of hundreds of

action potentials over the course of several minutes (Krook-Magnuson et al., 2011; Sheffield et al., 2011b). The action potentials occurring during persistent firing may originate from distal axons and backpropagate to the soma. This phenomenon has been shown to occur mostly in cells expressing the serotonin 5b receptor, which is found on NGFCs (Sheffield et al., 2011b). Interestingly, persistent firing can be induced by a variety of protocols, such as depolarisation step, synaptic stimulation and sine wave current injection (Klausberger et al., 2005; Sheffield et al., 2011a). I did not observe the occurrence of persistent firing in cell pairs when experiments are recorded with current clamp configuration in my project, possibly because insufficient action potentials were injected. In my experiments, up to 500 action potentials were injected at a frequency of 8.3 Hz (CV 0.75) over the course of 60 s. By contrast, it has been reported that ~800 action potentials were required to induce persistent firing in interneurons of the SLM (Sheffield et al., 2011b). In addition, it has been reported that application μ opioid receptor agonists (DAMGO) were able to reduce the likelihood of persistent firing occurring in Ivy cells, by doubling the amount of action potentials required to trigger this phenomenon (Krook-Magnuson et al., 2011; Sheffield et al., 2011b). Activation of μ opioid receptor often hyperpolarises neurons, even if the number of initial action potentials required to induce persistent firing did not increase in an artificially hyperpolarised neuron (Krook-Magnuson et al., 2011; Sheffield et al., 2011b). This is because the effect of μ opioid receptor is not limited only to the soma. By using a stronger hyperpolarisation current to extend hyperpolarisation to axons, the number of action potentials required to induce persistent firing in μ opioid receptor activation was raised (Krook-Magnuson et al., 2011; Sheffield et al., 2011b).

Persistent firing is an example of neuron's ability to integrate a large amount of signal (hundreds of action potentials) over a relatively long time window (minutes). Functionally, one role of persistent firing is the generation of oscillations. Persistent firing

occurs at frequencies that match commonly observed oscillations, such as beta and gamma (Sheffield et al., 2011b) oscillations. Another possible function for persistent firing is to represent a cellular correlate of working memory storage (Egorov et al., 2002). The mechanism for persistent firing is uncertain. Since it is known that NGFCs form gap junctions between themselves and other interneurons (Price et al., 2005b; Zsiros and Maccaferri, 2005), one possible explanation is that persistent firing may rely on gap junctions (Sheffield et al., 2011b). It is possible that NO can be released by interneurons during persistent firing, which may be involved in regulating the synaptic integration of action potentials through FSI. However, it has been demonstrated that blocking $GABA_A$, $GABA_B$, AMPA and NMDA receptors does not affect persistent firing (Sheffield et al., 2011b).

A recent study has revealed a novel modulatory system present in the NGFC type. Specifically, it has been reported that NGFCs represent a local source of insulin in the cerebral cortex (Molnár et al., 2014). In particular, exogenous application of insulin reduces the excitability of neocortical neurons, and this effect was mimicked by the physiological activation of NGFCs. Furthermore, K-ATP channels and intracellular calcium contribute to insulin receptor-mediated action of NGFCs. However, this study could not identify the mechanism of insulin release from these neurons. Since insulin is a peptide, it is possible that a rise in dendritic Ca^{2+} is required as neuropeptide release was shown to be dependent on dendritic Ca^{2+} entry (Ludwig et al., 2002). It is known that insulin controls the metabolism through regulating brain glucose level and thus, can modulate neural circuits (Biessels et al., 1998). Interestingly, insulin can also directly modulate the molecular composition of neurons through an insulin-dependent recruitment of $GABA_A$ receptors (Wan et al., 1997). It is possible that insulin and NO released from NGFCs have opposite effects on targeted neurons to finely tune the efficacy of GABAergic synapses.

Finally, it is also important to note that FSI was detectable only in approximately 40% of all synaptically coupled pairs that are recorded without any bias, and that this percentage rose to around 80% when only nNOS-expressing interneurons of the SLM were tested. This finding agrees with the observation that some, but not all NGFCs express nNOS (Tricoire et al., 2010) and that only a third of nNOS-expressing cells coexpress the NOsGC receptor (Szabadits et al., 2007).

4.3. Voltage imaging of bAP in interneurons

Because the firing of postsynaptic neurons was observed to evoke FSI, the next logical step was to test whether bAPs were present in these neurons. I pursued this by recording bAPs with voltage imaging at different dendritic sites (range, 20–120 µm from the soma). It is known that different interneuron types have different dendritic aspects and ion channel distribution (Klausberger and Somogyi, 2008). With two photon Ca^{2+} imaging, it was found that hippocampal NGFCs are fairly resistant to decrement in AP backpropagation and this contrasts with other interneurons of the SLM (Price et al., 2008). However, there are limitations of using Ca^{2+} imaging to study AP, for example, the speed of Ca^{2+} imaging is limiting for the optimal recording of fast APs. Here I show for the first time, the optical recording of bAPs in hippocampal interneurons with VSD. I found that bAPs were present in all interneurons of the SLM tested and they were particularly robust in NGFCs.

Data obtained in cortex and few other brain areas strengthen the latter conclusion. The APs of dendritic targeting cortical interneurons actively backpropagate far into their dendritic branches without significant decrement, resulting in uniformly global Ca^{2+} accumulations (Goldberg and Yuste, 2005). In contrast, bAPs of interneurons that target the soma of postsynaptic cells are severely limited to proximal dendrites because of the selective dendritic expression of A-type K^+ channels (Goldberg and Yuste, 2005). Both dendritic and perisomatic targeting interneurons have been observed with the soma in the SLM (Vida et al., 1998), and this might explain the resulting heterogeneity of my data. Moreover, dendritic branching is likely to be an important factor. Via sharp electrode dendritic recording, Hausser & coll. showed constant bAP along single, minimally branched and long dendrites of cortical layer V pyramidal cells. In contrast, more branched cells, such as Purkinje cells in the cerebellum, show rapid

decrement in AP amplitude with distance (Vetter et al., 2001). NGFCs, which possess a fairly simple dendritic arborisation, seem to fit this view. I also found that 4-AP, but not TEA, broadened optical dendritic APs. The antagonist TEA at 1mM concentration targets Kv3 channels but does not affect Ia-type K^{+} channel, whereas 4-AP blocks Kv3 and Ia channels (Goldberg et al., 2003); this phenomenon could be explained by the observation that most interneurons in the SLM express the Ia channel.

bAPs were also detected in the dendrites after the injection of the *in vivo* firing used as stimulation protocol to induce FSI, suggesting a faithful propagation of the signal during physiologically relevant firing. Previous data obtained by Ca^{2+} imaging or dual dendritic and somatic patch-clamp recording of hippocampal or cortical interneurons reported significant attenuation of bAPs with distance from the soma because of the higher density of K^{+} channels in distal dendrites (Goldberg et al., 2003; Aponte et al., 2008; Topolnik et al., 2009; Hu et al., 2010; Evstratova et al., 2011). Other studies reported more robust bAPs in dendrites of interneurons by using Ca^{2+} (Rozsa et al., 2004) or voltage imaging (Casale and McCormick, 2011). The conclusion that emerges from my data and from previous studies is consistent with neuron type-specific attenuation of bAPs along the dendrites of various interneuron types.

Since the amount of dye bound to cell membrane at different locations can vary, the interpretation of un-calibrated VSD signals along dendrites can be methodologically problematic. To rectify this problem, I have used a long lasting hyperpolarising current pulse into the soma as a reference signal, assuming that it would spread with minimal attenuation along the dendrites of the interneurons, and this is in analogy to what was previously shown in cerebellar Purkinje cells (Vetter et al., 2001); this strategy proved sto be successful in the majority of attempt. In my experiments, the calibrated VSD data gave similar results to the un-calibrated data. It has been suggested that a high concentration of VSD have non-specific pharmacological effect on the recording neuron

and that excitation with strong lighting may introduce phototoxicity (Stuart and Palmer, 2006). I have avoided the possibility of side effects introduced by VSDs by withdrawing the recording pipette after the initial filing period and allowing a recovery period of one to two hours (i.e.. allowing the dye to distribute within the neuron and allowing the neuron to recover to more physiological condition), before re-patching the same neuron with a recording pipette but in the absence of the dye. In this manner, the neuron would not be overloaded with VSD.

Despite the risk of phototoxicity, the use of intense light for excitation greatly improves signal to noise ratio, I have attempted to mitigate phototoxicity by resorting to a very short exposure time (10 ms for bAP recording) and allowing at least one minute of recovery time between trials as well as avoiding light exposure to the soma (recordings are made at least 20 μM away from the soma). In the case of my calibration protocol, because a long recording period was required, I have reduced the excitation intensity significantly and reduced noise through processing multiple trials (> 9). In this way, high signal to noise ratio was achieved and the recorded neurons showed no sign of injury.

Whole cell voltage imaging techniques are still relatively novel in this field of study. My project has made several technical advancements in this area. Particularly, I was able to optically record VSD data in interneurons for the first time as whole cell voltage imaging techniques has proven to be technically demanding, especially when applied to interneurons. There are several reasons for this. First, the anatomy of interneurons is often not planar when compared to principal cells (i.e. their dendrites are not restricted to the same plane) - this makes imaging difficult as it is not possible to focus on all parts of the dendrites at the same time. Fortunately, this problem is less severe in NGFCs as the dendrites of NGFCs are fairly planar compared to other interneurons and therefore, more suitable for voltage imaging. In particular, the first 100 μM of NGFCs dendrites are often planar and most data were recorded from sites that fall

within this range. Secondly, interneurons are more compact and have a lower tolerance for dye loading compared with principal cells. This issue was adressed using re-patching techniques, an approach that I have discussed above. Third, because interneurons are more compact, it is relatively more difficult to find a site for dye loading with the patching pipette without damaging the integrity of the cell membrane as compared to principal cells. Pyramidal cells, which are longer than interneurons, are easier to patch towards the end of the cell body to avoid the nucleus and reduce damage. In contrast, the patch has to be carried out very carefully for interneurons, and I have reduced the problem of membrane damage by using a smaller pipette while patching at the edge of the cell body.

4.4 Dendritic calcium is required for FSI

Since increase in dendritic calcium is critical in activating molecular machinery to release retrograde signals, I have studied the level of dendritic calcium in cell pairs that display FSI. I have observed that the L-type Ca^{2+} channels, but not Ca^{2+} stores, mediate FSI induction, since this phenomenon was blocked by nifedipine, a specific L-type Ca^{2+} channel antagonist. Since a low frequency of presynaptic stimulation was utilised (once per 60 s), bath application of the L-type Ca^{2+} channel antagonist nimodipine had no effects on baseline uIPSCs. This result is consistent with a previous study showing that L-type Ca^{2+} channels do not alter IPSCs at low frequency stimulation (Jensen and Mody, 2001). Thus, as for the release of GABA at hippocampal synapses, my data suggest that L-type Ca^{2+} channels are use-dependent (in my experiments the *in vivo* firing pattern injected was in the theta frequency range).

My results are consistent with the finding that L-type Ca^{2+} channels, in addition to N-type Ca^{2+} channels, initiate DSI (Lenz et al., 1998). A dendritic release of retrograde signals shares some properties with the axonal release, but also has relevant differences. For example, a dendritic release of retrograde signalling molecules can be less spatially controlled than axonal release, because different domains of the dendrites can receive excitatory inputs that depolarises them.

Dendritic Ca^{2+} dependency of retrograde messengers is common. For example, studies comparing the suppression evoked by caged Ca^{2+} and by rise in Ca^{2+} level induced by postsynaptic depolarisation suggest that the increase in residual Ca^{2+} trigger eCB release (Wang and Zucker, 2001). Dendritic calcium levels of concentrations in µM range are needed to evoke eCB release in control conditions (Wang and Zucker, 2001; Brenowitz et al., 2006). This is consistent with the occurrence of FSI, since cell pairs which displayed FSI arrived at an average dendritic Ca^{2+} concentration of ~ 1.2 µM in my

experiments. In contrast, cell pairs that did not display FSI was observed to achieve an average dendritic Ca^{2+} concentration of only ~ 0.5 μM. The release of eCB depends on both the amplitude and duration of the dendritic Ca^{2+} signal, as studies have shown that a sustained increase in residual Ca^{2+} is effective in releasing eCBs (Brenowitz et al., 2006). The synthesis of NO is dependent on nNOS, which is highly sensitive to regulation by Ca^{2+} and calmodulin. For example, it was observed that the presence of Ca^{2+} could increase the rates of NO synthesis in a concentration-dependent manner (Mayer et al., 1992).

It has been reported that internal Ca^{2+} stores play a prominent role in dendritic release of retrograde signals, because release from internal stores can amplify Ca^{2+} level due to calcium-induced calcium release (Ross et al., 2005). However, my data showed that pharmacological blockade of internal Ca^{2+} stores did not abolish FSI. Interestingly, when I monitored dendritic Ca^{2+} levels during the stimulation protocol that was used to induce FSI, I found a precise correlation between the presence of FSI and supralinear Ca^{2+} signal.

It is worth noting that the extent to which dendritic Ca^{2+} levels increased between recordings varied considerably. I did not explore the mechanisms underlying this variability and several factors could be involved. For example, bAP could contribute to the amount of dendritic Ca^{2+} increase. It has been demonstrated that dendritic Ca^{2+} concentration in cortical bitufted interneurons increases linearly with bAP trains of increasing frequency using simultaneous dendritic recording and calcium imaging demonstrated that d (Kaiser et al., 2001). In addition, distance-dependent distribution of potassium currents may also contribute to the occurrence of bAP evoked Ca^{2+} transient (Goldberg et al., 2003). Another factor could be that a heterogeneous Ca^{2+} buffering properties and various Ca^{2+} extrusion rate are likely to exist among different types of interneurons. It has been suggested that the level of differential Ca^{2+} buffering capacity

between hippocampal interneurons and pyramidal cells could explain the different kinetics and amplitudes of calcium transients between them (Rozsa et al., 2004). Specifically, hippocampal SR interneurons were not affected by thapsigargin (which blocks calcium-ATPase and depletes the internal stores), whereas pyramidal cells show a reduction in bAP evoked calcium increase; indicating that intracellular calcium stores do not contribute to bAP evoked calcium transients in interneurons (Rozsa et al., 2004). Moreover, the variable distribution of dendritic Ca^{2+} channels may also contribute to a differential level of dendritic Ca^{2+} increase. For example, an heterogeneous expression of VGCCs has been reported in CA1 pyramidal cells (Isomura et al., 2002).

4.5. FSI is mediated by nitric oxide

Next, I identified NO as the signal mediating FSI. My data are consistent with the idea that prolonged physiological firing of the postsynaptic cell leads to Ca^{2+}-dependent release of NO from dendrites, which activates presynaptic NOsGC receptors; this in turn depresses GABA release from axon terminals. My pharmacological results clearly shows the involvement of NO as a signal mediating FSI: the non-specific nNOS inhibitor L-NAME blocked FSI in virtually all cell pairs tested and the specific NOsGC receptor blocker ODQ abolished FSI in all cell pairs tested. Furthermore, the NO precursor L-arginine potentiated FSI, and the NO donor SNP occluded FSI and pairs of tdTomato-nNOS-expressing neurons displayed a significantly higher frequency of FSI occurrence compared with randomly recorded pairs. A dendritic release of NO is consistent with its gaseous nature that does not require vesicles for its release (Garthwaite, 2008).

My data also shows that FSI can occasionally be observed in autapses that are formed on presynaptic cells immediately after the postsynaptic cell firing. However, both the likelihood of detection and the magnitude of FSI were much lower compared with those observed in unitary inhibitory events in paired recording experiments. One reason could be that NO is likely to be released from the postsynaptic cell, which has a limited diffusion distance (up to 100 μM) (Garthwaite, 2008; Lourenco et al., 2014). At the same time, the presynaptic autapse may be located further away from putative sites of NO release in comparison with regular synaptic sites, and therefore, may receive weaker NO signalling and exhibit a correspondingly weaker FSI response. Nevertheless, my data indicate that the strength of autaptic signal could be regulated by NO via FSI.

My results are consistent with data showing high expression of the NOsGC receptor in the SLM, and with the detection of the molecular machinery for retrograde NO signalling, such as NOs in hippocampal interneurons (Szabadits et al., 2007) in

addition to CA1 pyramidal cells (Burette et al., 2002). Functionally, it has been reported that NO that is released from CA1 pyramidal cells retrogradely mediates DSI (Makara et al., 2007). However, this effect by NO was only observed after prior activation of the muscarinic acetylcholine receptor, and it was triggered by the steady depolarisation of the postsynaptic neuron (Makara et al., 2007).

Current understanding of NOsGC receptors suggests the existence of several potential molecular pathways that follow NOsGC activation. The activation of NOsGC synthesises cGMP, and this is crucial for NO signalling in the brain (Boulton et al., 1994; Ahern et al., 2002). There are at least three molecular targets for cGMP that contribute to the function of NO in the brain. One target for cGMP is the hyperpolarisation activated cyclic nucleotide gated (HCN) channels (Zagotta and Siegelbaum, 1996), which has been shown to be present in hippocampal interneurons (Maccaferri and McBain, 1996; Lörincz et al., 2002). A second target is the cGMP-dependent phosphodiesterase, which is also expressed in hippocampal interneurons (van Staveren et al., 2002; Domek-Łopacińska et al., 2005). Finally, another target for cGMP is the cGMP-dependent protein kinase (PKG), which have been observed in hippocampal interneurons (Kleppisch et al., 1999; Feil et al., 2005). This heterogeneity within the cGMP signalling pathway could explain the diversity of NO–NOsGC–cGMP pathway that can either facilitate or inhibit GABAergic neurotransmission.

My findings that NO act to inhibit presynaptic GABA release is consistent with a previous study that also demonstrated an inhibitory role of NO on neuronal signalling (Liu et al., 1997); namely the application of a NO donor inhibits the activity of neurons in the supraoptic nucleus of the rat hypothalamus. However, NO has been also shown to have the opposite effect of facilitating GABA release. For example, NO increases synaptic GABA release in rat paraventricular nucleus neurons and this process is likely to be carried out through PKG activation targeted by cGMP (Li et al., 2004).

I have not studied the downstream pathways triggered by FSI of synaptic inhibition in hippocampal interneurons. However, it is relevant to briefly discuss the molecular pathways that are known to be involved in the retrograde signalling mediated by eCB that underlies DSI. This effect is primarily brought by two consequences from the activation of CB1 receptors: 1) inhibition of VGCC and adenylyl cyclase; 2) activation of inwardly rectifying K^+ channel and MAP kinase. It could be that the molecular effectors of FSI are similar. It is important to note that in addition to cGMP production, NO is known to have several targets such as ryanodine receptors via nitrosylation (Eu et al., 2003). My data provided pharmacological evidence that NOsGC is the main effector of FSI by showing that a NOsGC antagonist was able to block FSI.

In addition to the regulation of GABAergic signalling, NO is also known for its vasodilation properties. Indeed, it has been reported that bath application of NO donor onto acute rat cortical slices causes dilation of blood vessels, and this vasodilation effect can also be elicited through electrical stimulation of single nNOS expressing interneuron in the cortex (Cauli et al., 2004). This coupling between neuronal activities of interneurons expressing nNOS and vasodilation has also been reported in other brain structures such as the cerebellum, where electrical stimulation of nNOS-postive stellate cells induces vasodilation by release of NO that can be measured using NO-sensitive electrode (Rancillac et al., 2006). However, the picture is more complicated in the case for NGFCs. It is known that nNOS-positive NGFCs also express NPY, which is a potent vasoconstrictor (Cauli et al., 2004). A study has reported vasodilation and vasoconstriction effects induced by direct release of NO or NPY, respectively, and mediated by activation of serotonin 3A receptors that are present on nNOS-type II interneurons in the cortex which co-expresses nNOS and NPY (Vucurovic et al., 2010; Perrenoud et al., 2012). Therefore, it is likely that NGFCs which co-express nNOS and NPY may exert a dual control over cerebral blood flow. In this regard, however, it is

important to keep in mind that the overall effect for an unknown interneuron type that expresses both nNOS and NPY is vasodilation (Cauli et al., 2004). However, the release site for NO and NPY may be different, and this factor may provide site specificity to the effects mediated by these two agents. Particularly, NO is likely to be released from the dendrites of NGFCs, in agreement with the present study, whereas NPY is more likely released by axon terminals. The differential site of release for these two agents would act to finely tune blood and oxygen supply to neuronal circuits.

4.6. Implications of nitric oxide signalling

The evidence that NO is a retrograde signal released from postsynaptic GABAergic neurons to transiently depress synaptic inhibition is unprecedented, to my knowledge. An eCB is the classical retrograde mediator of DSI, including synaptic connections between hippocampal interneuron-principal cell (Kreitzer and Regehr, 2001; Ohno-Shosaku et al., 2001; Wilson and Nicoll, 2001), and it also mediates the self-induced hyperpolarisation of low-threshold spiking dendrite-targeting cortical interneurons (Bacci et al., 2004). My finding enriches the repertoire of pyramidal cell's control of the inhibition from interneurons. Such NO-mediated modulation appears to be particularly appropriate to control GABA released from interneuron types that do not express CB1 receptors. It is conceivable that the rise in dendritic calcium level required for DSI may influence several signalling cascades in addition to the eCB system, including the NO system. It is well established that NO can be synthesised by neurons in a calcium dependent manner (Prast and Philippu, 2001), particularly from L-arginine by NO synthase (NOS). Because NO is a gaseous molecule that freely crosses membranes, it is well suited as a retrograde messenger.

Selective expression of receptor molecules in subsets of presynaptic terminals allows retrograde messengers to dynamically regulate network functions in the brain. For example, selective expression of CB1 receptors by CCK-expressing and other interneurons of the hippocampus allow postsynaptic neurons to specifically regulate synaptic inhibition from these interneuron types (Katona et al., 1999). As a result, when pyramidal cells release eCBs following depolarisation, they will selectively suppress synapses from certain class of cells, namely CCK-positive basket cells (Wilson and Nicoll, 2001). The NO-dependent FSI represents an additional way to modulate hippocampal inhibitory synapses. This novel mechanism could be widespread in various

brain areas. Apart from NGFCs and interneurons of the SLM studied in the current project, several types of hippocampal interneurons are known to express the NO machinery. For example, nNOS expressing Ivy cells which are located in the SR and targets the proximal dendrites of pyramidal cells.

The selective regulation of specific populations of interneurons by different retrograde signalling systems would provide differential control of gating signals in the brain. This would allow excitatory signals in cortical regions to be better controlled by local interneurons. A study has hypothesised the possibility of this selective regulation (Vogels and Abbott, 2009). The authors suggest that excitatory signals are gated by the selective regulation of specific populations of interneurons, and selective suppression of interneuron populations could provide means of reducing inhibition. In this way, the balance of excitation and inhibition is regulated, and this allows excitatory inputs to effectively activate their designated population of neurons. This suppression of inhibition can be controlled, for example, through the classical DSI phenomenon of the eCB system, or via the NO-dependent FSI mechanism I have presented here.

In my project I have demonstrated the role for NO in GABAergic synapses, as a retrograde signalling molecule that functions to suppress synaptic inhibition. However, depending on the circuit, NO may be produced pre- or postsynaptically and its function also varies. In comparison with more conventional neurotransmitters such as glutamate and GABA, NO is special due to its gaseous nature which allows it to diffuse freely through aqueous and lipid environments, therefore it is more difficult to predict its site of action. The advantage provided by this property is that NO may enable simultaneous signalling to both pre- and postsynaptic elements. In my experiments I have demonstrated that NO is likely to be released from the dendrites of the postsynaptic neuron and acts presynaptically. However, once released, NO could exert its effect postsynaptically too, given that the NO receptor, NOsGC can be found on both sides of

certain inhibitory synapses (Szabadits et al., 2007). It is important to note that my data cannot firmly exclude a purely presynaptic mechanism, although the kinetics of uIPSCs during FSI was indistinguishable from that of control uIPSCs, a result that makes a postsynaptic modulation of the $GABA_A$ receptor unlikely. Additional functional tests to investigate presynaptic versus postsynaptic mechanisms (such as the CV analysis of the synaptic responses) were precluded by the need of collecting tens of uIPSCs to perform this analysis. This would have required unrealistic long-lasting recordings due to the well-known requirement of low-frequency stimulation to evoke stable NGFC-mediated IPSCs (Tamás et al., 2003; Price et al., 2005). It is worth noting that the subunit composition of NOsGC in pyramidal cells and interneurons differ. As mentioned before, NOsGC is a heterodimeric enzyme composed of two different subunits α (1 – 2) and β (1 – 2) (Russwurm et al., 2001; Russwurm and Koesling, 2002). However, only two kinds of functionally important subunits of NOsGC are known in the hippocampus: the $\alpha_1\beta_1$ and $\alpha_2\beta_1$ complexes. Studies have shown that α_1 subunit of NOsGC is present in interneurons and their terminals, but it is not detectable in pyramidal cells (Szabadits et al., 2007). Thus, if NO can act postsynaptically, there may be a difference between pyramidal cells and interneurons. Using immunoperoxidase (DAB) staining, the α_1 subunit of NOsGC can be found in all layers of the hippocampus from the alveus to SLM, including both perisomatic and dendritic targeting GABAergic neurons, and strongest staining has been observed in somata, proximal dendrites, and axons (Szabadits et al., 2007).

NO has also been associated with the modulation at excitatory synaptic terminals. It has been reported that bath application of a nNOS inhibitor blocks LTP, and this inhibition is partially occluded by high concentration of L-arginine, suggesting that the involvement of NO (O'Dell et al., 1991). In addition, inhibitors of guanylyl cyclase or cGMP-dependent protein kinase block potentiation by either titanic stimulation or low-

frequency stimulation paired with postsynaptic cell firing in cultured hippocampal neurons. Furthermore, bath application of a cGMP analogue (8-Br-cGMP) or injection of cGMP into the presynaptic neuron produces activity-dependent LTP (Arancio et al., 1995). Additionally, NO has been found to modulate excitatory synapses in other brain areas as well. In rat rostral ventral medulla neurones, endogenous NO was found to potentiate glutamate release for 10 – 20 mins through cGMP, PKG and presynaptic N-type calcium channels (Huang et al., 2003). Moreover, in the cerebellar parallel fibre-Purkinje cell synapse, NO has been demonstrated to be required for a presynaptic form of LTP, however this effect is dependent on cAMP rather than cGMP (Jacoby et al., 2001). In general, since the activation of the NO receptor synthesis cGMP, it is likely that NO has a direct effect on the modulation of LTP. As described previously, postsynaptic firing leads to calcium influx which is required for LTP following a rise in calcium concentration, NO is released and further facilitates LTP. Despite NO acts by facilitating the potentiation of glutamatergic, excitatory synapses on a longer time period, my data suggest that on a short term, NO does not affect glutamatergic, excitatory synapses impinging on hippocampal interneurons of the SLM. Thus, it could be that NO has different functions over different time courses, leading to complex scenarios of chemical modulators of neuronal networks.

Interestingly, some previous studies have demonstrated that apart from its modulatory functions, NO itself can function as a neurotransmitter. For example, recording from neurones in the pond snail (*Lymnaea stagnalis*) at synapses between a nitrenergic neuron and postsynaptic neuron, a slow NO-mediated EPSPs is detected that could trigger postsynaptic spiking (Park et al., 1998) . This NO-mediated EPSP has a fixed delay of ~ 200 ms, reaching peak amplitude after ~ 500 ms, and returns to baseline after ~ 1 s. In addition, the NO-mediated EPSP was observed after bursts of presynaptic activity, but not from single presynaptic action potentials. However, when the

concentration of Ca^{2+} and Mg^{2+} in the bathing medium was increased, unitary NO-mediated EPSPs could be observed (Park et al., 1998). In addition, application of exogenous NO produced sustained response of the neurones (Park et al., 1998), suggesting that the decaying phase of the EPSP is not caused by tachyphylaxis (loss of responsiveness) but likely due to the transient nature of NO.

Another example of NO signalling is from recording from nitrergic nerves innervating the colon (Hwang et al., 2008). In this study, the authors reported NO-mediated IPSPs. Specifically, a single shock to the nerves elicited a biphasic inhibitory potential, an initial fast phase caused by release of a purine and then a second, slower phase that is the result of NO release. The NO-mediated IPSP is slower than the NO-mediated EPSP recorded in snail neurone, because the former peaks after ~3 s and returns to baseline after ~8 s (Hwang et al., 2008).

4.7. The involvement of cannabinoid in FSI

The eCB signalling system is the most popular and better known retrograde signalling system, as it is responsible for DSI of interneuron-principal cell connections (Kreitzer and Regehr, 2001; Ohno-Shosaku et al., 2001; Wilson and Nicoll, 2001), as well as between hippocampal interneurons (Ali, 2007). The CB1 receptors are very abundant in many brain regions, including the hippocampus (Freund et al., 2003), and they are primarily located on presynaptic boutons. The postsynaptic cells are believed to represent the primary source of eCBs.

In the hippocampus, the majority of CB1 receptors are localised in the SP and SR, and especially at the junction between SP and SR (Tsou et al., 1998; Katona et al., 1999). This anatomical localisation is consistent with the DSI phenomenon between pyramidal cells and CCK-positive basket cells which soma and dendrites are mainly located in the SR. The CB1 receptors are also found in other strata such as the SO and SLM but to a less extent (Tsou et al., 1998). Indirect evidence suggests that NGFCs do not express CB1 receptors, and a study has reported that nNOS and CCK show no co-localisation (Szabadics et al., 2007). In addition, it is known that Ivy cells, which are similar to NGFCs, do not express CB1 receptors (Somogyi et al., 2012). However, whether NGFCs express CB1 receptors has not been determined yet. My functional data demonstrate that at least some NGFCs express the CB1 receptor. A previous study performed in our lab reported that a subset of NGFCs and other interneurons of the SLM (< 50%) express mRNA for CCK (Price et al., 2005). Interestingly, a heterogeneous expression of mRNA in interneurons of the SLM has been observed (Figure 4.7.1). It is worth noting that two subtypes of NGFCs exists, a NOS-positive type that is derived from the median ganglionic eminence, and a NOS-negative type that originates from the caudal ganglionic eminence (Tricoire et al., 2010; Tricoire and Vitalis, 2012). However,

the expression of CCK is not correlated with the two subtypes of NGFCs. Namely, NGFCs have been found to express CCK only, NOS only, or both CCK and NOS (Price et al., 2005). In addition, using immunofluorescence, I have carried out preliminary investigations and my results suggest that CCK and nNOS signals do overlap for a small set of neurons of the SLM (Figure 4.7.2). This preliminary result is actually consistent with my electrophysiological and pharmacological experiments showing that in some cell pair in which NGFC was the presynaptic cell, FSI could be blocked by the CB1R antagonist AM251. In this context, it is important to keep in mind the observation that in cell pairs where AM251 was not effective against FSI, subsequent bath application of L-NAME was able to abolish this phenomenon.

My data suggest that eCB and NO signalling may act independently, since I have observed FSI in a small subset of cell pairs which were not responsive to CB1R antagonist but responded to nNOS antagonist. However, my functional data could not firmly establish whether there is a functional interaction or a parallel activation of CB1 and NO receptor signals and whether they occur in the same or in different pairs of neurons. In principle, the effect of NO could be achieved in two ways (Figure 4.7.3). Firstly, cGMP (the product of NOsGC) could trigger FSI directly or act downstream of CB1R activation. In this way, NO and eCB system could function in parallel. My data indicate this model is possible, due to the observation that L-NAME blocked FSI in a subset of cell pairs in which AM251 had no effect. In addition, as mentioned previously, the molecular targets of CB1R and NOsGC could converge. For example, several studies haven shown that the activation of CB1Rs inhibits VGCCs in order to reduce presynaptic transmitter release (Freund et al., 2003). In synergy with this action, cGMP (product of NOsGC) could also inhibit VGCCs via the activation of HCN channels (Huang et al., 2011). As a matter of fact, in my experiments, FSI was sensitive to AM251 in the majority of cell pairs (6/9), suggesting that CB1R might be involved. A second mode of

action may exist, namely, cGMP could act through CB1R or act upstream of CB1R activation. According to this model, however, NO could only trigger FSI in CB1R-positive neurons. In hippocampal pyramidal cells, NO has been demonstrated to contribute to DSI in the presence of the muscarinic agonist carbachol (Makara et al., 2007). In this study, the authors suggest NO and eCB systems interact with each other rather than act in parallel (Makara et al., 2007). The authors found that NO donor increased the level of cGMP preferentially in CB1R positive terminals, suggesting a link between the eCB and the NO system. In addition, electron microscopic investigation revealed that nNOS was postsynaptically located at symmetrical synapses formed by CB1R immunopositive axon terminals, which is also immunopositive for NOsGC. Importantly, the authors also demonstrated that the effect of ODQ and 8-Br-cGMP (an analogue of the product of NOsGC) on DSI was inhibited if the cells were pre-treated with the CB1R antagonist AM251. Conversely, application of the CB1R agonist WIN 55,212-2 was able to elicit DSI in the presence of NOsGC antagonist ODQ. These experiments indicate to a functional interaction between the NO and eCB signalling systems instead of a independent, parallel pathway to modulate the release of GABA (Makara et al., 2007). Another alternative is that NOsGCs expressed at postsynaptic level potentiate the eCB production and contribute to DSI. However, this seems to be unlikely as the great majority of experimental results suggest a presynaptic site for NO.

My data cannot rule out the possibility that NO may act upstream of CB1R. In the future, it might be useful to see whether blockade of NO receptors in the presence of CB1R agonists can interfere with FSI. However, future experiment on eCB and NO signalling interaction should take into account that in a subset of my experiments, cell pairs which displayed FSI were independent of eCB (3/9, blockade of CB1 receptor did not interfere with FSI), suggesting that the NO-mediated signalling is independent from the CB1R signalling. A final technical consideration should be added when

pharmacological data on CB1R are interpreted: the specific CB1R antagonist AM251 requires a long period of pre-treatment to act in slices and fully block CB1Rs. Therefore a negative result obtained with this antagonist must be interpreted with caution and possibly a positive control demonstrating its efficacy on another cellular parameter should be obtained. In my pharmacology experiments, a the putative action of this antagonist was evaluated 5-10 minutes after the drug had reached the recording chamber. Furthermore, NO-dependent retrograde modulation of synaptic inhibition in interneurons does not require the activation of cholinergic receptors, in contrast to pyramidal cells (Makara et al,., 2007). This difference could be due to higher levels of NO in the interneurons than in pyramidal cells, so that the concentration of NO needs to be elevated by another signalling system (i.e., acetylcholine) before eliciting detectable effects in the latter but not in the former neurons. Finally, other eCB independent retrograde signalling suppression of synaptic transmission exists. For example, opioids are reported to act as a retrograde signalling molecule to suppress excitatory transmission in the hypothalamus (Iremonger and Bains, 2009).

In other brain regions complex interactions between retrograde signalling systems has been also known. Initial studies of oxytocin signalling in the hypothalamus suggested a simple scheme where oxytocin is released from postsynaptic supraoptic magnocellular neurons and travels retrogradely to reduce presynaptic probability of glutamate release by activating oxytocin receptors (Hirasawa et al., 2001). Particularly, the activation of the oxytocin receptor with a a specific agonist caused a decrease in the synaptic strength, as well as an increase in paired-pulse ratio which indicates presynaptic action. However, further experiments revealed a more complicated picture: the authors found that application of CB1R antagonists also blocked presynaptic suppression mediated by oxytocin, whereas oxytocin receptor antagonists did not block this suppression in the presence of CB1R agonists at glutamergic synapses (Hirasawa et

al., 2004). One explanation for these observations is that oxytocin once released, acts in an autocrine manner, activating oxytocin receptors on postsynaptic cells and promoting the release of eCBs, which represent the actual retrograde messengers (Regehr et al., 2009).

	GAD 65	GAD 67	CaB	CR	PV	CCK	NPY	SOM	VIP	DYN	Enk	b-NOS
NG cells												
0405-1	y	y	y	y	n	y	y	y	n	n	y	y
0407-3	y	y	n	n	n	n	y	n	n	n	n	n
0407-4	y	y	n	n	n	y	y	y	n	n	y	y
0407-5	y	y	n	n	n	n	n	n	n	n	y	n
0408-1	y	y	n	y	n	n	y	n	n	n	n	n
0408-2	y	y	y	n	n	n	y	n	n	n	n	y
0408-4	y	y	y	y	n	y	y	n	n	y	n	n
0408-5	y	y	n	n	n	n	y	n	n	n	n	n
0413-4	y	y	n	y	n	y	y	y	n	n	n	y
0419-2	y	y	n	n	n	n	y	y	n	n	n	n
0419-3	y	y	n	n	n	n	y	n	n	n	n	y
0420-4	y	y	n	n	n	y	n	n	n	n	n	y
0518-1	y	y	n	n	n	n	n	n	n	n	n	n
0518-2	y	y	n	y	n	y	y	n	n	n	y	y
0525-3	y	y	n	n	n	n	y	n	n	n	n	n
Total	15	15	3	5	0	6	12	4	0	1	4	7
Non-NG cells												
0407-1	y	y	n	n	n	n	y	y	n	n	y	y
0407-6	y	y	n	y	n	y	n	n	n	n	y	y
0413-2	y	y	n	n	n	n	n	n	n	n	y	n
0413-6	y	y	n	y	n	y	n	n	n	n	n	y
0420-5	y	y	y	n	y	n	n	y	n	n	y	n
0517-1	y	y	n	n	n	n	y	n	n	n	y	y
0517-2	y	y	y	y	n	y	n	y	n	n	y	n
0517-3	y	y	y	n	n	y	n	n		n	n	y
0518-3	y	y	n	y	n	y	n	y	n	n	y	y
0518-4	y	y	y	n	n	y	n	y	n	n	y	y
0525-1	y	y	n	n	n	n	n	n	n	n	n	n
Total	11	11	4	4	1	6	2	5	0	0	8	7

y, Yes; n, no; GAD 65 and 67, glutamic acid decarboxylases 65 and 67; CaB, calbindin; PV, parvalbumin; CR, calretinin; VIP, vasointestinal peptide; SOM, somatostatin; CCK, cholecystokinin; Dyn, dynorphin; Enk, enkephalin.

Figure 4.7.1 PCR results for anatomically identified SLM interneurons

The mRNA for CCK, which is associated with the expression of CB1 receptors, has been found in both NGFCs and other interneurons of the SLM that either expresses the b-NOS mRNA or not.

Figure taken from Price et al., 2005

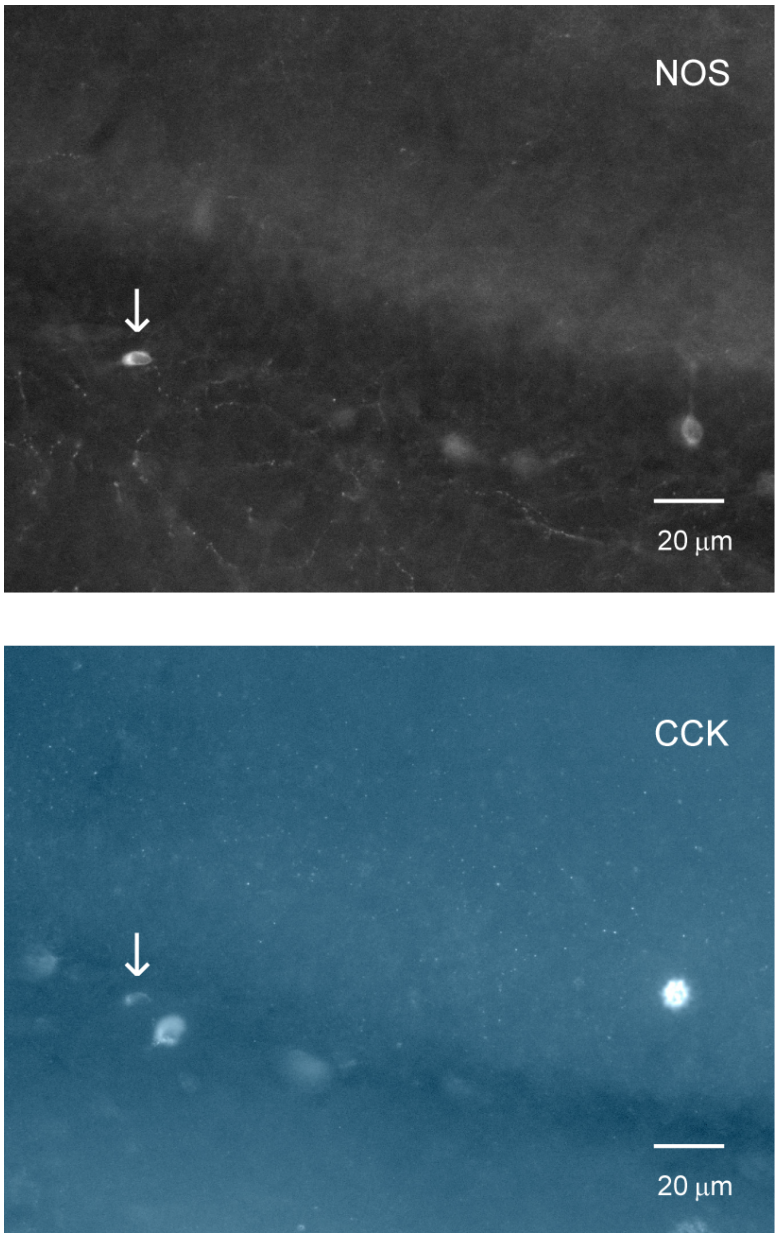

Figure 4.7.2 Immunofluorescent image showing a CCK and NOS positive cell

Top picture, NOS immunofluorescent labelling. Bottom picture, CCK immunofluorescent labelling. The arrow denotes the cell that is positive for both NOS and CCK.

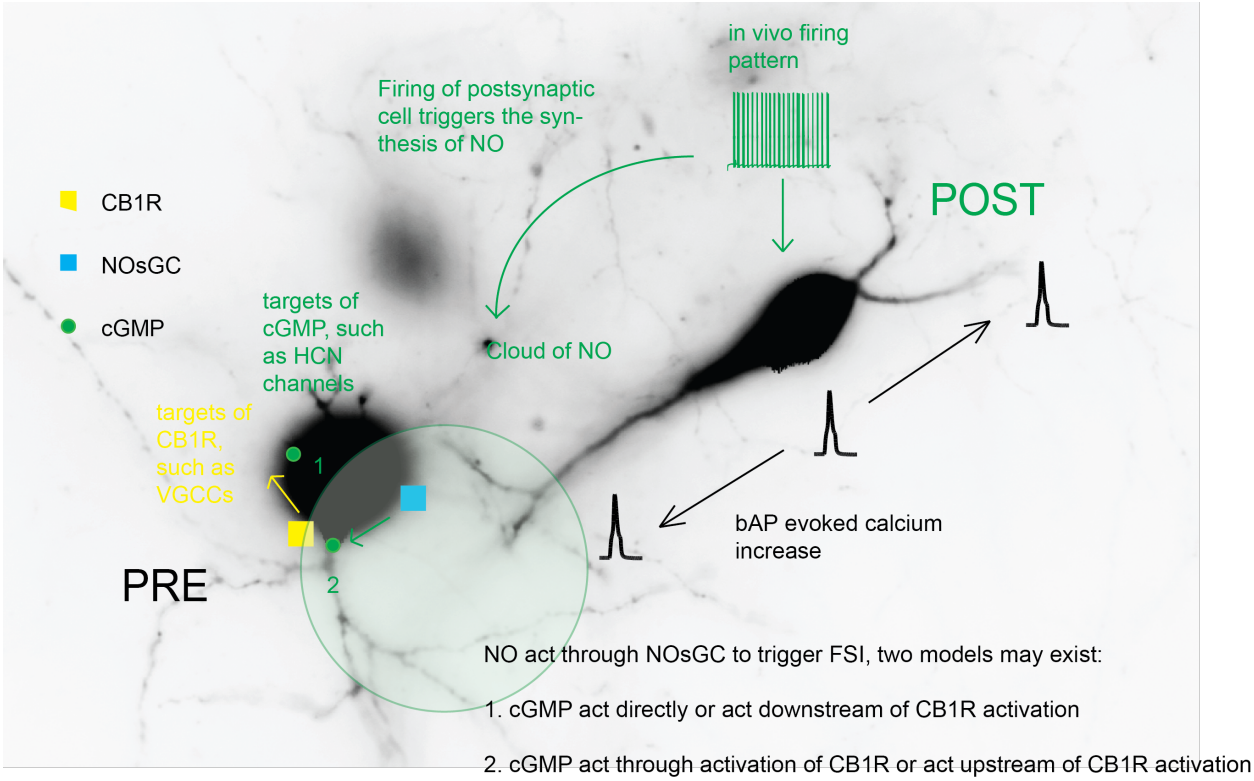

Figure 4.7.2 Scheme showing two methods of NOsGC activity

NO released from the postsynaptic cell activates NOsGC to produce cGMP, which in turn, could act directly or downstream of CB1R activation in order to trigger FSI. Alternatively, cGMP could act through CB1R or upstream of CB1R activation.

4.8. Functional role of FSI in the hippocampal network

What is the functional role of FSI in the hippocampal networks? FSI provides the postsynaptic neurons with the ability to control specific synaptic inputs to them and therefore controlling network activity. Retrograde signals have been shown to reduce to strength of synaptic inputs through negative feedback in hippocampal pyramidal cells. For example, eCB dependent DSI phenomenon in which postsynaptic firing evokes the release of eCB that in turn reduces incoming feedfoward inhibition (Kreitzer and Regehr, 2001; Ohno-Shosaku et al., 2001; Wilson and Nicoll, 2001). Negative feedback can have crucial physiological consequences. For example, eCB antagonists have been shown to suppress seizures in the hippocampus by altering the balance between synaptic excitation and inhibition (Marsicano et al., 2003; Monory et al., 2006). My data indicate that interneurons of the SLM display FSI. The SLM is an area of integration containing several excitatory inputs and local but also distant inhibitory inputs (Soltesz and Jones, 1995; Capogna, 2011; Melzer et al., 2012). Feedforward inhibition (Buzsáki, 1984; Pouille and Scanziani, 2001; Jarsky et al., 2005; Price et al., 2008) limits the temporal summation of EPSPs and generates a narrow “window of excitability” during which action potentials can occur in the postsynaptic neuron. Previous studies in the hippocampus and cortex have demonstrated that active pyramidal cells can trigger DSI, to reduce incoming feedfoward inhibition, as a method to increase their own excitability. Here I report that interneurons can also control their own excitability with FSI.

I have attempted to address the important topic of the physiological consequences of FSI on cell’s synaptic integration and used a dynamic clamp approach to inject EPSP conductance. First, I have observed that NGFC-mediated slow IPSPs modify the size of unitary EPSPs evoked by the stimulation of fibres present in the SLM, such as the perforant pathway originating from the EC. Crucially, this effect was

transiently attenuated by coincident-occurring FSI. Chains of interneurons are likely to coordinate the spatiotemporal organisation of distinct but connected networks (Mizuseki et al., 2009; Chamberland and Topolnik, 2012). I speculate that FSI occurring in interneurons of the SLM transiently strengthens the rhythmic coordination between the EC and the CA1 area of the hippocampus.

My data suggest the involvement of the *in vivo* firing pattern on network properties, and NO is able to act as a retrograde signalling molecule to influence presynaptic transmitter release. However, it is important to note that the same *in vivo* firing pattern when replayed in NGFCs *in vitro*, elicited a strong synaptic depression called mid-term depression with recovery constant around 10 mins (Karayannis et al., 2010). This mid-term depression seems to be specific to NGFC synapses since it does not occur with uIPSCs evoked by other types of interneurons of the SLM (Karayannis et al., 2010). This raises additional question to why it is required for the cell to reduce incoming inhibition if their synaptic output is already silenced. Perhaps *in vivo*, NGFCs may exhibit less synaptic depression and FSI act in a way to 'prime' the postsynaptic cell in order to ready the cell for firing when recovered. However, currently, it is not known whether NGFCs *in vivo* display similar synaptic depression after firing of action potentials at theta frequency (Fuentealba et al., 2010). Although postsynaptic cell types other than NGFCs (4/21) have been observed in a subset of FSI pairs, it is likely that FSI is able to to 'prime' the postsynaptic cell for future activity in these cell pairs.

Different types of interneurons show different changes in synaptic plasticity when undergo depolarisation. Specifically, in CA1, basket and bistratified cells receive EPSPs that display paired-pulse and short-term depression (Ali et al., 1998) , by contrast, OLM cells receive EPSPs that display paired pulse and short-term facilitation (Ali and Thomson, 1998). These interneurons also behave differently during different network oscillations. For example, O-LM cells are active and fire rhythmically at the trough of

theta waves when pyramidal cells are active but remain silent during sharp waves *in vivo* (Klausberger et al., 2003). However, the EPSP input alone is not the only determinant of neuron firing, and other factors are likely to determine their firing properties and in turn modulate their postsynaptic targets in a brain-state-dependent manner. Indeed, using paired recordings *in vitro,* a study has shown that CCK-positive SC associated interneurons in the SR are able to trigger DSI and to influence its inhibitory input from other CCK-positive SC associated interneurons (Ali, 2007). Specifically, uIPSP is reduced by about 50% following depolarisation of the postsynaptic CCK-positive SC associated interneuron, and this suppression of inhibition is blocked by CB1R antagonist. My data are consistent with those reported by Ali, however, the messenger involved in my experiments is NO rather than eCB.

Interneuron to interneuron connection often leads to an increased activity of the target of the secondary interneurons (disinhibition), as the activity of the presynaptic (primary) interneuron inhibits the postsynaptic (secondary) interneuron. Since increasing firing rate of the primary interneuron reduces inhibition from other inhibitory interneurons onto it, thus increasing its excitability and reducing the activity of secondary interneurons, in turn further increases the activity of the targets of the secondary interneurons (through more disinhibition). Therefore, when FSI occurs, the excitability of postsynaptic pyramidal cell should transiently increase due to short-term reduced inhibition.

Another possible function for FSI is to dynamically regulate network properties. In particular, FSI utilises NO as a retrograde signalling molecule and this has several functional implications. As mentioned in previous chapter, the differential expression pattern of eCB and NO provides selective regulation of populations of interneurons. On a network level, NGFCs targets the distal dendrites of pyramidal cells and receives inputs from the EC. In addition, NGFCs are known to form extensive network with other NGFCs, as well as with other interneurons of the SLM through chemical and electrical

synapses (Price et al., 2005; Zsiros and Maccaferri, 2005); and it has been suggested that electrical coupling between interneurons is critical in generating oscillations in interneuron networks (Hestrin and Galarreta, 2005). The inhibitory influences of such networks can be pivotal for pyramidal cell rhythmic activity. However, it is known that NGFCs have two different developmental origins and the key difference is that one population (derived from median ganglionic eminence) is nNOS-positive and the other one (caudal ganglionic eminence) is nNOS-negative (Tricoire et al., 2010; Tricoire and Vitalis, 2012). Apart from the expression of nNOS, these two populations of NGFCs are very similar. The NO dependent FSI phenomenon may partly explain a functional role for the existence of two populations of NGFCs, in which nNOS-positive NGFCs are selectively able to increase their excitability and feedforward inhibition when subject to higher level of activity, and provide a differential level of activity among neuronal networks. This use-dependent control of excitability would not occur in nNOS-negative NGFCs.

4.9. Conclusion and future works

My results make significant progress to the understanding of hippocampal NGFCs and of the physiological role of NOS-expressing neurons. Here I report an unexpected physiological role for NGFC firing. Experimentally, I have re-played NGFC firing pattern recorded *in vivo* during theta rhythm in *in vitro* recorded NGFCs. I found that such firing triggered a transient decrease in the strength of synaptic inhibition impinging onto the active cell. I termed this phenomenon “firing induced suppression of inhibition” (FSI) because of its formal analogy with the well-known phenomenon of “depolarisation-induced suppression of inhibition” (DSI). The data suggest that FSI is likely due to the calcium-dependent retrograde release of NO from the dendrites of postsynaptic NGFCs to inhibit the release of GABA from presynaptic interneurons. I also demonstrated the physiological impact of this phenomenon by showing that when FSI takes place the strength of incoming excitatory postsynaptic potentials onto NGFC is transiently sharpened.

I have used a multidisciplinary approach consisting of electrophysiological recording of synaptically-coupled and anatomical identified pairs of neurons, single cell voltage imaging and calcium imaging. I think my data are innovative and important for several reasons. First, the data indicates a novel and clear-cut physiological role for NO expressed by several hippocampal and cortical GABAergic cells including NGFCs. Second, they demonstrate retrograde synaptic plasticity initiated by an “*in vivo* firing pattern”, in contrast to more commonly-used less physiologically-relevant prolonged depolarisation of the postsynaptic neuron. Third, the data reveals backpropagated AP detected from the dendrites of interneurons with a much faster (~100 fold) time resolution compared to standard calcium imaging.

I believe that the present study defines novel features of synaptic communication

between neurons and that it will be influential for future research. However, there are several questions remain to be answered. First, the NO machinery is widely expressed in the hippocampus, therefore will other nNOS expressing cell types, such as Ivy cell and pyramidal cells, display FSI when subject to *in vivo* firing pattern? Makara et al. has reported a NO dependent DSI phenomenon in hippocampal pyramidal cells that requires cholinergic activation (Makara et al., 2007), whereas FSI does not. Another difference is that the conditioning protocol used in that study consisted of a depolarisation voltage step. It would be interesting to see whether firing patterns recorded *in vivo* and re-played *in vitro* would trigger NO-mediated FSI. In addition, it would be important to study in details whether CB1R and NO receptor-mediated retrograde signalling act in parallel or co-exist in the same neuron type. My data suggest a heterogeneous arrangement in which NO is responsible for FSI in the majority of cases, but eCB is also responsible in a subset of neurons. However, my data cannot firmly conclude wether eCB and NO signalling act in parallel or interact with each other. My data suggest that eCB and NO signalling may be independent, since I have observed FSI in a small subset of cell pairs which were not responsive to CB1R antagonist but responded to nNOS antagonist. However, FSI was sensitive to AM251 in the majority of cell pairs, and it has been reported that NO act upstream of eCB signalling pathway in DSI from hippocampal interneurons (Makara et al., 2007). This important issue could be studied by examining the molecular targets downstream eCB and NO receptors, namely CB1 receptors and NOsGC, and by conducting pharmacology experiments in the presence of either CB1R blockers or NO signalling blockers.

In the future, it would be also important to determine in more details the neuron types involved in FSI. By comparison to DSI, which is usually carried out by CCK-positive basket cells, the FSI phenomenon apparently can involve several interneuron types in addition to NOS-expressing NGFCs. Unfortunately, I was unable to determine

the neuron identity of about 50% of post-synaptically recorded neurons because of technical reasons. From the cell pairs that I successfully recovered, the majority of them appeared to be NGFCs, but other cell types were recovered too, such as basket cells and perforant pathway associated interneurons. Furthermore, it is likely that other interneurons cell types may display FSI too, such as Scaffer collateral associated cells.

Another interesting aspect that deserves future investigation is that the data obtained suggest a positive correlation between bAP, rise in dendritic calcium and FSI. However, I could not define the nature of this relation in details. It would be interesting to test if there is a causal relationship between the two phenomena. This could be done using simultaneous voltage and calcium imaging on dendrites of interneurons (Canepari et al., 2008), which would allow better examination of the mechanism of VGCC activation-induced rise in dendritic calcium.

Finally, the functional role of FSI remains to be better elucidated. Using dynamic clamp technique, my data indicate that FSI transiently strengthens the rhythmic coordination between the EC and CA1 area of the hippocampus through suppression of inhibition to the postsynaptic cell. However, the physiological role of FSI on a global network scale is not known. I speculate that FSI would allow a differential level of excitability among SLM interneurons, namely nNOS/NOsGC positive and nNOS/NOsGC negative populations, to selectively control the excitability of pyramidal cells. The ideal approach would be to selectively eliminate FSI, i.e. by disrupting the NO machinery in the SLM and then studying the consequences. Pharmacological approaches have advantage of rapidly affecting signalling systems but can be non-specific since the NO machinery is abundant in the hippocampus. A genetic approach may help to answer this question. For example, the selective elimination of CB1 receptors in presynaptic terminals of specific types of cells have provided a more detailed dissection of the function of retrograde signalling systems (Marsicano et al., 2003).

In summary, the present study demonstrates a novel feature of synaptic communication between interneurons of the hippocampus termed firing-induced suppression of inhibition (FSI). Specifically, injecting a theta-associated activity pattern of NGFCs recorded *in vivo* into NGFCs in rat hippocampal slices caused a transient reduction in unitary IPSP/C amplitude. FSI indirectly increased the amplitude of EPSPs and therefore enhanced the spatial and temporal summation of excitatory inputs to NGFCs, and in turn regulating their inhibition of pyramidal cells.

REFERENCES

Ahern GP, Klyachko VA, Jackson MB (2002) cGMP and S-nitrosylation: two routes for modulation of neuronal excitability by NO. Trends Neurosci 25:510–517.

Alger BE, Nicoll RA (1982) Pharmacological evidence for two kinds of GABA receptors on rat hippocampal pyramidal cells studied in vitro. J Physiol 328.

Alger BE, Pitler TA, Wagner JJ, Martin LA, Morishita W, Kirov SA, Lenz RA (1996) Retrograde signalling in depolarization-induced suppression of inhibition in rat hippocampal CA1 cells. J Physiol 496:197–209.

Ali AB (2007) Presynaptic inhibition of GABAA receptor-mediated unitary IPSPs by cannabinoid receptors at synapses between CCK-positive interneurons in rat hippocampus. J Neurophysiol 98:861–869.

Ali AB, Deuchars J, Pawelzik H, Thomson AM (1998) CA1 pyramidal to basket and bistratified cell EPSPs: dual intracellular recordings in rat hippocampal slices. J Physiol 507 (Pt 1):201–217.

Ali AB, Thomson AM (1998) Facilitating pyramid to horizontal oriens-alveus interneurone inputs: dual intracellular recordings in slices of rat hippocampus. J Physiol 507 (Pt 1):185–199.

Andersen P, Bliss TV, Skrede KK (1971) Lamellar organization of hippocampal pathways. Exp brain Res 13:222–238.

Aponte Y, Bischofberger J, Jonas P (2008) Efficient Ca2+ buffering in fast-spiking basket cells of rat hippocampus. J Physiol 586:2061–2075.

Arancio O, Kandel ER, Hawkins RD (1995) Activity-dependent long-term enhancement of transmitter release by presynaptic 3',5'-cyclic GMP in cultured hippocampal neurons. Nature 376:74–80.

Bacci A, Huguenard JR (2006) Enhancement of spike-timing precision by autaptic transmission in neocortical inhibitory interneurons. Neuron 49:119–130.

Banks MI, White JA, Pearce RA (2000) Interactions between distinct GABA(A) circuits in hippocampus. Neuron 25:449–457.

Baumann SW, Baur R, Sigel E (2002) Forced subunit assembly in alpha1beta2gamma2 GABAA receptors. Insight into the absolute arrangement. The Journal of biological chemistry 277:46020-46025.

Bellamy TC, Garthwaite J (2001) "cAMP-specific" phosphodiesterase contributes to cGMP degradation in cerebellar cells exposed to nitric oxide. Mol Pharmacol 59:54–61.

Bianchi MT, Macdonald RL (2002) Slow phases of GABA(A) receptor desensitization: structural determinants and possible relevance for synaptic function. The Journal of physiology 544:3-18.

Biessels GJ, Kamal A, Urban IJ, Spruijt BM, Erkelens DW, Gispen WH (1998) Water maze learning and hippocampal synaptic plasticity in streptozotocin-diabetic rats: effects of insulin treatment. Brain Res 800:125–135.

Bliss TV, Lømo T (1973) Long-lasting potentiation of synaptic transmission in the dentate area of the anaesthetized rabbit following stimulation of the perforant path. J Physiol 232:331–356.

Bollan K, King D, Robertson LA, Brown K, Taylor PM, Moss SJ, Connolly CN (2003) GABA(A) receptor composition is determined by distinct assembly signals within alpha and beta subunits. The Journal of biological chemistry 278:4747-4755.

Boulton CL, Irving AJ, Southam E, Potier B, Garthwaite J, Collingridge GL (1994) The nitric oxide--cyclic GMP pathway and synaptic depression in rat hippocampal slices. Eur J Neurosci 6:1528–1535.

Bragin A, Jandó G, Nádasdy Z, Hetke J, Wise K, Buzsáki G (1995a) Gamma (40-100 Hz) oscillation in the hippocampus of the behaving rat. J Neurosci : Off J Soc Neurosci 15:47–60.

Bragin ANATOL, Jando G, Nadasdy Z, Van Landeghem M, Buzsáki G (1995b) Dentate EEG spikes and associated interneuronal population bursts in the hippocampal hilar region of the rat. J Neurophysiol 73:1691–1705.

Bredt DS, Snyder SH (1992) Nitric oxide, a novel neuronal messenger. Neuron 8:3–11.

Brenowitz SD, Best AR, Regehr WG (2006) Sustained elevation of dendritic calcium evokes widespread endocannabinoid release and suppression of synapses onto cerebellar Purkinje cells. J Neurosci : Off J Soc Neurosci 26:6841–6850.

Burette A, Zabel U, Weinberg RJ, Schmidt HH, Valtschanoff JG (2002) Synaptic localization of nitric oxide synthase and soluble guanylyl cyclase in the hippocampus. J Neurosci 22:8961–8970.

Buzsáki G (1984) Feed-forward inhibition in the hippocampal formation. Prog Neurobiol 22:131–153.

Buzsáki G (2002) Theta oscillations in the hippocampus. Neuron 33:325–340.

Canepari M, Vogt K, Zecevic D (2008) Combining voltage and calcium imaging from neuronal dendrites. Cell Mol Neurobiol 28:1079–1093.

Caraiscos VB, Elliott EM, You-Ten KE, Cheng VY, Belelli D, Newell JG, Jackson MF, Lambert JJ, Rosahl TW, Wafford KA, MacDonald JF, Orser BA (2004) Tonic inhibition in mouse hippocampal CA1 pyramidal neurons is mediated by alpha5 subunit-containing gamma-aminobutyric acid type A receptors. Proceedings of the National Academy of Sciences of the United States of America 101:3662-3667.

Capogna M (2011) Neurogliaform cells and other interneurons of stratum lacunosum-moleculare gate entorhinal-hippocampal dialogue. J Physiol 589:1875–1883.

Capogna M, Pearce RA (2011) GABA A,slow: causes and consequences. Trends Neurosci 34:101–112.

Cardin JA, Carlén M, Meletis K, Knoblich U, Zhang F, Deisseroth K, Tsai L-H, Moore CI (2009) Driving fast-spiking cells induces gamma rhythm and controls sensory responses. Nature 459:663–667.

Carr MF, Jadhav SP, Frank LM (2011) Hippocampal replay in the awake state: a potential substrate for memory consolidation and retrieval. Nat Neurosci 14:147–153.

Casale AE, McCormick DA (2011) Active action potential propagation but not initiation in thalamic interneuron dendrites. J Neurosci : Off J Soc Neurosci 31:18289–18302.

Cauli B, Tong X-K, Rancillac A, Serluca N, Lambolez B, Rossier J, Hamel E (2004) Cortical GABA interneurons in neurovascular coupling: relays for subcortical vasoactive pathways. J Neurosci : Off J Soc Neurosci 24:8940–8949.

Chaudhry FA, Reimer RJ, Bellocchio EE, Danbolt NC, Osen KK, Edwards RH, Storm-Mathisen J (1998) The vesicular GABA transporter, VGAT, localizes to synaptic vesicles in sets of glycinergic as well as GABAergic neurons. The Journal of neuroscience : the official journal of the Society for Neuroscience 18:9733-9750.

Chamberland S, Topolnik L (2012) Inhibitory control of hippocampal inhibitory neurons. Front Neurosci 6.

Cobb SR, Buhl EH, Halasy K, Paulsen O, Somogyi P (1995) Synchronization of neuronal activity in hippocampus by individual GABAergic interneurons. Nature 378:75–78.

Cobb SR, Halasy K, Vida I, Ny\íri G, Tamas G, Buhl EH, Somogyi P (1997) Synaptic effects of identified interneurons innervating both interneurons and pyramidal cells in the rat hippocampus. Neuroscience 79:629–648.

Collin T, Marty A, Llano I (2005) Presynaptic calcium stores and synaptic transmission. Curr Opin Neurobiol 15:275–281.

Connolly CN, Krishek BJ, McDonald BJ, Smart TG, Moss SJ (1996) Assembly and cell surface expression of heteromeric and homomeric gamma-aminobutyric acid type A receptors. The Journal of biological chemistry 271:89-96.

Cueni L, Canepari M, Luján R, Emmenegger Y, Watanabe M, Bond CT, Franken P, Adelman JP, Lüthi A (2008) T-type Ca2+ channels, SK2 channels and SERCAs gate sleep-related oscillations in thalamic dendrites. Nat Neurosci 11:683–692.

Deleuze C, Pazienti A, Bacci A (2014) Autaptic self-inhibition of cortical GABAergic neurons: Synaptic narcissism or useful introspection? Curr Opin Neurobiol 26:64–71.

Desmond NL, Scott CA, Jane JA, Levy WB (1994) Ultrastructural identification of entorhinal cortical synapses in CA1 stratum lacunosum-moleculare of the rat. Hippocampus 4:594–600.

Domek-Łopacińska K, van de Waarenburg M, Markerink-van Ittersum M, Steinbusch HWM, de Vente J (2005) Nitric oxide-induced cGMP synthesis in the cholinergic system during the development and aging of the rat brain. Brain Res Dev brain Res 158:72–81.

Dubruc F, Dupret D, Caillard O (2013) Self-tuning of inhibition by endocannabinoids shapes spike-time precision in CA1 pyramidal neurons. J Neurophysiol 110:1930–1944.

Edwards TM, Rickard NS (2007) New perspectives on the mechanisms through which nitric oxide may affect learning and memory processes. Neurosci Biobehav Rev 31:413–425.

Egorov AV, Hamam BN, Fransén E, Hasselmo ME, Alonso AA (2002) Graded persistent activity in entorhinal cortex neurons. Nature 420:173–178.

Elfant D, Pál BZ, Emptage N, Capogna M (2008) Specific inhibitory synapses shift the balance from feedforward to feedback inhibition of hippocampal CA1 pyramidal cells. Eur J Neurosci 27:104–113.

Empson RM, Heinemann U (1995) The perforant path projection to hippocampal area CA1 in the rat hippocampal-entorhinal cortex combined slice. J Physiol 484 (Pt 3):707–720.

Eu JP, Hare JM, Hess DT, Skaf M, Sun J, Cardenas-Navina I, Sun Q-A, Dewhirst M, Meissner G, Stamler JS (2003) Concerted regulation of skeletal muscle contractility by oxygen tension and endogenous nitric oxide. Proc Natl Acad Sci United States Am 100:15229–15234.

Evstratova A, Chamberland S, Topolnik L (2011) Cell type-specific and activity-dependent dynamics of action potential-evoked Ca2+ signals in dendrites of hippocampal inhibitory interneurons. J Physiol 589:1957–1977.

Feil S, Zimmermann P, Knorn A, Brummer S, Schlossmann J, Hofmann F, Feil R (2005) Distribution of cGMP-dependent protein kinase type I and its isoforms in the mouse brain and retina. Neuroscience 135:863–868.

Ferrari F, Ottani A, Vivoli R, Giuliani D (1999) Learning impairment produced in rats by the cannabinoid agonist HU 210 in a water-maze task. Pharmacol Biochem Behav 64:555–561.

Freund TF, Buzsáki G (1996) Interneurons of the hippocampus. Hippocampus 6:347–470.

Freund TF, Katona I (2007) Perisomatic inhibition. Neuron 56:33–42.

Freund TF, Katona I, Piomelli D (2003) Role of endogenous cannabinoids in synaptic signaling. Physiol Rev 83:1017–1066.

Fuentealba P, Begum R, Capogna M, Jinno S, Márton LF, Csicsvari J, Thomson A, Somogyi P, Klausberger T (2008) Ivy cells: a population of nitric-oxide-producing, slow-spiking GABAergic neurons and their involvement in hippocampal network activity. Neuron 57:917–929.

Fuentealba P, Klausberger T, Karayannis T, Suen WY, Huck J, Tomioka R, Rockland K, Capogna M, Studer M, Morales M, Somogyi P (2010) Expression of COUP-TFII nuclear receptor in restricted GABAergic neuronal populations in the adult rat hippocampus. J Neurosci : Off J Soc Neurosci 30:1595–1609.

Garthwaite J (2008) Concepts of neural nitric oxide-mediated transmission. Eur J Neurosci 27:2783–2802.

Garthwaite J, Boulton CL (1995) Nitric oxide signaling in the central nervous system. Annu Rev Physiol 57:683–706.

Gibb BJ, Garthwaite J (2001) Subunits of the nitric oxide receptor, soluble guanylyl cyclase, expressed in rat brain. Eur J Neurosci 13:539–544.

Glickfeld LL, Scanziani M (2006) Distinct timing in the activity of cannabinoid-sensitive and cannabinoid-insensitive basket cells. Nat Neurosci 9:807–815.

Goldberg JH, Tamas G, Yuste R (2003) Ca2+ imaging of mouse neocortical interneurone dendrites: Ia-type K+ channels control action potential backpropagation. J Physiol 551:49–65.

Goldberg JH, Yuste R (2005) Space matters: local and global dendritic Ca2+ compartmentalization in cortical interneurons. Trends Neurosci 28:158–167.

Gulyás AI, Szabó GG, Ulbert I, Holderith N, Monyer H, Erdélyi F, Szabó G, Freund TF, Hájos N (2010) Parvalbumin-containing fast-spiking basket cells generate the field potential oscillations induced by cholinergic receptor activation in the hippocampus. J Neurosci : Off J Soc Neurosci 30:15134–15145.

Hampson RE, Zhuang S-Y, Weiner JL, Deadwyler SA (2003) Functional significance of cannabinoid-mediated, depolarization-induced suppression of inhibition (DSI) in the hippocampus. J Neurophysiol 90:55–64.

He L, Wu LG (2007) The debate on the kiss-and-run fusion at synapses. Trends in neurosciences 30:447-455.

Hefft S, Jonas P (2005) Asynchronous GABA release generates long-lasting inhibition at a hippocampal interneuron-principal neuron synapse. Nat Neurosci 8:1319–1328.

Hestrin S, Galarreta M (2005) Electrical synapses define networks of neocortical GABAergic neurons. Trends Neurosci 28:304–309.

Hirasawa M, Kombian SB, Pittman QJ (2001) Oxytocin retrogradely inhibits evoked, but not miniature, EPSCs in the rat supraoptic nucleus: role of N- and P/Q-type calcium channels. J Physiol 532:595–607.

Hirasawa M, Schwab Y, Natah S, Hillard CJ, Mackie K, Sharkey KA, Pittman QJ (2004) Dendritically released transmitters cooperate via autocrine and retrograde actions to inhibit afferent excitation in rat brain. J Physiol 559:611–624.

Hosoi N, Holt M, Sakaba T (2009) Calcium dependence of exo- and endocytotic coupling at a glutamatergic synapse. Neuron 63:216-229.

Huang C-C, Chan SHH, Hsu K-S (2003) cGMP/protein kinase G-dependent potentiation of glutamatergic transmission induced by nitric oxide in immature rat rostral ventrolateral medulla neurons in vitro. Mol Pharmacol 64:521–532.

Huang Z, Lujan R, Kadurin I, Uebele VN, Renger JJ, Dolphin AC, Shah MM (2011) Presynaptic HCN1 channels regulate Cav3.2 activity and neurotransmission at select cortical synapses. Nature neuroscience 14:478-486.

Hu H, Martina M, Jonas P (2010) Dendritic mechanisms underlying rapid synaptic activation of fast-spiking hippocampal interneurons. Science 327:52–58.

Hwang SJ, O'Kane N, Singer C, Ward SM, Sanders KM, Koh SD (2008) Block of inhibitory junction potentials and TREK-1 channels in murine colon by Ca2+ store-active drugs. J Physiol 586:1169–1184.

Iremonger KJ, Bains JS (2009) Retrograde opioid signaling regulates glutamatergic transmission in the hypothalamus. J Neurosci : Off J Soc Neurosci 29:7349–7358.

Isomura Y, Fujiwara-Tsukamoto Y, Imanishi M, Nambu A, Takada M (2002) Distance-dependent Ni(2+)-sensitivity of synaptic plasticity in apical dendrites of hippocampal CA1 pyramidal cells. Journal of neurophysiology 87:1169-1174.

Jacoby S, Sims RE, Hartell NA (2001) Nitric oxide is required for the induction and heterosynaptic spread of long-term potentiation in rat cerebellar slices. J Physiol 535:825–839.

Jarsky T, Roxin A, Kath WL, Spruston N (2005) Conditional dendritic spike propagation following distal synaptic activation of hippocampal CA1 pyramidal neurons. Nat Neurosci 8:1667–1676.

Jensen K, Mody I (2001) L-type Ca2+ channel-mediated short-term plasticity of GABAergic synapses. Nat Neurosci 4:975–976.

Jensen O, Lisman JE (2005) Hippocampal sequence-encoding driven by a cortical multi-item working memory buffer. Trends Neurosci 28:67–72.

Kaiser KM, Zilberter Y, Sakmann B (2001) Back-propagating action potentials mediate calcium signalling in dendrites of bitufted interneurons in layer 2/3 of rat somatosensory cortex. The Journal of physiology 535:17-31.

Karayannis T, Elfant D, Huerta-Ocampo I, Teki S, Scott RS, Rusakov DA, Jones MV, Capogna M (2010) Slow GABA transient and receptor desensitization shape synaptic responses evoked by hippocampal neurogliaform cells. J Neurosci : Off J Soc Neurosci 30:9898–9909.

Katona I, Sperlágh B, Sík A, Käfalvi A, Vizi ES, Mackie K, Freund TF (1999) Presynaptically located CB1 cannabinoid receptors regulate GABA release from axon terminals of specific hippocampal interneurons. J Neurosci : Off J Soc Neurosci 19:4544–4558.

Kirsch GE, Shieh C-C, Drewe JA, Vener DF, Brownt AM (1993) Segmental exchanges define 4-aminopyridine binding and the inner mouth of K< sup>+ pores. Neuron 11:503–512.

Kitamura T, Pignatelli M, Suh J, Kohara K, Yoshiki A, Abe K, Tonegawa S (2014) Island Cells Control Temporal Association Memory. Science .

Klausberger T, Roberts JD, Somogyi P (2002) Cell type- and input-specific differences in the number and subtypes of synaptic GABA(A) receptors in the hippocampus. The Journal of neuroscience : the official journal of the Society for Neuroscience 22:2513-2521.

Klausberger T (2009) GABAergic interneurons targeting dendrites of pyramidal cells in the CA1 area of the hippocampus. Eur J Neurosci 30:947–957.

Klausberger T, Magill PJ, Márton LF, Roberts JDB, Cobden PM, Buzsáki G, Somogyi P (2003) Brain-state- and cell-type-specific firing of hippocampal interneurons in vivo. Nature 421:844–848.

Klausberger T, Marton LF, O'Neill J, Huck JHJ, Dalezios Y, Fuentealba P, Suen WY, Papp E, Kaneko T, Watanabe M, Csicsvari J, Somogyi P (2005) Complementary roles of cholecystokinin- and

parvalbumin-expressing GABAergic neurons in hippocampal network oscillations. J Neurosci : Off J Soc Neurosci 25:9782–9793.

Klausberger T, Somogyi P (2008) Neuronal diversity and temporal dynamics: the unity of hippocampal circuit operations. Science 321:53–57.

Kleppisch T, Pfeifer A, Klatt P, Ruth P, Montkowski A, Fässler R, Hofmann F (1999) Long-term potentiation in the hippocampal CA1 region of mice lacking cGMP-dependent kinases is normal and susceptible to inhibition of nitric oxide synthase. J Neurosci : Off J Soc Neurosci 19:48–55.

Kraus MM, Prast H (2002) Involvement of nitric oxide, cyclic GMP and phosphodiesterase 5 in excitatory amino acid and GABA release in the nucleus accumbens evoked by activation of the hippocampal fimbria. Neuroscience 112:331–343.

Kreitzer AC, Regehr WG (2001) Retrograde inhibition of presynaptic calcium influx by endogenous cannabinoids at excitatory synapses onto Purkinje cells. Neuron 29:717–727.

Krook-Magnuson E, Luu L, Lee S-H, Varga C, Soltesz I (2011) Ivy and neurogliaform interneurons are a major target of μ-opioid receptor modulation. J Neurosci 31:14861–14870.

Lenz RA, Alger BE (1999) Calcium dependence of depolarization-induced suppression of inhibition in rat hippocampal CA1 pyramidal neurons. J Physiol 521 Pt 1:147–157.

Lenz RA, Wagner JJ, Alger BE (1998) N- and L-type calcium channel involvement in depolarization-induced suppression of inhibition in rat hippocampal CA1 cells. J Physiol 512 (Pt 1):61–73.

Li D-P, Chen S-R, Finnegan TF, Pan H-L (2004) Signalling pathway of nitric oxide in synaptic GABA release in the rat paraventricular nucleus. J Physiol 554:100–110.

Lien C-C, Martina M, Schultz JH, Ehmke H, Jonas P (2002) Gating, modulation and subunit composition of voltage-gated K+ channels in dendritic inhibitory interneurones of rat hippocampus. J Physiol 538:405–419.

Lisman JE (1999) Relating hippocampal circuitry to function: recall of memory sequences by reciprocal dentate–CA3 interactions. Neuron 22:233–242.

Liu QS, Jia YS, Ju G (1997) Nitric oxide inhibits neuronal activity in the supraoptic nucleus of the rat hypothalamic slices. Brain Res Bull 43:121–125.

Llano I, Dreessen J, Kano M, Konnerth A (1991) Intradendritic release of calcium induced by glutamate in cerebellar Purkinje cells. Neuron 7:577–583.

Lörincz A, Notomi T, Tamás G, Shigemoto R, Nusser Z (2002) Polarized and compartment-dependent distribution of HCN1 in pyramidal cell dendrites. Nat Neurosci 5:1185–1193.

Lourenco J, Pacioni S, Rebola N, van Woerden GM, Marinelli S, DiGregorio D, Bacci A (2014) Non-associative potentiation of perisomatic inhibition alters the temporal coding of neocortical layer 5 pyramidal neurons. PLoS biology 12:e1001903.

Ludwig M, Sabatier N, Bull PM, Landgraf R, Dayanithi G, Leng G (2002) Intracellular calcium stores regulate activity-dependent neuropeptide release from dendrites. Nature 418:85–89.

Maccaferri G, McBain CJ (1996) The hyperpolarization-activated current (Ih) and its contribution to pacemaker activity in rat CA1 hippocampal stratum oriens-alveus interneurones. J Physiol 497 (Pt 1):119–130.

Magee JC (1998) Dendritic hyperpolarization-activated currents modify the integrative properties of hippocampal CA1 pyramidal neurons. J Neurosci 18:7613–7624.

Makara JK, Katona I, Nyíri G, Németh B, Ledent C, Watanabe M, de Vente J, Freund TF, Hájos N (2007) Involvement of nitric oxide in depolarization-induced suppression of inhibition in hippocampal pyramidal cells during activation of cholinergic receptors. J Neurosci : Off J Soc Neurosci 27:10211–10222.

Manns JR, Eichenbaum H (2006) Evolution of declarative memory. Hippocampus 16:795–808.

Marr D (1971) Simple memory: a theory for archicortex. Philos Trans R Soc London Ser B, Biol Sci:23–81.

Marsicano G, Goodenough S, Monory K, Hermann H, Eder M, Cannich A, Azad SC, Cascio MG, Gutiérrez SO, van der Stelt M, López-Rodriguez ML, Casanova E, Schütz G, Zieglgänsberger W, Di Marzo V, Behl C, Lutz B (2003) CB1 cannabinoid receptors and on-demand defense against excitotoxicity. Science 302:84–88.

Mátyás F, Freund TF, Gulyás AI (2004) Convergence of excitatory and inhibitory inputs onto CCK-containing basket cells in the CA1 area of the rat hippocampus. Eur J Neurosci 19:1243–1256.

Mayer B, Klatt P, Böhme E, Schmidt K (1992) Regulation of neuronal nitric oxide and cyclic GMP formation by Ca2+. J Neurochem 59:2024–2029.

McIntire SL, Reimer RJ, Schuske K, Edwards RH, Jorgensen EM (1997) Identification and characterization of the vesicular GABA transporter. Nature 389:870-876.

Melzer S, Michael M, Caputi A, Eliava M, Fuchs EC, Whittington MA, Monyer H (2012) Long-Range–Projecting GABAergic Neurons Modulate Inhibition in Hippocampus and Entorhinal Cortex. Science 335:1506–1510.

Miles R, Tóth K, Gulyás AI, Hájos N, Freund TF (1996) Differences between somatic and dendritic inhibition in the hippocampus. Neuron 16:815–823.

Mizuseki K, Sirota A, Pastalkova E, Buzsáki G (2009) Theta oscillations provide temporal windows for local circuit computation in the entorhinal-hippocampal loop. Neuron 64:267–280.

Molnár G, Faragó N, Kocsis ÁK, Rózsa M, Lovas S, Boldog E, Báldi R, Csajbók É, Gardi J, Puskás LG, Tamás G (2014) GABAergic neurogliaform cells represent local sources of insulin in the cerebral cortex. J Neurosci : Off J Soc Neurosci 34:1133–1137.

Monory K et al. (2006) The endocannabinoid system controls key epileptogenic circuits in the hippocampus. Neuron 51:455–466.

Moroz LL, Meech RW, Sweedler JV, Mackie GO (2004) Nitric oxide regulates swimming in the jellyfish Aglantha digitale. J Comp Neurol 471:26–36.

Morris RG (2003) Long-term potentiation and memory. Philosophical transactions of the Royal Society of London Series B, Biological sciences 358:643-647.

Namiki S, Kakizawa S, Hirose K, Iino M (2005) NO signalling decodes frequency of neuronal activity and generates synapse-specific plasticity in mouse cerebellum. J Physiol 566:849–863.

Neher E, Sakaba T (2008) Multiple roles of calcium ions in the regulation of neurotransmitter release. Neuron 59:861-872.

Nugent FS, Penick EC, Kauer JA (2007) Opioids block long-term potentiation of inhibitory synapses. Nature 446:1086–1090.

Nyilas R, Dudok B, Urbán GM, Mackie K, Watanabe M, Cravatt BF, Freund TF, Katona I (2008) Enzymatic machinery for endocannabinoid biosynthesis associated with calcium stores in glutamatergic axon terminals. J Neurosci 28:1058–1063.

Nyiri G, Freund TF, Somogyi P (2001) Input-dependent synaptic targeting of alpha(2)-subunit-containing GABA(A) receptors in synapses of hippocampal pyramidal cells of the rat. The European journal of neuroscience 13:428-442.

Ohno-Shosaku T, Maejima T, Kano M (2001) Endogenous cannabinoids mediate retrograde signals from depolarized postsynaptic neurons to presynaptic terminals. Neuron 29:729–738.

Oláh S, Füle M, Komlósi G, Varga C, Báldi R, Barzó P, Tamás G (2009) Regulation of cortical microcircuits by unitary GABA-mediated volume transmission. Nature 461:1278–1281.

Oliet SHR, Baimoukhametova DV, Piet R, Bains JS (2007) Retrograde regulation of GABA transmission by the tonic release of oxytocin and endocannabinoids governs postsynaptic firing. J Neurosci : Off J Soc Neurosci 27:1325–1333.

Ozaki M, Shibuya I, Kabashima N, Isse T, Noguchi J, Ueta Y, Inoue Y, Shigematsu A, Yamashita H (2000) Preferential potentiation by nitric oxide of spontaneous inhibitory postsynaptic currents in rat supraoptic neurones. J Neuroendocrinol 12:273–281.

O'Dell TJ, Hawkins RD, Kandel ER, Arancio O (1991) Tests of the roles of two diffusible substances in long-term potentiation: evidence for nitric oxide as a possible early retrograde messenger. Proc Natl Acad Sci United States Am 88:11285–11289.

O'Keefe J, Dostrovsky J (1971) The hippocampus as a spatial map. Preliminary evidence from unit activity in the freely-moving rat. Brain Res 34:171–175.

O'Keefe J, Recce ML (1993) Phase relationship between hippocampal place units and the EEG theta rhythm. Hippocampus 3:317–330.

Park JH, Straub VA, O'Shea M (1998) Anterograde signaling by nitric oxide: characterization and in vitro reconstitution of an identified nitrergic synapse. J Neurosci : Off J Soc Neurosci 18:5463–5476.

Pawelzik H, Hughes DI, Thomson AM (2003) Modulation of inhibitory autapses and synapses on rat CA1 interneurones by GABAA receptor ligands. J Physiol 546:701–716.

Pearce RA (1993) Physiological evidence for two distinct GABA< sub> A responses in rat hippocampus. Neuron 10:189–200.

Perrenoud Q, Rossier J, Férézou I, Geoffroy H, Gallopin T, Vitalis T, Rancillac A (2012) Activation of cortical 5-HT(3) receptor-expressing interneurons induces NO mediated vasodilatations and NPY mediated vasoconstrictions. Front Neural circuits 6.

Pinal CS, Tobin AJ (1998) Uniqueness and redundancy in GABA production. Perspectives on developmental neurobiology 5:109-118.

Pitler TA, Alger BE (1992) Postsynaptic spike firing reduces synaptic GABAA responses in hippocampal pyramidal cells. J Neurosci : Off J Soc Neurosci 12:4122–4132.

Pope HG, Gruber AJ, Hudson JI, Huestis MA, Yurgelun-Todd D (2001) Neuropsychological performance in long-term cannabis users. Arch Gen Psychiatry 58:909–915.

Pouille F, Scanziani M (2001) Enforcement of temporal fidelity in pyramidal cells by somatic feed-forward inhibition. Science 293:1159–1163.

Pouille F, Scanziani M (2004) Routing of spike series by dynamic circuits in the hippocampus. Nature 429:717–723.

Price CJ, Cauli B, Kovacs ER, Kulik A, Lambolez B, Shigemoto R, Capogna M (2005) Neurogliaform neurons form a novel inhibitory network in the hippocampal CA1 area. J Neurosci 25:6775–6786.

Price CJ, Scott R, Rusakov DA, Capogna M (2008) GABA(B) receptor modulation of feedforward inhibition through hippocampal neurogliaform cells. J Neurosci : Off J Soc Neurosci 28:6974–6982.

Rancillac A, Rossier J, Guille M, Tong X-K, Geoffroy H, Amatore C, Arbault S, Hamel E, Cauli B (2006) Glutamatergic Control of Microvascular Tone by Distinct GABA Neurons in the Cerebellum. J Neurosci : Off J Soc Neurosci 26:6997–7006.

Regehr WG, Carey MR, Best AR (2009) Activity-dependent regulation of synapses by retrograde messengers. Neuron 63:154–170.

Remondes M, Schuman EM (2002) Direct cortical input modulates plasticity and spiking in CA1 pyramidal neurons. Nature 416:736–740.

Rizzoli SO, Betz WJ (2005) Synaptic vesicle pools. Nature reviews Neuroscience 6:57-69.

Rossi DJ, Hamann M (1998) Spillover-mediated transmission at inhibitory synapses promoted by high affinity alpha6 subunit GABA(A) receptors and glomerular geometry. Neuron 20:783–795.

Ross WN, Nakamura T, Watanabe S, Larkum M, Lasser-Ross N (2005) Synaptically activated ca2+ release from internal stores in CNS neurons. Cell Mol Neurobiol 25:283–295.

Rozsa B, Zelles T, Vizi ES, Lendvai B (2004) Distance-dependent scaling of calcium transients evoked by backpropagating spikes and synaptic activity in dendrites of hippocampal interneurons. The Journal of neuroscience : the official journal of the Society for Neuroscience 24:661-670.

Russwurm M, Koesling D (2002) Isoforms of NO-sensitive guanylyl cyclase. Mol Cell Biochem 230:159–164.

Russwurm M, Wittau N, Koesling D (2001) Guanylyl cyclase/PSD-95 interaction: targeting of the nitric oxide-sensitive alpha2beta1 guanylyl cyclase to synaptic membranes. J Biol Chem 276:44647–44652.

Salinas E, Sejnowski TJ (2001) Correlated neuronal activity and the flow of neural information. Nat Rev Neurosci 2:539–550.

Schneggenburger R, Sakaba T, Neher E (2002) Vesicle pools and short-term synaptic depression: lessons from a large synapse. Trends in neurosciences 25:206-212.

Scoville WB, Milner B (1957) Loss of recent memory after bilateral hippocampal lesions. J Neurol neurosurgery, Psychiatry 20.

Sheffield ME, Best TK, Mensh BD, Kath WL, Spruston N (2011a) Slow integration leads to persistent action potential firing in distal axons of coupled interneurons. BMC Neurosci 12.

Sheffield MEJ, Best TK, Mensh BD, Kath WL, Spruston N (2011b) Slow integration leads to persistent action potential firing in distal axons of coupled interneurons. Nat Neurosci 14:200–207.

Simon A, Oláh S, Molnár G, Szabadics J, Tamás G (2005) Gap-junctional coupling between neurogliaform cells and various interneuron types in the neocortex. J Neurosci : Off J Soc Neurosci 25:6278–6285.

Sohal VS, Zhang F, Yizhar O, Deisseroth K (2009) Parvalbumin neurons and gamma rhythms enhance cortical circuit performance. Nature 459:698–702.

Soltesz I, Deschenes M (1993) Low-and high-frequency membrane potential oscillations during theta activity in CA1 and CA3 pyramidal neurons of the rat hippocampus under ketamine-xylazine anesthesia. J Neurophysiol 70:97–116.

Soltesz I, Jones RS (1995) The direct perforant path input to CA1: excitatory or inhibitory? Hippocampus 5:101–103.

Somogyi P, Klausberger T (2005) Defined types of cortical interneurone structure space and spike timing in the hippocampus. The Journal of physiology 562:9-26.

Somogyi J, Szabo A, Somogyi P, Lamsa K (2012) Molecular analysis of ivy cells of the hippocampal CA1 stratum radiatum using spectral identification of immunofluorophores. Front Neural circuits 6.

Stuart GJ, Palmer LM (2006) Imaging membrane potential in dendrites and axons of single neurons. Pflügers Arch 453:403–410.

Sudhof TC (2004) The synaptic vesicle cycle. Annual review of neuroscience 27:509-547.

Szabadics J, Tamás G, Soltesz I (2007) Different transmitter transients underlie presynaptic cell type specificity of GABAA,slow and GABAA,fast. Proc Natl Acad Sci United States Am 104:14831–14836.

Szabadits E, Cserép C, Ludányi A, Katona I, Gracia-Llanes J, Freund TF, Nyíri G (2007) Hippocampal GABAergic synapses possess the molecular machinery for retrograde nitric oxide signaling. J Neurosci 27:8101–8111.

Tamas G, Buhl EH, Somogyi P (1997) Massive autaptic self-innervation of GABAergic neurons in cat visual cortex. J Neurosci 17:6352–6364.

Tamas G, Lorincz A, Simon A, Szabadics J (2003) Identified sources and targets of slow inhibition in the neocortex. Science 299:1902–1905.

Taniguchi H, He M, Wu P, Kim S, Paik R, Sugino K, Kvitsiani D, Kvitsani D, Fu Y, Lu J, Lin Y, Miyoshi G, Shima Y, Fishell G, Nelson SB, Huang ZJ (2011) A resource of Cre driver lines for genetic targeting of GABAergic neurons in cerebral cortex. Neuron 71:995–1013.

Topolnik L, Chamberland S, Pelletier J-G, Ran I, Lacaille J-C (2009) Activity-dependent compartmentalized regulation of dendritic Ca2+ signaling in hippocampal interneurons. J Neurosci : Off J Soc Neurosci 29:4658–4663.

Tricoire L, Pelkey KA, Daw MI, Sousa VH, Miyoshi G, Jeffries B, Cauli B, Fishell G, McBain CJ (2010) Common origins of hippocampal Ivy and nitric oxide synthase expressing neurogliaform cells. J Neurosci 30:2165–2176.

Tricoire L, Vitalis T (2012) Neuronal nitric oxide synthase expressing neurons: a journey from birth to neuronal circuits. Front Neural circuits 6.

Tsou K, Brown S, Sañudo-Peña MC, Mackie K, Walker JM (1998) Immunohistochemical distribution of cannabinoid CB1 receptors in the rat central nervous system. Neuroscience 83:393–411.

Van Staveren WCG, Glick J, Markerink-van Ittersum M, Shimizu M, Beavo JA, Steinbusch HWM, de Vente J (2002) Cloning and localization of the cGMP-specific phosphodiesterase type 9 in the rat brain. J Neurocytol 31:729–741.

Varvel SA, Hamm RJ, Martin BR, Lichtman AH (2001) Differential effects of delta 9-THC on spatial reference and working memory in mice. Psychopharmacology 157:142–150.

Varvel SA, Lichtman AH (2002) Evaluation of CB1R knockout mice in the Morris water maze. J Pharmacol Exp Ther 301:915–924.

Vetter P, Roth A, Häusser M (2001) Propagation of action potentials in dendrites depends on dendritic morphology. J Neurophysiol 85:926–937.

Vida I, Halasy K, Szinyei C, Somogyi P, Buhl EH (1998) Unitary IPSPs evoked by interneurons at the stratum radiatum-stratum lacunosum-moleculare border in the CA1 area of the rat hippocampus in vitro. J Physiol 506 (Pt 3):755–773.

Vogels TP, Abbott LF (2009) Gating multiple signals through detailed balance of excitation and inhibition in spiking networks. Nat Neurosci 12:483–491.

Vucurovic K, Gallopin T, Ferezou I, Rancillac A, Chameau P, van Hooft JA, Geoffroy H, Monyer H, Rossier J, Vitalis T (2010) Serotonin 3A receptor subtype as an early and protracted marker of cortical interneuron subpopulations. Cereb cortex 20:2333–2347.

Wang Y, Manis PB (2008) Short-term synaptic depression and recovery at the mature mammalian endbulb of Held synapse in mice. Journal of neurophysiology 100:1255-1264.

Wang J, Zucker RS (2001) Photolysis-induced suppression of inhibition in rat hippocampal CA1 pyramidal neurons. J Physiol 533:757–763.

Wan Q, Xiong ZG, Man HY, Ackerley CA, Braunton J, Lu WY, Becker LE, MacDonald JF, Wang YT (1997) Recruitment of functional GABA(A) receptors to postsynaptic domains by insulin. Nature 388:686–690.

Wespatat V, Tennigkeit F, Singer W (2004) Phase sensitivity of synaptic modifications in oscillating cells of rat visual cortex. J Neurosci : Off J Soc Neurosci 24:9067–9075.

White JA, Chow CC, Rit J, Soto-Treviño C, Kopell N (1998) Synchronization and oscillatory dynamics in heterogeneous, mutually inhibited neurons. J Comput Neurosci 5:5–16.

Wilson RI, Nicoll RA (2001) Endogenous cannabinoids mediate retrograde signalling at hippocampal synapses. Nature 410:588–592.

Zagotta WN, Siegelbaum SA (1996) Structure and function of cyclic nucleotide-gated channels. Annu Rev Neurosci 19:235–263.

Zarnowska ED, Keist R, Rudolph U, Pearce RA (2009) GABAA receptor alpha5 subunits contribute to GABAA,slow synaptic inhibition in mouse hippocampus. J Neurophysiol 101:1179–1191.

Zhang X-M, Zhu J (2011) Kainic Acid-induced neurotoxicity: targeting glial responses and glia-derived cytokines. Curr Neuropharmacol 9:388–398.

Zsiros V, Maccaferri G (2005) Electrical coupling between interneurons with different excitable properties in the stratum lacunosum-moleculare of the juvenile CA1 rat hippocampus. J Neurosci : Off J Soc Neurosci 25:8686–8695.

Zucker RS, Regehr WG (2002) Short-term synaptic plasticity. Annual review of physiology 64:355-405.